



TECHNISCHE
UNIVERSITÄT
WIEN

DISSERTATION

GLUEBALLS AND GAUGE/GRAVITY DUALITY

UNRAVELING THE MYSTERIES OF THE (STRONG) FORCE

ausgeführt zum Zwecke der Erlangung des akademischen Grades eines Doktors der
technischen Wissenschaften unter der Anleitung von

Univ.-Prof. Dr. **Anton Rebhan**

Institut für Theoretische Physik (E136)

eingereicht an der Technischen Universität,
Fakultät für Physik

von

Dipl.-Ing. **Frederic Brünner**

Matrikelnummer 00726861

Schegargasse 17/2/8

1190 Wien

Wien, 1.9.2020

Dipl.-Ing. Frederic Brünner



Die approbierte gedruckte Originalversion dieser Dissertation ist an der TU Wien Bibliothek verfügbar.
The approved original version of this doctoral thesis is available in print at TU Wien Bibliothek.

KURZFASSUNG

Was sind Glueballs und woran kann man sie erkennen?

Die starke Wechselwirkung hält nicht nur in Nukleonen Quarks und Gluonen zusammen, sondern ist auch für die Existenz zahlreicher sehr kurzlebiger gebundener Zustände (Mesonen und Baryonen) verantwortlich, die in Beschleunigerexperimenten beobachtet werden können. Darüber hinaus gibt es auch eine Anzahl an Teilchen, die zwar nach theoretischen Überlegungen zu finden sein sollten, die man bisher jedoch noch nicht identifizieren konnte. Dazu gehören sogenannte *Glueballs*: Zustände, die nur aus Gluonen, den mit der starken Kernkraft assoziierten Teilchen, bestehen. Glueballs werden von der Gittereichtheorie vorhergesagt, wobei die leichtesten bei einer Energie von unter 2 GeV erwartet werden. In diesem Energiebereich wurden bereits mehrere infrage kommende Zustände experimentell nachgewiesen, weswegen eine theoretische Vorhersage für das Zerfallsmuster eines Glueballs notwendig ist, um diesen darunter identifizieren zu können.

Das Ziel dieser Arbeit ist daher die Berechnung der Zerfallsraten von Glueballs, ein in der Quantenchromodynamik (QCD) schwieriges und ungelöstes Problem. Mittel zum Zweck ist die Dualität zwischen Eich- und Gravitationstheorien. Das Problem der starken Kopplung bei niedrigen Energien wird umgangen, indem die stark gekoppelte Eichtheorie auf eine schwach gekoppelte Supergravitationstheorie abgebildet wird. Verwendet wird dabei das Witten-Sakai-Sugimoto-Modell, eine auf der Typ-IIA Stringtheorie basierende Realisierung der Dualität. Diese Methode ermöglicht die Untersuchung der Wechselwirkungen von Glueballs und Mesonen in einer Theorie, welche der QCD ähnelt. So erhalten wir viele nichttriviale Ergebnisse für die Zerfallskanäle unterschiedlicher Glueballzustände. Der leichteste Glueball wird besonders im Hinblick auf die Auswirkung endlicher Quarkmassen auf die Zerfallsraten untersucht. Die gewonnenen Ergebnisse sind konsistent mit experimentellen Daten für den isoskalaren Zustand $f_0(1710)$. Der ungemischte pseudoskalare Glueball besitzt sehr spezifische Zerfallsmuster: jede mögliche Kombination von Zerfallsprodukten enthält mindestens ein η - oder η' -Meson. Die Masse des Tensorglueballs ist laut Modellvorhersage deutlich kleiner als die Prognose der Gittereichtheorie.

Erhöht man die Masse jedoch auf Werte, die mit der Gittereichtheorie kompatibel sind, so finden wir, dass der Zustand besonders instabil ist. Ebenso ergibt sich, dass auch der Pseudovektorglueball ein sehr instabiler Zustand ist, d.h. dass er sehr schnell zerfällt.

ABSTRACT

What are glueballs and how do we recognize them?

Beyond holding together quarks and gluons to form nucleons, the strong interaction is responsible for the existence of a vast number of distinct short-lived bound states (mesons and baryons) observable in collider experiments. However, there are particles expected to exist based on theoretical considerations, but which have not been found yet. A subset of them are so-called *glueballs*: states made purely of gluons, particles associated with the strong force. Glueballs are predicted by lattice gauge theory, the lightest of which are expected to be found at energies below 2 GeV. Because there are several candidate states in this energy region detected in various experiments, a theoretical prediction for the decay pattern of a glueball is necessary to identify it among them.

The aim of this work is the computation of decay rates of glueballs, a difficult and unsolved problem in quantum chromodynamics (QCD). Our method of choice is the framework of gauge/gravity duality. The problem of strong coupling at low energies is circumvented by mapping strongly coupled gauge theory to weakly coupled supergravity. We make use of the Witten-Sakai-Sugimoto model, a specific realisation of gauge/gravity duality based on type-IIA string theory. It allows us to study the interactions of glueballs and mesons for a theory similar to QCD. As a consequence, we obtain many nontrivial results for the decay channels of various glueball states. The lightest scalar glueball is studied with a particular emphasis on the effects of finite quark mass on the decay rates. Our results are found to be consistent with experimental data for the $f_0(1710)$ isoscalar state. The unmixed pseudoscalar glueball is shown to possess very specific decay patterns: every possible combination of decay products will always include at least one η or η' meson. The tensor glueball, whose mass comes out much smaller than predicted by lattice gauge theory, is shown to be a broad state when its mass is extrapolated to values compatible with lattice results. Finally, the pseudovector glueball also turns out to be very broad, i.e., it decays very fast.



Die approbierte gedruckte Originalversion dieser Dissertation ist an der TU Wien Bibliothek verfügbar.
The approved original version of this doctoral thesis is available in print at TU Wien Bibliothek.

ACKNOWLEDGEMENTS

This work would not have been possible without the influence, energy, and support of many extraordinary people I have had the honour to spend time with during my journey. This section is dedicated to them.

First of all, I would like to thank **Anton Rebhan**, who ignited my interest in quantum field theory through his excellent lecture series, and subsequently agreed to become both my diploma thesis and doctoral supervisor. With his enthusiasm and nearly indomitable focus he not only greatly influenced my approach to scientific research, he also introduced me to the magic of rotating A4 sheets by 90° in order to comfortably write down lengthy equations. I am grateful for having had the chance to study with you!

I also want to thank my two other collaborators on the "glueball project": **Denis Parganlija**, who shared his passion and insight on the phenomenology of hadrons with me, as well as **Josef Leutgeb**, whose fresh and talented approach made our joint work very enjoyable.

My time as a doctoral student was greatly enriched by the opportunity to spend a total of six months abroad. For that, I sincerely thank the doctoral program **Doktoratskolleg Particles & Interactions**. Furthermore I would like to express my gratitude towards **Philip Candelas**, **James Sparks**, and **Andrei Starinets** for making my stay at the University of Oxford possible and very exciting, and likewise towards **Johanna Erdmenger** for a great time at the Max Planck Institute for Physics in Munich.

As my research interest extends beyond the topic of this thesis, I had the chance to establish collaborations with **Vyacheslav P. Spiridonov** and **Diego Regalado**, and I would like to thank them both for inspiring and fruitful interactions during which I learned a lot.

I also would like to thank a number of people from the Institute for Theoretical Physics at TU Wien, beginning with **Daniel Grumiller** for his generous support, and **Harald Skarke** for enjoyable discussions on mathematical topics. Special thanks go to **Ayan Mukhopadhyay**, whose friendship and enthusiastic approach towards physics has been very encouraging, not only professionally but on a personal level too. My office

mates **Christian Ecker**, **Alexander Haber**, **David Müller**, and **Alexander Soloviev** contributed to a great time as a PhD student, and without them my time at the institute would not have been as joyful. I also would like to thank **Iva Lovrekovic** for many interesting discussions, and last but not least **Max Riegler**, who has been a great comrade for many years, as well as a source of inspiration.

Hannes Kolroser has my thanks for being the one who intruduced me to the idea of studying physics. Had we not met by the age of ten, who knows where I would be now?

My parents **Elisabeth** and **Karl Brünner** always encouraged me to follow my passions and I consider myself very lucky to have them and their continuous support in my life. My sincere thanks to both of you!

Finally, I want to thank **Marie-Thérèse Steinmann**, my partner, companion and friend, for supporting me with the serenity of a true Jedi in all stages of my doctoral studies. Without her and her sheer endless stream of ideas and creativity, this thesis would not have been the same. You have turned the past eight years of my life into a journey of personal growth and I owe you my gratitude. Thank you!

CONTENTS

LIST OF PUBLICATIONS	1
LIST OF FIGURES	3
LIST OF TABLES	5
0 PREFACE	7
1 INTRODUCTION	9
2 STRING THEORY	17
2.1 From Hadrons to Strings and Back Again	17
2.2 Supergravity Actions	20
2.3 D-brane Actions	23
3 GAUGE/GRAVITY DUALITY	25
3.1 History	25
3.2 The Correspondence	27
3.3 Bottom-Up vs. Top-Down Holography	31
4 A DUAL OF PURE YANG-MILLS THEORY	33
4.1 Witten's Construction	33
4.2 The Spectrum of Glueballs	36
4.3 Explicit Form of the Solutions	42
4.4 Dual operators	46
4.5 Comparison with Lattice Results	47

5 THE SAKAI-SUGIMOTO MODEL	49
5.1 Introducing Flavour Branes	49
5.2 Mesons and Interactions	51
5.3 The Mass of η_0	57
5.4 Introducing Finite Quark Mass	58
5.5 The Gluon Condensate	65
5.6 Mass Scale and Glueball Spectrum	66
6 SCALAR GLUEBALL - CHIRAL LIMIT	69
6.1 Generalities	69
6.2 Decay to Two Pseudoscalars	71
6.3 Decay to Four Pseudoscalars	76
6.4 Decay to Two Vector Mesons	82
6.5 Comparison with Experiment	83
7 SCALAR GLUEBALL - MASSIVE QUARKS	87
7.1 Glueball Coupling to the Pseudoscalar Mass Term	87
7.2 Results	89
7.3 Constraints on $\eta\eta'$ Decay	90
8 TENSOR GLUEBALL	97
8.1 Vertices	97
8.2 Decay to Two Pions	97
8.3 Decay to Two Vector Mesons	98
8.4 Results	99
9 PSEUDOSCALAR GLUEBALL	103
9.1 Vertices	103
9.2 Results - Decay Rates	107
9.3 Results - Production Rates	111
10 PSEUDOVECTOR GLUEBALL	117

10.1 Vertices 117

10.2 Results 120

11 CONCLUSION 121

A COMPUTING AMPLITUDES 123



Die approbierte gedruckte Originalversion dieser Dissertation ist an der TU Wien Bibliothek verfügbar.
The approved original version of this doctoral thesis is available in print at TU Wien Bibliothek.

LIST OF PUBLICATIONS

This thesis is based on the publications

- F. **Brünner**, J. **Leutgeb** and A. **Rebhan**,
A broad pseudovector glueball from holographic QCD,
Phys.Lett. B **788** (2019) 431-435.
- F. **Brünner** and A. **Rebhan**,
Holographic QCD predictions for production and decay of pseudoscalar glueballs,
Phys.Lett. B **770** (2017) 124-130.
- F. **Brünner** and A. **Rebhan**,
Constraints on the $\eta\eta'$ decay rate of a scalar glueball from gauge/gravity duality,
Phys. Rev. D **92** (2015), 121902.
- F. **Brünner** and A. **Rebhan**,
Nonchiral enhancement of scalar glueball decay in the Witten-Sakai-Sugimoto model,
Phys. Rev. Lett. **115** (2015), 131601.
- F. **Brünner**, D. **Parganlija** and A. **Rebhan**,
Glueball Decay Rates in the Witten-Sakai-Sugimoto Model,
Phys. Rev. D **91** (2015), 106002.

Parts of the results have been published in the following conference proceedings articles:

- F. **Brünner** and A. **Rebhan**,
Predictions for production and decay of the pseudoscalar glueball from the Witten-Sakai-Sugimoto model,
PoS EPS-HEP2017, **545** (2017).
- A. **Rebhan**, F. **Brünner** and D. **Parganlija**,
Glueball decay patterns in top-down holographic QCD,
PoS EPS-HEP2015, **421** (2015).

- **F. Brünner, D. Parganlija and A. Rebhan,**
Top-down Holographic Glueball Decay Rates,
AIP Conf. Proc. **1701** (2016) 090007.

- **F. Brünner and A. Rebhan,**
Glueball Decay in the Witten-Sakai-Sugimoto Model and Finite Quark Masses,
PoS CD 15 (2015) **124**.

- **F. Brünner, D. Parganlija and A. Rebhan,**
Holographic Glueball Decay,
Acta Phys. Polon. Supp. 7 (2014), **533**.

LIST OF FIGURES

1.1	The spectrum of glueballs in lattice gauge theory	11
4.1	The geometry of the Witten model	35
4.2	Comparison between supergravity and lattice gauge theory results for the spectrum of glueballs	48
5.1	Embedding of probe branes in the Witten-Sakai-Sugimoto model	50
5.2	Dependence of the mass of η , η' , and of the pseudoscalar mixing angle on the Witten-Veneziano mass	64
5.3	Comparison between supergravity and lattice gauge theory results for the spectrum of glueballs after fixing the mass scale to experimental data	67
6.1	Feynman diagram for scalar glueball decay into two pseudoscalar mesons	73
6.2	Feynman diagrams for the decay of a scalar glueball into four pseudoscalars mesons	77
6.3	Feynman diagram for the decay of a scalar glueball into four π^0 mesons .	78
7.1	Comparison of ratios of scalar glueball decay rates to experimental data for a glueball mass equal to that of $f_0(1500)$	93
7.2	Comparison of ratios of scalar glueball decay rates to experimental data for a glueball mass equal to that of $f_0(1710)$	94
9.1	Pseudoscalar glueball decay rate into a scalar glueball and an η/η' meson	109
9.2	Partial decay widths of a pseudoscalar glueball into three pseudoscalar mesons	110
9.3	Feynman diagrams for pseudoscalar glueball production	113
9.4	Pseudoscalar glueball production rates 1	114

9.5 Pseudoscalar glueball production rates 2 115

LIST OF TABLES

3.1	Map of concepts in gauge/gravity duality.	30
4.1	Mass spectrum of glueballs in the holographic model	40
6.1	Comparison of the results for scalar glueball decay rates with experimental data of the $f_0(1500)$ isoscalar in the chiral case	84
6.2	Comparison of the results for scalar glueball decay rates with experimental data of the $f_0(1710)$ isoscalar in the chiral case	85
7.1	Holographic results and experimental data regarding nonchiral enhancement for the $f_0(1710)$ meson	90
7.2	Comparison of holographic results with experimental data both for the $f_0(1500)$ and the $f_0(1710)$ isoscalar in the nonchiral case	91
8.1	Holographic results for decay rates of the tensor glueball	101
10.1	Holographic results for decay rates of the tensor glueball	120

0 PREFACE

“Crazy thing is...it's true. The Force, the Jedi. All of it. It's all true.”

Han Solo

In a time long before I decided to study physics, I was a huge fan of science fiction and fantasy. I loved to dive into fictional worlds, and took great pleasure in learning as much as I could about these alternate realities. One of these, which I particularly enjoyed, was the Star Wars universe. I was deeply fascinated by the Jedi, as well as the Force.

Many years later, when I had turned into an aspiring physicist with a great interest in theoretical particle physics, the opportunity arose to pursue doctoral research on the topic of the strong interaction governing the behaviour of quarks, gluons, and their composite states known as hadrons. After a while, a couple of articles on the topic were published, and some of the results gained attention in the media. In particular, a successful popular science channel on YouTube dedicated a video¹ to a paper by my supervisor Anton Rebhan and me. In this excellent video, which by now has more than 700.000 views, as well as other press releases, glueballs were referred to as particles of "pure force". This is due to the fact that glueballs are made of gluons, particles associated with the strong force. In the comment section of the video, people quickly made a connection to Star Wars: the conclusion that scientists were looking for "the Force" was drawn. It was probably no coincidence that Star Wars Episode VII had been released within the same week.

Thus, the circle is complete, and I have turned a childhood passion into a professional activity! As I've been told that physicists were allowed to be a bit nerdy, I have decided to honour my interest in Star Wars by painting this thesis in its colours. The reader is

¹SciShow, "The Quest for Glueballs", <https://www.youtube.com/watch?v=FpwpnVRABYk>

advised to take some of it with a grain of salt.

Beyond this, I want to mention that my effort with this thesis was to present its content as accessible as possible. As my work touches many different fields, including string theory, gravity, quantum field theory, as well as the phenomenology of particles, I have decided to give brief introductions to relevant concepts wherever I deemed it necessary. Furthermore, I have already summarised the main results of this thesis briefly at the end of the introduction, for those not interested in technical details.

1 INTRODUCTION

“Use the Force, Luke.”

Obi-Wan Kenobi

The discovery of the AdS/CFT (Anti-de-Sitter/Conformal Field Theory) correspondence [1] is without doubt one of the most important theoretical developments of the last few decades. There are several reasons for this, among them the fact that it allows for a perturbative study of nonperturbative problems in quantum field theory that are hard or impossible to solve by conventional methods. Other reasons include the possibility of insights on quantum gravity, and it also provides a framework in which string theory can actually tell us something about the real world, independently of its status as a theory of everything. Gauge/gravity duality, as the more general version of the correspondence not limited to AdS or CFT is called, is also often referred to as holography, because it relates gauge theories without gravity to gravitational theories in higher-dimensional spacetimes. This principle has been and continues to be applied successfully to a variety of fields, such as condensed matter physics, heavy ion phenomenology, and quantum information.

Beyond these technical reasons, the AdS/CFT-correspondence and its possible generalisations to more and more realistic systems leads to exciting questions one may ask: what does it mean that a physical system of elementary particles in our four-dimensional world can be equivalently described in terms of gravitational excitations in a higher-dimensional curved background? The statement of the correspondence is that within its range of validity all observables, i.e., anything our detectors can measure, would be completely identical in both descriptions. Is a dual description of the whole of our reality possible? If the answer is yes, what makes the four-dimensional description special so that

we have discovered it first, and only with great effort have come to a (in a certain sense) more complicated, dual description? Is it the principle of evolution that has limited us to a four-dimensional way of thinking, and is it possible that on a distant planet, alien beings may be accustomed to thinking about their reality in terms of higher-dimensional gravity? However, an answer to these questions lies beyond the scope of this thesis, and henceforth we will concern ourselves only with the more trivial technicalities of particle physics.

A field that is particularly plagued by its nonperturbative nature is the study of the strong interactions at low energy. Because of asymptotic freedom, which implies a large coupling constant at the energy scales of interest, quantum chromodynamics cannot be treated perturbatively in this region, leaving the wealth of hadronic physics beyond direct control. Bound states of quarks and gluons can therefore only be described by techniques like effective field theory or lattice QCD. The former is useful to some degree when studying interactions of mesons and baryons, whereas the latter allows for precise predictions on the spectrum of resonances. Unfortunately, to this day there is no coherent approach for describing hadrons and their interactions systematically. Because of this, their spectrum is far from well understood, despite the abundance of data from various collider experiments.

An important problem arises already on a very elementary level. In a world without quarks, gluons would not propagate freely, but would form bound states in accordance with the principle of confinement. The idea of a bound state of gluons dates back to the very early days of QCD, see for example [2] or [3]. These particles, which appear natural due to the self-interacting nature of the strong force, became known as *gluonia* or *glueballs*, and play an important role in the full understanding of the low energy hadronic spectrum. Just like states for which the corresponding quantum numbers can be inferred from a constituent quark model, the possible values of J^{PC} for glueballs (i.e., their angular momentum, parity, and charge conservation quantum numbers) are deduced from considering systems of two or three constituent gluons. The lowest-lying ground states arising from two gluons are the *scalar* with 0^{++} , the *tensor* with 2^{++} , and the *pseudoscalar* with 0^{-+} . For systems of three gluons we obtain states with 1^{++} , 1^{+-} , 1^{--} , and 3^{--} .

Due to the strongly interacting nature of QCD at low energy, it is very hard to extract

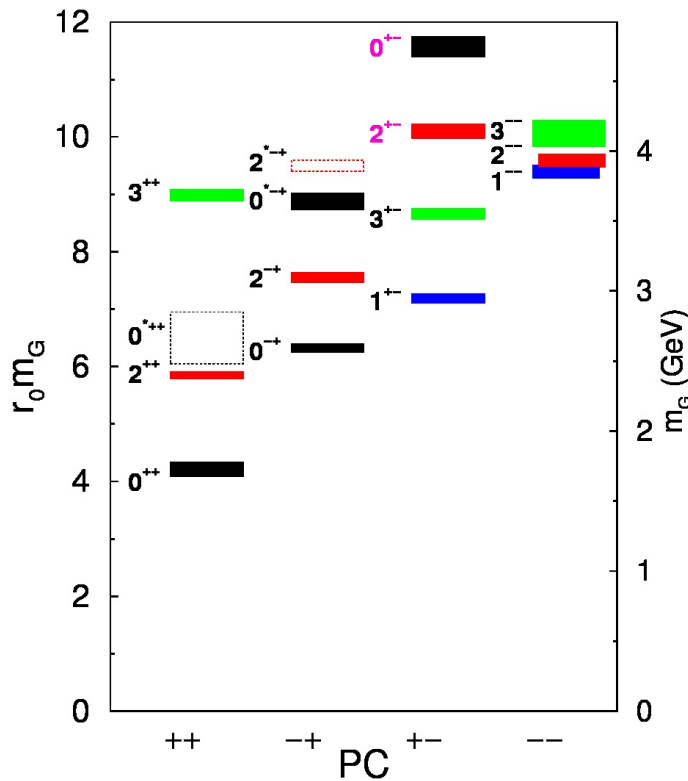


Figure 1.1: The spectrum of glueballs in lattice gauge theory according to Morningstar and Peardon [5].

more properties of glueballs from this theory alone. In fact, proving the very existence of glueballs, i.e., the presence of a mass gap in the spectrum of pure quantum Yang-Mills theory, is an important yet unsolved mathematical problem that has found its place among the Millennium Problems posed by the Clay Mathematics Institute [4]. For this reason, predictions on the mass spectrum of glueballs come from lattice gauge theory. Fig. 1.1 shows the results of a well-known study by Morningstar and Peardon [5] that illustrates the richness of the spectrum. Most notably, the lightest glueball is predicted to be lighter than 2 GeV, while a tensor, a pseudoscalar, as well as an excited scalar are found at roughly 2.5 GeV, and a pseudovector (1^{+-}) slightly below 3 GeV, followed by a large number of other states beyond the 3 GeV mark.

As fundamental as these states may be, not a single one has so far been identified unambiguously in experiment. This is in part because of an unsatisfactory experimental

situation and in part because for glueballs of certain quantum numbers, there is more than one candidate state with the same quantum numbers in the relevant mass region. This is because mesons, i.e., hadrons composed of pairs of quarks and antiquarks, are a priori indistinguishable from glueballs based on mass and quantum number alone. Experiment tells us that there is a very large number of so-called resonances, highly unstable particles characterised by their total decay rate $\Gamma \propto 1/\tau$, also known as their decay width, where τ is their mean lifetime¹, a small fraction of which could in principle be glueballs.

Let us comment briefly on the experimental status of glueball candidates.

The Particle Data Group (PDG) [6] lists five isospin-zero scalar states (known as *isoscalars*) below 2 GeV: $f_0(500)$ (the σ meson), $f_0(980)$, $f_0(1370)$, $f_0(1500)$, and $f_0(1710)$, where the last two states are narrow and are often considered in the literature as candidates for the lightest scalar glueball [7, 8, 9, 10, 11, 12, 13, 14, 15, 16]. Broad scalar glueball states around 1 GeV have been discussed in [17, 18, 19, 20]. For the tensor glueball there are also several states with the right quantum numbers in the relevant mass region: $f_2(1950)$, $f_2(2010)$, $f_2(2300)$, and $f_2(2340)$, as well states whose quantum numbers are not yet confirmed, like $f_J(2220)$. The identification of a glueball among these states has been the subject of various studies, without conclusive results [21, 22, 23, 24, 25]. Finally, the lowest-lying pseudoscalar glueball has been argued to be in the mass region slightly below 1.5 GeV, and to be identified with the $\eta(1405)$ meson [26]. However, lattice gauge theory predicts this state to be found around 2.6 GeV, both in quenched and unquenched² computations [27, 28, 29]. Therefore it can be safely assumed that the issue is not resolved. The situation is even worse for the pseudovector glueball, where the status of possible candidates is completely unclear.

So how would one go about identifying a glueball?

Resonances are not only characterised by their mass and their total decay rate, but also by their decay products. Depending on their mass, hadronic particles may in principle

¹Consequently, short-lived resonances are referred to as *broad*, as opposed to those decaying not as quickly, which are called *narrow*.

²The *quenched approximation* refers to the absence of dynamical quarks.

decay into a variety of different lighter particles, each of which is referred to as belonging to a distinct decay channel. The individual decay rates for each of the channels, together with the particle mass, may then be considered a unique signature usable to identify a specific resonance. Given a theoretical prediction for glueball decay rates as well as their masses, one may then search for compatible resonances among the experimental data.

There is, however, an additional issue. Two particles with the same quantum numbers may in principle mix with each other, i.e., exist in superposition such that the energy of a resonance cannot be unambiguously associated with either one. Mathematically, this phenomenon may be described by a so-called mixing matrix that tells us how much of each particle type is contained within a given state. Thus, resonances of interest could in principle be results of the mixing of a glueball with a quark-antiquark state. Once again, a solid theoretical prediction for the mixing matrix would be able to solve this problem.

Concerning the problem of too little experimental data, we can only hope for more to materialise in the future. However, as explained above, the situation could already be greatly improved by a solid theoretical prediction on the couplings of glueballs to ordinary mesons. The problem is that QCD at low energies is strongly coupled, and therefore perturbative techniques cannot be used to extract the relevant information from the theory. Furthermore, because lattice gauge theory unfortunately is unable to predict decay rates and traditional effective models do not allow for a systematic derivation of interaction vertices, new methods are called for. This is where gauge/gravity duality enters: while a holographic dual of QCD itself is not known, it is possible to calculate decay rates in duals of closely related models. The problem of strong coupling is circumvented by mapping the gauge theory problem to one formulated in the framework of weakly coupled gravity, where the calculations are doable in a relatively straightforward manner. After the degrees of freedom on the gravity side are identified correctly, interaction vertices may be derived rigorously, at least in the framework of "top-down" holography we will be using. This approach has the benefit of requiring only a minimal number of input parameters, which is an advantage compared to both "bottom-up" holographic models and conventional methods in effective field theory such as the nonlinear sigma model.

The present thesis is concerned with systematically studying glueball decay rates in the

Sakai-Sugimoto model [30], a holographic model based on a specific construction of pairs of N_f probe D8- and anti-D8 branes corresponding to quarks and antiquarks. They are placed in a background of a stack of D4-branes corresponding to a dual to five-dimensional Yang-Mills theory that is effectively four-dimensional below a certain compactification scale, as first formulated by Witten [31]. As is characteristic for holographic theories, a tractable holographic dual arises from this construction of D-branes in Type IIA string theory in the large N_c and large but fixed λ limit, where λ is the 't Hooft coupling. In this region of the parameter space, one may work in the supergravity approximation of string theory, which amounts to solving problems of classical gravity.

While this limit, as well as the presence of a fifth, compact dimension clearly deviate from quantum chromodynamics, which is supposed to completely describe all hadronic interactions correctly at $N_c = 3$, the two theories nevertheless have important features in common, e.g. the mechanism of chiral symmetry breaking that is important for the low energy phenomenology we are interested in. From this point of view alone it would already be worthwhile to examine it as a toy-model to learn about hadronic interactions. It turns out, as we will briefly review in later sections, that the Sakai-Sugimoto model not only reproduces features of low-energy QCD correctly on a qualitative level, but also to a large degree quantitatively. For example, the well-known decay rates of ρ and ω mesons come out close to the experimental value. This lends some credibility to the endeavour of predicting glueball decay channels in this framework, even though it should still be considered an uncontrolled approximation to QCD.

This thesis contains a number of results and predictions on glueball decay, the most important of which we want to summarise in the following:

- **Scalar glueball (0^{++})** - The spectrum of glueballs in Witten's background contains two distinct scalar states, represented by towers of gravitational excitations corresponding to two distinct polarisations: the *dilatonic* and the *exotic* one, where the latter is named as such because it corresponds to a polarisation in the compactified direction not present in real life QCD. We find that the predictions for the ratio of decay rate to mass, Γ/M , of the exotic glueball, which also comes out far too light as compared to lattice predictions, are not in good agreement with any of the

experimental candidate states. This still holds true after artificially extrapolating the mass of the state beyond the prediction of the model to the physical values of the experimental candidates. Our proposal for an explanation is that because this state arises from an extra dimension, it should be excluded when comparing with four-dimensional QCD. The dilatonic glueball comes out in the correct mass region (a little below 1.5 GeV) and shows agreement with results for the glueball candidate $f_0(1710)$, and not so good agreement with $f_0(1500)$ (after slightly extrapolating the mass in both cases) [32]. Our results furthermore predict a significant decay into four and six pseudoscalar mesons, due to the existence of a coupling to intermediate ρ and ω mesons. Including finite quark mass into the Sakai-Sugimoto model strengthens this conclusion: the resulting enhancement of decay into mesons containing strange quarks is in good agreement with experimental data for the $f_0(1710)$ isoscalar for a reasonable range of parameter values [33]. This also leads to interesting constraints on the decay rate into η and η' mesons [34]. Note that mixing between glueballs and quark-antiquark scalars may only arise as a string effect that is difficult to incorporate into the supergravity effective actions, and is currently out of reach. For this reason our results are valid under the assumption of weak mixing, and therefore an interpretation of glueball candidates as predominantly glue states.

- **Tensor glueball (2^{++})** - The mass of the tensor glueball in Witten's model is degenerate with the dilatonic scalar, and as such deviates considerably from the lattice result. At the model value, the tensor glueball cannot decay into two vector mesons, and hence Γ/M is significantly lower than when extrapolating the mass to values of 2 GeV and beyond [32]. At the lattice value for a mass of roughly 2.4 GeV the tensor glueball comes out as a very broad state. The final states are again dominated by four and six pseudoscalar mesons, as in the case of the scalar glueball. The introduction of quark mass does not lead to additional interaction vertices for the tensor glueball.
- **Pseudoscalar glueball (0^{-+})** - Our main predictions for an unmixed pseudoscalar glueball are that every possible set of final states of the decay has to contain at least

one η or η' meson, and that the remaining particles are given by the final states of the decay of an intermediate scalar glueball [35]. We also use the same interaction vertices to derive predictions for the production rates of pseudoscalar glueballs.

- **Pseudovector glueball (1^{+-})** - The main conclusion of our computation is that the pseudovector glueball is a very broad state [36]. Already for the conservative estimate of the mass of the state given by the model value, the ratio Γ/M is of order one. Taken at face value, the consequence of this is that it will be very hard to establish experimental evidence for a state of this kind.

The structure of this thesis is as follows: in chapter **2**, we give a brief introduction to string theory, as well as to the actions relevant for concrete calculations in later chapters. In chapter **3**, we discuss the basics of gauge/gravity duality, and in chapter **4**, we show how a theory of glueballs that follows from a construction by Witten can be realised in this framework. In chapter **5**, we present the (Witten-)Sakai-Sugimoto-model, a holographic theory of quark-antiquark states that arises by adding flavour branes to the setup of the previous chapter. In subsequent chapters we present our results on glueball decay, starting with the scalar glueball in the case of massless and massive quarks in chapters **6** and **7**, continuing with the tensor glueball in chapter **8**, the pseudoscalar glueball in chapter **9**, and the pseudovector glueball in chapter **10**. We conclude in chapter **11**, and present relevant aspects of the computation of decay rates in appendix **A**.

2 STRING THEORY

“Your focus determines your reality.”

Qui-Gon Jinn

2.1 FROM HADRONS TO STRINGS AND BACK AGAIN

The fact that gauge/gravity duality emerged from string theory as a way of studying the physics of strongly coupled gauge theories is remarkable for many reasons. One of them is the circumstance that string theory itself was originally born out of an attempt to describe the spectrum of hadrons. This endeavour was quickly dropped however, when it turned out that string theory had some features that were not desirable in this context, and the principle of natural selection of theories chose quantum chromodynamics as the correct framework to describe the strong interaction. Let us nevertheless briefly recapitulate this story, in order to get some perspective on how things have come full circle with the discovery of gauge/gravity duality.

Half a century ago, particle physicists were in the situation of trying to understand why there was such a large amount of distinct hadrons, strongly interacting resonances. Hadrons were found to be aligned along a so-called Regge trajectory, determined by the equation

$$\alpha' m^2 = J, \quad (2.1)$$

m being the mass and J the spin of the resonance, and α' the constant Regge slope. It was measured to have the universal value of roughly 1 GeV^{-2} . The relation even held for

hadrons of high spin, of which there was also a great number. It was hard to imagine a theory of so many fundamental particles, let alone particles of high spin, as all the working examples of renormalisable theories were limited to low spin. This was strong indication that there had to be a more fundamental framework that remained to be uncovered.

Another problem that arose around the same time was that of $s \leftrightarrow t$ duality in resonant scattering. The letters s and t denote Mandelstam variables occurring in scattering amplitudes in quantum field theory. In a given scattering process, the total scattering amplitude will receive contributions from tree-level Feynman diagrams that contain internal lines both of momentum \sqrt{s} and \sqrt{t} . These processes are referred to as s -channel and t -channel, respectively. $s \leftrightarrow t$ duality refers to the case where contributions of both channels are equal. As simple as this sounds, it is hard to realise in an actual physical process, as it would occur only if masses and couplings are chosen in a very specific way. However, evidence emerged that this duality was actually present in the scattering of hadronic resonances. Veneziano proposed an analytic form for an amplitude invariant under the exchange of s and t , which relied on the Regge behaviour of the resonances [45]. Unfortunately it turned out that it was incompatible with experimental data on hadronic scattering, and as such “dual models” were no longer interesting as theories of the strong interactions.

The Veneziano amplitude eventually found its place as the correct description of scattering processes in string theory. The problem that the amplitude required the existence of massless states, in particular a massless spin two particle incompatible with observation of the hadron spectrum, had turned into an interesting feature. A consistent theory of quantum gravity would require a particle of exactly this type, in the form of the graviton. For this and many other reasons string theory attracted a lot of researchers and quickly became and still is a very active subfield of modern-day theoretical high energy physics.

String theory, as the name suggests, is the theory of the interactions of strings, one-dimensional fundamental objects moving through space-time, replacing the traditional picture of point-like elementary particles as the fundamental constituents of matter. The concept of a world line is replaced by that of a world sheet, the region in space-time defined by the movement of a one-dimensional object. The starting point of a mathematical

formulation of string theory is the question: what does the action minimized by the dynamics of a string look like? The answer, in flat space-time, is given by the Nambu-Goto action:

$$S_{\text{NG}} = -T \int d\sigma d\tau \sqrt{(\dot{X}^\mu X'_\mu)^2 - \dot{X}^2 X'^2}, \quad (2.2)$$

with the embedding of the string world sheet $X^\mu = X^\mu(\sigma, \tau)$ being parametrised as a function of the world sheet coordinates σ and τ , where $\dot{X}^\mu \equiv \frac{\partial X^\mu}{\partial \tau}$ and $X'^\mu \equiv \frac{\partial X^\mu}{\partial \sigma}$. The prefactor T is the string tension. The action is proportional to the area of the world sheet, and therefore any solution to the equations of motion will minimise this quantity.

These simple starting assumptions lead to an unexpectedly rich body of phenomena. The key realisation is that after quantisation, distinct levels of excitation of strings correspond to distinct physical particles. String theory is a candidate for a theory of everything because it naturally incorporates a graviton, a massless spin-two excitation, in addition to the degrees of freedom of a nonabelian gauge theory, such as the standard model. However, a concrete confirmation of string theory as a fundamental framework for describing our world is still lacking. This might in part be due to the small size of strings, smaller than the resolution of our detectors, and in part due to another prediction of string theory: in order for the theory to be consistent, one requires a total of (at least) 10 space-time dimensions. As we only observe four, the question arises how this could ever be compatible with nature as we experience it. The standard route to resolve this problem is to postulate that the other (six) dimensions are compact and small, such that they would only play a direct role in phenomena occurring at energies beyond the reach of current collider experiments. Unfortunately, this does not resolve the issue unambiguously: there is a huge number of possible compactifications, a circumstance known as the landscape problem. Right now, there is no criterion known that would single out one geometry or class of geometries, leading to a derivation of the standard model from first principles. Despite this limitation, string theory has proven to be an immensely important tool both in mathematics and theoretical physics, and in the intersection of both subjects. For example, not mentioning the AdS/CFT correspondence, string theory has contributed greatly to the understanding of supersymmetric gauge theories and their various dualities. Therefore,

even if string theory would never live up to the dream of being a successful fundamental theory of everything, it is clear that it will remain an important part of theoretical physics.

So why is the total number of dimensions in string theory greater than four? The precise number of space-time dimensions follows from consistence requirements such as the closure of the Poincaré algebra. In the case of bosonic strings, strings that do not give rise to fermionic excitations, the so-called critical dimension is 26. This theory is unstable, as it contains a tachyonic mode of imaginary mass. This problem is solved by introducing fermions and making the theory supersymmetric. This modification is referred to as superstring theory and has critical dimension 10.

String theory is more than just a perturbation theory of strings. Many of its interesting features arise because there is a highly nontrivial nonperturbative description in terms of hypersurfaces on which strings may end. These were discovered in [46] and named D-branes, due to the Dirichlet boundary conditions imposed on open strings. D-branes are dynamical objects, charged under the various form fields of a given string theory, and also act as a source of gravity, curving the space-time around them. As discussed in more detail in other parts of this thesis, the world volume dynamics generated by endpoints of open strings on D-branes play an important role in gauge/gravity duality and its application to the phenomenology of hadrons. In the low energy limit that is of interest in this case, when the string picture is no longer apparent, string theory is approximated by supergravity, and the world volume theory on D-branes is given by an ordinary (gauge) field theory. In the following two sections we describe the relevant actions.

2.2 ◆ SUPERGRAVITY ACTIONS

It is important to mention that there is not just one type of string theory, but several varieties related by certain duality transformations. The theories commonly arising in the context of holography are known as type IIA and type IIB string theories. The field content and the numbers of dimensions of D-branes permitted in each of them are different. The original version of the AdS/CFT correspondence discovered by Maldacena belongs to the type IIB category, while the holographic model that is the focus of this thesis is a solution

to type IIA. The motivation for this will be discussed later. As we want to consider the large N and large but fixed λ limits, which correspond to the limit of weak gravity, it suffices to consider the low energy approximation known as type IIA supergravity. It is convenient to start with the eleven-dimensional supergravity that is the low-energy limit of M-theory, and to obtain type IIA supergravity by dimensional reduction. In the following we will review the relevant actions, taking the expositions in [47] and [48] as a rough guideline.

Let us begin by discussing the field content of eleven-dimensional supergravity. There are in total two bosonic fields. One of them is the graviton that may be represented by the vielbein e_M^A , where the index A corresponds to the tangent space and transforms nontrivially under local Lorentz transformations, while the index M corresponds to the base-space and transforms nontrivially under general coordinate transformations. The spacetime metric, which will be our object of choice to work with for actual computations, is constructed as

$$g_{MN} = \eta_{AB} e_M^A e_N^B, \quad (2.3)$$

where η_{AB} is the flat tangent space metric. The graviton is a traceless symmetric tensor transforming under the little group $SO(9)$ and therefore contains 44 degrees of freedom.

The other bosonic field is a rank-three antisymmetric tensor, the three-form field A_3 , which is associated with gauge invariance of the theory under

$$A_3 \rightarrow A_3 + d\Gamma_2, \quad (2.4)$$

with a two-form Γ_2 . Gauge invariance leads to transversality of physical polarisations, of which there are 84.

In a supersymmetric theory a total of 128 bosonic degrees of freedom has to be matched by 128 fermionic ones. These are contained in the gravitino ψ_M , which acts as a gauge field for local supersymmetry. It transforms under the spin group $\text{Spin}(9)$, the covering group of $SO(9)$, and for each value of the index M carries a Majorana spinor with 32 components. Due to gauge invariance, there are 128 independent physical degrees of freedom.

The action of the theory is restricted by general coordinate invariance, local Lorentz invariance, gauge invariance, and local supersymmetry, and was first constructed in [49]. As we are only interested in classical solutions, it suffices to consider the bosonic part. The latter is given in terms of the fields by

$$S_{11D} = \frac{1}{2\kappa_{11}^2} \int d^{11}x \sqrt{-g} \left(R - \frac{1}{2} |F_4|^2 \right) - \frac{1}{12\kappa_{11}^2} \int A_3 \wedge F_4 \wedge F_4. \quad (2.5)$$

The first term is the Einstein-Hilbert term with the Ricci scalar $R \equiv g^{MN} R_{MN}$, the second term is the square of the four form field strength $F_4 = dA_3$, with

$$|F_p|^2 = \frac{1}{p!} g^{M_1 N_1} g^{M_2 N_2} \dots g^{M_p N_p} F_{M_1 M_2 \dots M_p} F_{N_1 N_2 \dots N_p}, \quad (2.6)$$

and the third term is a Chern-Simons term. By convention, the prefactor is determined by the eleven-dimensional gravitational coupling constant κ_{11} that is related to the corresponding Newton's constant G_{11} and the Planck length ℓ_P by

$$2\kappa_{11}^2 = 16\pi G_{11} = (2\pi)^8 \ell_P^9. \quad (2.7)$$

The action of type IIA supergravity is obtained from eleven-dimensional supergravity by dimensional reduction. This means that we compactify a direction we call x_{11} on a circle of radius $R = g_s \ell_s$ and keep only the zero modes in the Fourier expansions of the fields. The metric is reduced by decomposing the eleven-dimensional line element as

$$ds^2 = g_{MN} dx^M dx^N = e^{-\frac{2}{3}\Phi} g_{mn} dx^m dx^n + e^{\frac{4}{3}\Phi} (dx^{11} + A_m dx^m)^2, \quad (2.8)$$

where g_{mn} is the ten-dimensional metric, A_m is a U(1) gauge field, and Φ is a scalar field, the dilaton, which appears in Eq. (3.3). The string coupling constant is given by the vacuum expectation value of its exponential:

$$g_s = \langle \exp \Phi \rangle. \quad (2.9)$$

Finally, the eleven-dimensional three-form reduces to the three-form A_3 with the components¹

¹When both forms appear simultaneously, we will use the superscript "11D", otherwise the meaning

$$A_{mno} = A_{mno}^{11D} \quad (2.10)$$

and the two-form B_2 with the components

$$B_{mn} = A_{mn,11}^{11D}. \quad (2.11)$$

The action of IIA supergravity may be written in terms of these fields contained in the string world sheet sigma model action. We can decompose it according to the sectors of type IIA string theory the fields correspond to, namely the Ramond-Ramond (RR) and the Neveu-Schwarz (NS) sectors. There is again a Chern-Simons (CS) term that contains fields from both sectors. The total bosonic action is then given by

$$S_{\text{IIA}} = S_{\text{NS}} + S_{\text{RR}} + S_{\text{CS}}, \quad (2.12)$$

with

$$S_{\text{NS}} = \frac{1}{2\kappa_{10}^2} \int d^{10}x \sqrt{g} e^{-2\Phi} \left(R + 4\partial_\mu \Phi \partial^\mu \Phi - \frac{1}{2} |H_3|^2 \right), \quad (2.13)$$

$$S_{\text{RR}} = -\frac{1}{4\kappa_{10}^2} \int d^{10}x \sqrt{g} \left(|F_2|^2 + |\tilde{F}_4|^2 \right), \quad (2.14)$$

and

$$S_{\text{CS}} = -\frac{1}{4\kappa_{10}^2} \int B_2 \wedge F_4 \wedge F_4, \quad (2.15)$$

where $\kappa_{10}^2 = \kappa_{11}^2 / 2\pi R$, $H_3 = dB_2$, $F_2 = dA_1$, and $\tilde{F}_4 = dA_3 + A_1 \wedge H_3$.

2.3 ◆ D-BRANE ACTIONS

D-branes, as mentioned before, may be thought of both as nonperturbative dynamical objects in their own right, as well as hypersurfaces on which strings may end. From the latter point of view one may ask what the correct description would be at low energies, where the stringy nature of interactions should not be apparent. This question is answered in terms of an effective action for the massless modes of the strings on the $p+1$ -dimensional world volume of a Dp -brane. For a stack of N D-branes these will correspond to the gauge should be clear from the context.

field of a $U(N)$ gauge theory. We will be interested in the behaviour of these degrees of freedom, represented by the field strength $F = dA + A \wedge A$, in the presence of background fields both from the NS and the RR sector, as described by the actions in the previous section. The interactions with the NS fields are described by the Dirac-Born-Infeld (DBI) action, which is given by

$$S_{\text{DBI}} = -T_p \int d^{p+1}x e^{-\Phi} \text{Tr} \sqrt{-\det(g_{MN} + \mathcal{F}_{MN})}, \quad (2.16)$$

where $T_p = \frac{1}{\kappa_{10}^2} (4\pi^2 \alpha')^{\frac{3-p}{2}}$ is the D-brane tension and $\alpha' = \ell_s^2$, with

$$\mathcal{F}_{MN} \equiv B_{MN} + 2\pi\alpha' F_{MN}. \quad (2.17)$$

The trace is to be taken on the generators of the gauge group, with $\text{Tr} T^a T^b = \delta^{ab}$. For the calculations throughout this thesis we will use the fact that the integrand of Eq.(2.16) may be expanded in small fluctuations of \mathcal{F}_{MN} according to the symmetrised-trace-prescription [50]. The result is given to quartic order by

$$\begin{aligned} \text{STr} \sqrt{-\det(g_{MN} + \mathcal{F}_{MN})} &= 1 + \frac{1}{4} \text{Tr} g^{MN} g^{PQ} \mathcal{F}_{MP} \mathcal{F}_{NQ} \\ &- \frac{1}{12} \text{Tr} g^{MN} g^{PQ} g^{RS} g^{TU} (\mathcal{F}_{MP} \mathcal{F}_{RQ} \mathcal{F}_{NT} \mathcal{F}_{SU} + \frac{1}{2} \mathcal{F}_{MP} \mathcal{F}_{RQ} \mathcal{F}_{ST} \mathcal{F}_{NU} \\ &- \frac{1}{4} \mathcal{F}_{MP} \mathcal{F}_{NQ} \mathcal{F}_{RT} \mathcal{F}_{SU} - \frac{1}{8} \mathcal{F}_{MP} \mathcal{F}_{RT} \mathcal{F}_{NQ} \mathcal{F}_{SU}) + \mathcal{O}(\mathcal{F}^6). \end{aligned} \quad (2.18)$$

Interactions with RR fields are governed by an action similar to a Chern-Simons term:

$$S_{\text{CS}} = iT_p \int \text{Tr} \exp(B_2 + 2\pi\alpha' F_2) \wedge \sum_q C_q. \quad (2.19)$$

The structure of the nonvanishing terms resulting after expanding the exponential is determined by the requirement that the degrees of the form add up to the number of space-time dimensions of the world volume of the D-brane.

3 GAUGE/GRAVITY DUALITY

“Many of the truths that we cling to depend on our point of view.”

Obi-Wan Kenobi

3.1 HISTORY

The two major breakthroughs in the physics of the 20th century were the understanding of gravity as curvature of spacetime in the form of general relativity, as well as the realisation that matter is fundamentally governed by the rules of quantum mechanics. The latter has led to quantum field theory, a comprehensive framework for describing with high precision the nongravitational interactions of matter up to relativistic scales, culminating in the Standard Model of particle physics, whose theoretical and experimental exploration dominated the second half of the century. Its experimental confirmation was finally complete with the discovery of the Higgs boson only a few years ago.

Despite these successes, a complete picture of all fundamental interactions has not yet been achieved. This is due to the fact that while general relativity is in very good agreement with observational data, it is still an inherently classical (i.e., non-quantum) theory. There are reasons to expect that a classical description of space-time cannot hold under all circumstances. The Planck scale, the smallest scale that may be formed by making use of the natural constants c , G , and \hbar , is often cited as the scale which should serve as a natural cut-off for the regime where quantum field theory and gravity may be treated separately. It is expected that a full theory of quantum gravity is necessary to describe the physics arising at this scale. In regions of very high curvature, for example,

properties of space-time should be governed by quantum gravity. Much effort has gone into trying to formulate such a theory, but so far no satisfying answer has been found. A good candidate available at present is string theory, which is in principle a fully functional theory of quantum gravity. Unfortunately, experimental confirmation that it actually describes the space-time geometry of our universe is still missing. The search for quantum gravity has nevertheless been very productive, in the sense that it has led to other interesting results, one of which is the discovery gauge/gravity duality.

The foundations of gauge/gravity duality date back to the formulation of the holographic principle [37, 38]. In [37], 't Hooft discusses cut-offs in quantum field theory and the idea that a physical cut-off is given naturally in terms of black holes: when reaching very high energies, a physical process may result in the formation of a microscopic black hole, if the energy density in a given small region of spacetime would at some point be high enough. As is well known due to Bekenstein, the entropy of a black hole scales with surface area, not volume. 't Hooft goes one step further and claims that all degrees of freedom determining the physics at these scales should be encoded in the surface, and that a description in one dimension less, i.e. a $2+1$ dimensional one, should be completely equivalent to a $3+1$ dimensional one. Susskind [38] makes 't Hooft's idea more concrete by using light cone quantisation for partons, and discusses possible connections to string theory.

Another important hint towards gauge/gravity duality came almost 20 years earlier, also from 't Hooft [39]. He studied the large- N limit of QCD and discovered that in this limit, the theory simplifies into an expansion consisting of planar diagrams. These diagrams are equivalent to those of a free string theory with coupling constant $1/N$. This is remarkable but maybe not surprising, given that string theory was originally discovered in an attempt to understand the hadronic spectrum (see the previous Chapter for more detail).

The real breakthrough, in which the above ideas were made precise, came only when Maldacena formulated the AdS/CFT correspondence [1], the first concrete example of a full holographic duality. By duality we mean the complete equivalence of two distinct

frameworks in the sense that they agree on all observables. The AdS/CFT correspondence is remarkable because it relates a theory without gravity to one with gravity: $\mathcal{N} = 4$ supersymmetric Yang-Mills theory with gauge group $U(N)$ in the large- N limit in four dimensions, which is also a conformal field theory, is dual to an $AdS_5 \times S^5$ solution of type IIB supergravity.

3.2 ◆ THE CORRESPONDENCE

In the absence of a rigorous proof, a heuristic explanation for the AdS/CFT correspondence goes as follows [40]:

Consider a stack of N D3-branes. Their world volume, on which open strings may end, is a four-dimensional submanifold of the full ten-dimensional space. Separated from this world volume along a coordinate r , closed strings may propagate in a region of the space time referred to as the bulk. As string theory permits open strings to join to form closed strings, interactions between these two regions may take place in the form of processes akin to Hawking radiation. The total action of this system is then of the form

$$S = S_{\text{bulk}} + S_{\text{brane}} + S_{\text{interactions}}. \quad (3.1)$$

One may now ask what this system would look like at low energy, when the string picture is no longer apparent. This amounts to taking the limit $\alpha' \rightarrow 0$, making the interaction term in (3.1) vanish, as it is proportional to α'^2 . In the bulk, massive string modes disappear and we are left with supergravity, i.e., free gravity, while on the world volume of the branes we obtain four-dimensional $\mathcal{N} = 4$ supersymmetric Yang-Mills theory, an $SU(N)$ gauge theory without gravity that possesses conformal symmetry.

There is an alternative way of looking at the system described above. Instead of examining the behaviour of the solution of string theory (D3-branes) at low energy, we may instead first consider the low energy limit of string theory itself, i.e., supergravity, and solve it. We obtain what is known as p -branes, and again we find two decoupled physical systems, one at large and another at small r . This time, however, both are systems composed of gravitational degrees of freedom. It turns out that in the limit $r \rightarrow 0$, the

geometry of a p -brane is that of an $\text{AdS}_5 \times S^5$ space-time.

Consistency of both approaches towards taking the low energy limit requires that both descriptions near $r \rightarrow 0$ are identical, and hence we obtain an equivalence between $\mathcal{N} = 4$ supersymmetric Yang-Mills theory and gravity on $\text{AdS}_5 \times S^5$ in a particular region of the latter. This region is referred to as the boundary, as the four-dimensional Minkowski space on which the gauge theory lives is located at infinity in the standard coordinates (Poincaré coordinates) used to describe Anti-de-Sitter space.

What is not obvious from the arguments laid out so far is that one has to impose certain conditions on the parameters of the theories for the supergravity limit to hold. In particular, the so-called AdS-radius must be large in comparison to the string length, and quantum string corrections must be small. The former implies $g_s N \propto g_{YM}^2 N \gg 1$, while the latter is realised by $g_s \rightarrow 0$. Combining the two, we also obtain the condition $N \rightarrow \infty$, in order to keep $g_s N$ large but fixed. With the identification of the 't Hooft coupling $\lambda \equiv g_{YM}^2 N$, the conditions are usually phrased as

$$N \rightarrow \infty, \quad \lambda \gg 1, \quad (3.2)$$

i.e., the so-called large- N limit and the limit of large but fixed 't Hooft coupling. This fits together nicely with the observation regarding planar diagrams in the large N limit and string theory discussed in the previous section. Furthermore, $\lambda \gg 1$ is important because at large N , λ is the effective coupling of the gauge theory and as such, the latter is strongly coupled, which implies that perturbation theory is not applicable. However, the gravity part of this so-called duality is weakly coupled. This has important implications, as it opens up the possibility of mapping a problem that is hard to solve on the gauge theory side due to strong coupling to the weakly coupled gravity side, and solve it there. This is the general idea the work described in the later chapters of this thesis relies upon.

One interesting check of consistency for the duality worth mentioning at this point is the fact that the R-symmetry group of the gauge group $SU(4) \simeq SO(6)$ corresponds to isometries of the S^5 part of the geometry. This is a manifestation of the principle that global symmetries on the field theory side correspond to gauge symmetries on the gravity

side.

So what does it mean for two theories to be related by duality? It means that no matter how different the degrees of freedom of the theories are, they have to lead to the same results for all physical observables. To be precise, the most general statement of the AdS/CFT correspondence is usually expressed in terms of the string partition function and expectation values. The formulation commonly used is the following [41, 42, 43]:

$$\langle \exp \left[\int d^4x \Phi_0(\vec{x}) \mathcal{O}(\vec{x}) \right] \rangle_{\text{CFT}} = \mathcal{Z}_{\text{string}} [\Phi(\vec{x}, z)|_{z=0} = \Phi_0(\vec{x})]. \quad (3.3)$$

On the left hand side we have a field theory quantity, namely the generating functional of correlation functions. The latter are computed by taking functional derivatives with respect to Φ_0 and evaluating the result at $\Phi_0 = 0$. On the right hand side we have the string partition function that depends on the dilaton field Φ , whose boundary conditions are chosen such that it agrees with the field Φ_0 on the boundary where the field theory "lives" (in terms of the coordinate z , the boundary being at $z = 0$). The field Φ on the right hand side is the dilaton, whose expectation value determines the string coupling, and its boundary value, Φ_0 , couples to the field theory operator \mathcal{O} . This equation is taken to be equivalent to a correspondence between the operator \mathcal{O} and the field Φ , and according to the statement of the correspondence, an analogous formula holds for any field arising on the gravity side. The importance of this cannot be understated: the partition function contains the full physical information of the string theory, just as correlation functions of operators make up all observables of a quantum field theory. If this formula is true, which has not been proven rigorously, all physical observables can be computed either in one framework or the other.

While Maldacena's example was the first, many other instances of gauge/gravity duality were discovered later. The physical systems one may study with this technology are manifold, ranging from condensed matter systems to gauge theories that are similar, albeit not identical, to quantum chromodynamics. One example of the latter is the subject of study of this thesis. It is important to note that gauge/gravity duality exists for certain non-conformal and non-supersymmetric theories. For an introduction to the topic of gauge/duality that features a number of applications, see [44].

gauge theory	gravity dual
degree N of the gauge group	number of branes, curvature radius
flat space time on which the gauge theory lives	boundary of higher-dimensional geometry
global symmetry	gauge symmetry
gauge invariant operators	fields acting as sources to these operators
particle mass	eigenvalue in wave equation
energy scale	radial coordinate in the AdS -space
renormalisation group flow	movement along the radial coordinate

Table 3.1: Map of concepts in gauge/gravity duality.

Finally, we present a table (3.1) that shows how concepts from the gauge theory side are mapped to the gravity dual. These are very general, and hold beyond the original example of the AdS/CFT correspondence discussed above.

Let us finish by commenting on these identifications. 1.) The degree N of the gauge group, e.g. $SU(N)$ in the standard example, arises from the number of branes in the stack that generates the physical system. Only when it is large, i.e., the number of branes is high, we are able to obtain sufficiently small curvature such that the supergravity limit is applicable. 2.) From the point of view of the gravity solution, the field theory lives on its boundary at infinity with respect to the so-called holographic coordinate that is part of the AdS space. Depending on the precise solution, this boundary is not necessarily four-dimensional. 3.) Gauge fields on the gravity side couple to Noether currents associated with global symmetries at infinity, which are realised as symmetries on the field theory side. 4.) Gauge invariant operators couple to classical fields on the gravity side, i.e., the latter act as sources to the former. This principle is reflected in Eq. (3.3). 5.) Consequently, the mass of physical states associated with these operators may be extracted by solving classical wave equations for the fields on the gravity side. To be precise, the mass appears as an eigenvalue in said equations. 6.) Another feature related to the above is the fact that the energy scale of the theory at hand is identified with the distance along the holographic coordinate. This identification can be understood intuitively from the relation of the energy of a wave and its wavelength. 7.) Furthermore, movement along

this coordinate corresponds to the renormalisation group flow of the gauge theory.

3.3 ◆ **BOTTOM-UP VS. TOP-DOWN HOLOGRAPHY**

There is one question that immediately arises: how can one discover new instances of gauge/gravity duality? How do we know if a given gauge theory has a gravity counterpart, and if it does, how do we know what it looks like? There are two approaches to this problem. One is to assume that AdS/CFT correspondence holds and to write down the interactions of classical fields in an appropriate AdS background by hand, modelling the gravity system in such a way that the desired properties of the boundary theory may be captured. Possible choices include the field content, the symmetries, whether the theory is confining or not, as well as the incorporation of finite temperature. This philosophy is known as the *bottom-up* approach to holography. The freedom in the choice of interactions allows for a great amount of flexibility in modelling various phenomena. One downside is the fact that this freedom often comes with a large number of free parameters that have to be fixed by fitting the model to physical observables. This may severely limit the predictivity of such an approach, and can be compared to the situation in phenomenological field theories for the interactions of hadrons at low energy.

In this thesis we will consider a different approach that offers comparatively little freedom, and as a consequence comes only with a small number of parameters one has to fit in order for the model to become predictive. This happens precisely when the AdS geometry, and all the fields living in it, are actually solutions to string theory, as in the case of Maldacena's original example discussed in the previous section. As a consequence, interactions are completely fixed by the low energy effective action of string theory, and one speaks about *top-down* holography. It is convenient that one does not have to deal with the full machinery of string theory, but with its low-energy approximation in the form of supergravity. Supergravity in eleven and ten dimensions is well known, and the relative simplicity of the corresponding Lagrangians, which we have presented in the previous chapter, allows for their straightforward application to holographic computations. Another advantage is that the field theory side can be deduced directly from the low energy world

volume theory on stacks of branes. However, the downside is that it can happen that gravity solutions dual to a field theory of interest are not known or do not exist. In that case, one might have to settle for duals of theories that are not identical, but as closely related as possible to the theory in question. This is the case for the work presented in this thesis, where the goal is to describe the phenomenology of quantum chromodynamics, a theory for which a gravity dual is currently not accessible.

4 A DUAL OF PURE YANG-MILLS THEORY

“Luminous beings are we, not this crude matter.”

Yoda

4.1 WITTEN'S CONSTRUCTION

The $\text{AdS}_5 \times S^5$ geometry introduced as a dual of the large- N limit of $\mathcal{N} = 4$ super Yang-Mills theory describes a deconfined plasma of gluons and their supersymmetric partners. It has been studied thoroughly in an attempt to learn about universal properties of deconfined matter that might hold also for a realistic quark-gluon plasma as produced in relativistic heavy ion collisions. The phenomenology of hadrons remains out of reach for this model, as it would require a confining theory as a starting point. However, shortly after the discovery of the AdS/CFT correspondence, Witten introduced a version of the duality in which the field theory side exhibits confinement [31].

Starting with the $\text{AdS}_5 \times S^5$ geometry, a confining theory is obtained by compactifying one of the directions of the boundary theory on a circle. This introduces a mass scale and confining behaviour of Wilson loops. As a consequence, the boundary theory lives on an $\mathbb{R}^{2,1} \times S^1$ background, and the theory is effectively three-dimensional below the compactification scale. While this has its own merit and is certainly worth studying, in order to obtain a theory that is closer towards the goal of finding a dual of four-dimensional quantum chromodynamics, we need a geometry that admits a four-dimensional dual, at least below a certain energy scale.

The solution is to realise that there exists an $\text{AdS}_7 \times \text{S}^4$ solution to eleven-dimensional supergravity. It arises as the near horizon limit of a stack of M5-branes, or equivalently in the ten-dimensional type IIA picture from a stack of N_c D4-branes. Confinement may be introduced by a version of this solution compactified on a circle with periodicity $2\pi/M_{\text{KK}}$, where M_{KK} is the corresponding Kaluza-Klein mass, and the line element is given by

$$ds^2 = \frac{r^2}{L^2} (f(r)dx_4^2 + \eta_{\mu\nu}dx^\mu dx^\nu + dx_{11}^2) + \frac{L^2}{r^2} \frac{dr^2}{f(r)} + \frac{L^2}{4} d\Omega_4^2, \quad (4.1)$$

with $f(r) = 1 - r_{\text{KK}}^6/r^6$, where L is the AdS-radius, $r \in [r_{\text{KK}}, \infty)$ is the holographic coordinate bounded from below by $r_{\text{KK}} = M_{\text{KK}}L^2/3$, and $d\Omega_4^2$ is the line element of a unit four-sphere. Greek indices indicate 4d Minkowski space and run from 0 to 3, while x_4 is the aforementioned compactified direction. The x_{11} -direction may be compactified in order to reduce to string theory, with periodicity $2\pi g_s l_s$, where g_s and l_s are string coupling and length, respectively. This direction is then absent in the dual type IIA string theory picture, where the corresponding line element in the string-frame is obtained from Eq. (2.8).

The function $f(r)$ guarantees that the geometry, which may be thought of as an Euclidean black hole, ends at $r = r_{\text{KK}}$. Going down from infinity, the precise form of $f(r)$ contracts the circle from its maximal size at infinity to zero at the horizon. The resulting shape of the (x_4, r) subspace is shown in Fig. 4.1.

In order for this geometry to be a stable solution, it needs to be supported by a non-vanishing Ramond-Ramond four-form flux given by

$$\int_{\text{S}^4} F_4 = N_c \frac{\kappa_{10}}{\sqrt{\alpha' \pi}}, \quad (4.2)$$

which fixes F_4 to be proportional to the volume form of the S^4 .

The field theory dual to supergravity in this background is intrinsically five-dimensional. However, physical observables are not affected by the extra-dimension below the compactification scale M_{KK} , and the dynamics are effectively four-dimensional.

The parameters L , g_s , l_s , and M_{KK} of the gravity solution are related to the four-dimensional gauge-theory parameters g_{YM} and N_c by

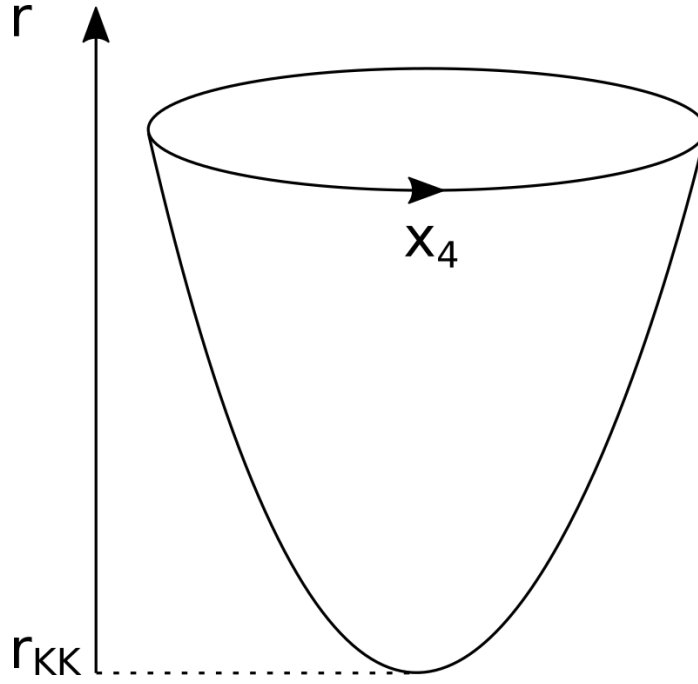


Figure 4.1: Visual representation of the (x_4, r) subspace of the geometry described by the line element in Eq. (4.1).

$$g_{\text{YM}}^2 = 2\pi g_s l_s M_{\text{KK}}, \quad N_c = \frac{L^3}{8\pi g_s l_s^3}. \quad (4.3)$$

Let us briefly check the limit of validity of the above solution, using the criteria presented in section 2.2. The condition that the radius L should be much larger than the string length l_s leads to

$$\frac{L^3}{l_s^3} = 8\pi g_s N_c \gg 1. \quad (4.4)$$

But $g_s N_c$ can also be written as

$$g_s N_c = \frac{g_{\text{YM}}^2 N_c}{2\pi l_s M_{\text{KK}}}, \quad (4.5)$$

which implies $\lambda \equiv g_{\text{YM}}^2 N_c \gg 1$. Finally, because the requirement of small quantum string corrections corresponds to $g_s \rightarrow 0$, the finite value of $8\pi g_s N_c$ leads to $N_c \rightarrow \infty$.

Thus we are dealing with a strongly coupled field theory in the large- N_c limit. Beyond this, Wilson loops display area-law behaviour, indicating confinement of all degrees of

freedom, i.e., the circumstance that all particles are singlets with respect to the gauge group $U(N_c)$.

Let us discuss the other symmetries of the field theory. The latter naturally inherits the space-time isometries of the compactified AdS_7 space at infinity, which are translated into the Poincaré group of the field theory. Furthermore, there is the isometry group of the S^4 , $SO(5)$. This translates into the R-symmetry group of the field theory, $Sp(2) \simeq SO(5)$, which corresponds to $\mathcal{N} = 2$ in five dimensions. We are consequently dealing with $\mathcal{N} = 2$ supersymmetric Yang-Mills theory. There is a subtlety to this: supersymmetry is only preserved as long as we impose periodic boundary conditions on gauginos (fermions in the $\mathcal{N} = 2$ vector multiplet) along the x_4 -circle. We may therefore choose to break supersymmetry by imposing antiperiodic boundary conditions on gauginos, which subsequently become massive. This is the method Witten has used to construct a holographic dual of nonsupersymmetric Yang Mills theory. Compactification turns the x_4 -component of the gauge field into an adjoint scalar that obtains mass from one-loop corrections, as a mass term is no longer protected by supersymmetry, and what remains is a massless four-dimensional gauge field in the adjoint representation of the gauge group $U(N_c)$. The spectrum is effectively the same as that of an $SU(N_c)$ theory, as the $U(1)$ part of $U(N_c)$ is infrared free and hence decoupled at low energies. As the theory is confining, the degrees of freedom are, apart from the aforementioned adjoint scalar, glueballs, and the holographic construction allows for the determination of their spectrum, as we will see in the following section.

4.2 ◆ THE SPECTRUM OF GLUEBALLS

The spectrum of glueballs of the theory discussed in the previous section has been studied extensively in the literature. The first correct and comprehensive study that captured all physically interesting fluctuations was performed by Brower, Mathur, and Tan [51]. In the following we will recapitulate the main aspects of their considerations, and elaborate on a few points in more detail.

The spectrum of fluctuations in eleven-dimensional supergravity is obtained by solving

the linearised equations of motion derived from Eq. (2.5). There are two categories of fluctuations: those of the metric, given by the substitution

$$g_{MN} \rightarrow g_{MN} + \delta g_{MN}, \quad (4.6)$$

as well as fluctuations of the three-form field:

$$A_3 \rightarrow A_3 + \delta A_3. \quad (4.7)$$

Let us begin by studying fluctuations of the metric, and for this purpose define $h_{MN} \equiv \delta g_{MN}$. The linearised equations of motion are then given by

$$-\frac{1}{2}\nabla_\sigma\nabla^\sigma h_{\mu\nu} - \frac{1}{2}\nabla_\mu\nabla_\nu h_\sigma{}^\sigma + \frac{1}{2}\nabla^\sigma\nabla_\nu h_{\mu\sigma} + \frac{1}{2}\nabla^\sigma\nabla_\mu h_{\nu\sigma} + \frac{4}{L^2}h_{\mu\nu} = 0, \quad (4.8)$$

where ∇_μ denotes the covariant derivative with respect to the background metric. Solutions to these equations in the rest frame, are generically of the form

$$h_{MN} = \epsilon_{MN}(r)e^{ik_0x_0}, \quad (4.9)$$

where $\epsilon_{MN}(r)$ encodes both the traceless polarisation tensor and the dependence of the modes on the holographic coordinate r , and the discrete mass parameter will be realised through $k_0 = im$. For the purpose of determining the spin content, we will fix the gauge as $h_{0N} = 0$. In flat space, we may also choose $h_{rN} = 0$. In AdS_7 space time, this is strictly only valid at $r \rightarrow \infty$, but we can work with this choice as long as we are simply interested in determining the spin content.

These fluctuations are decomposed into distinct independent solutions that fall into different representations of the isometries (the little group) of the compactified $\text{AdS}_7 \times \text{S}^4$ geometry. At r tending to infinity, the little group of four-dimensional flat space in the x_1, x_2, x_3 and x_{11} directions is given by the group of four-dimensional rotations, namely $\text{SO}(4)$. Independent solutions therefore correspond to irreducible representations of this group. We are therefore left to determine 14 independent components of the polarisation tensor. Under $\text{SO}(4)$, we obtain a 9-dimensional, a 4-dimensional, and a one-dimensional

representation. These may again be decomposed into distinct spins under $SO(3)$, the group of three-dimensional rotations in x_1 , x_2 and x_3 , as follows:

The nine-dimensional representation splits into a five-dimensional spin-2 representation with

$$h_{ij} - \frac{1}{3}\delta_{ij}h_{kk} \neq 0, \quad (4.10)$$

a three-dimensional spin-1 representation with

$$h_{i,11} = h_{11,i} \neq 0, \quad (4.11)$$

and a one-dimensional spin-0 representation with

$$h_{11,11} = -3h_{11} = -3h_{22} = -3h_{33} \neq 0. \quad (4.12)$$

The four-dimensional representation splits into a three-dimensional spin-1 representation with

$$h_{\tau i} = h_{i\tau} \neq 0, \quad (4.13)$$

and a one-dimensional spin-0 representation with

$$h_{\tau,11} = h_{0\tau} \neq 0. \quad (4.14)$$

Finally, there is the one-dimensional spin-0 representation with

$$h_{\tau\tau} = -4h_{11} = -4h_{22} = -4h_{33} = -4h_{11,11} \neq 0. \quad (4.15)$$

In addition to these states, which all arise from the AdS_7 part of the geometry, there is a scalar fluctuation of the S^4 part that does not break the $SO(5)$ symmetry of the space.

Let us now consider fluctuations of the three-form field. Physical solutions may be obtained by looking for solutions whose nonzero components carry indices other than those corresponding to the coordinates x_0 and r . Decomposing again under $SO(4)$ we obtain a four-dimensional and a six-dimensional irreducible representation. These may be separated into representations of $SO(3)$ as follows:

The four-dimensional representation splits into a three-dimensional spin-1 representation with

$$A_{ij,11} \neq 0, \quad (4.16)$$

and a one-dimensional spin-0 representation with

$$A_{ijk} \neq 0. \quad (4.17)$$

The six-dimensional representation splits into a three-dimensional spin-1 representation with

$$A_{i\tau,11} \neq 0, \quad (4.18)$$

and another three-dimensional spin-1 representation with

$$A_{ij\tau} \neq 0. \quad (4.19)$$

In total, there are five distinct representations of $SO(4)$ (three for the AdS_7 metric and two for the three-form field), and one scalar from fluctuations of the S^4 metric. This means that we can expect six distinct towers of values for the mass of the fluctuations. States corresponding to distinct representations of $SO(3)$, but to the same representation of $SO(4)$, are degenerate in mass. The spectrum is correspondingly determined by six distinct eigenvalue equations, which also fix the dependence of the fluctuations on the radial coordinate r . The equations are given, in the notation of [51] and in units of $L = 1$ and $r_{KK} = 1$, by

$$\frac{d}{dr}(r^7 - r) \frac{d}{dr} T_4(r) + m^2 r^3 T_4(r) = 0, \quad (4.20)$$

$$\frac{d}{dr}(r^7 - r) \frac{d}{dr} V_4(r) + \left[m^2 r^3 - \frac{9}{r(r^6 - 1)} \right] V_4(r) = 0, \quad (4.21)$$

$$\frac{d}{dr}(r^7 - r) \frac{d}{dr} S_4(r) + \left[m^2 r^3 + \frac{432r^5}{(5r^6 - 2)^2} \right] S_4(r) = 0, \quad (4.22)$$

mode	S_4	T_4	V_4	N_4	M_4	L_4
J^{PC}	0^{++}	$0^{++}/2^{++}$	0^{-+}	1^{+-}	1^{--}	0^{++}
$n=0$	7.30835	22.0966	31.9853	53.3758	83.0449	115.002
$n=1$	46.9855	55.5833	72.4793	109.446	143.581	189.632
$n=2$	94.4816	102.452	126.144	177.231	217.397	277.283
$n=3$	154.963	162.699	193.133	257.959	304.531	378.099
$n=4$	228.709	236.328	273.482	351.895	405.011	492.171

Table 4.1: The mass spectrum of glueballs obtained from numerically solving Eqs. (4.20)-(4.25). Results are given for $L = 1$ and $r_{\text{KK}} = 1$, i.e., m^2 is shown in units of $M_{\text{KK}}^2/9$ of

$$\frac{d}{dr}(r^7 - r) \frac{d}{dr} N_4(r) + \left[m^2 r^3 - 27r^5 + \frac{9}{r} \right] N_4(r) = 0, \quad (4.23)$$

$$\frac{d}{dr}(r^7 - r) \frac{d}{dr} M_4(r) + \left[m^2 r^3 - 27r^5 - \frac{9r^5}{r^6 - 1} \right] M_4(r) = 0, \quad (4.24)$$

and

$$\frac{d}{dr}(r^7 - r) \frac{d}{dr} L_4(r) + [m^2 r^3 - 72r^5] L_4(r) = 0. \quad (4.25)$$

Note that because the $h_{rN} = 0$ gauge may not be used in AdS_7 space, the equations were determined by making use of the full form of the modes as given in the next section.. They may be solved by imposing the boundary conditions

$$\frac{d}{dr} H(r)|_{r=1} = 0, \quad H(r=1) \neq 0, \quad \lim_{r \rightarrow \infty} H(r) = 0, \quad (4.26)$$

where $H(r)$ represents any of the solutions to Eqs. (4.20)-(4.25). Other boundary conditions are possible; however, they are only relevant for finding solutions corresponding to modes transforming nontrivially under τ -parity, an operation we will explain shortly. Solutions are normalised by requiring that the supergravity actions lead to a canonical four-dimensional kinetic term after integrating over all extra dimensions. We will quote

the results of this normalisation procedure towards the end of this section, along with the explicit form of all relevant fluctuations.

The eigenvalue spectrum obtained from solving these equations is given in Table 4.1. Note that we have also shown spin, parity and charge conjugation quantum numbers J^{PC} associated with the modes. These are determined by dimensionally reducing the fluctuations to type IIA string theory inserting them into the D4-brane effective action, and observing which operators they are coupled to. The behaviour of the operator under the transformations then determines the quantum numbers. Since the theory is five-dimensional, a clarification on quantum numbers is in order:

As the fifth dimension is compactified, we define parity to act on the components of the gauge field through a reflection of the *three* spatial coordinates x_i for $i \in \{1, 2, 3\}$:

$$\begin{aligned} P &: A_0(x_0, x_i, \tau) \rightarrow A_0(x_0, -x_i, \tau) \\ P &: A_i(x_0, x_i, \tau) \rightarrow -A_i(x_0, -x_i, \tau) \\ P &: A_\tau(x_0, x_i, \tau) \rightarrow A_\tau(x_0, -x_i, \tau). \end{aligned} \quad (4.27)$$

For the compact direction, we refer to the reversal of orientation of the circle as τ -parity, and define its action on the gauge field as

$$\begin{aligned} P_\tau &: A_0(x_0, x_i, \tau) \rightarrow A_0(x_0, x_i, -\tau) \\ P_\tau &: A_i(x_0, x_i, \tau) \rightarrow A_i(x_0, x_i, -\tau) \\ P_\tau &: A_\tau(x_0, x_i, \tau) \rightarrow -A_\tau(x_0, x_i, -\tau). \end{aligned} \quad (4.28)$$

As we will see in Section 5, τ -parity is modified for fermionic degrees of freedom. Glueball states transforming odd under P_τ will not be considered, as this transformation plays no role in four-dimensional QCD, which we are comparing with. Charge conjugation is defined as usual.

4.3 ◆ EXPLICIT FORM OF THE SOLUTIONS

Let us now write out explicitly all glueball fluctuations that will be studied in this thesis. The lightest glueball and its excitations correspond to a scalar mode, whose eigenvalues are shown in the first column in Table 4.1. The solution was derived for the first time in [52], and is given by

$$\begin{aligned}
h_{\tau\tau} &= -\frac{r^2}{L^2} f(r) H_E(r) G_E(x) \\
h_{\mu\nu} &= \frac{r^2}{L^2} H_E(r) \left[\frac{1}{4} \eta_{\mu\nu} - \left(\frac{1}{4} + \frac{3r_{\text{KK}}^6}{5r^6 - 2r_{\text{KK}}^6} \right) \frac{\partial_\mu \partial_\nu}{M_E^2} \right] G_E(x) \\
h_{11,11} &= \frac{r^2}{L^2} \frac{1}{4} H_E(r) G_E(x) \\
h_{rr} &= -\frac{L^2}{r^2} f(r)^{-1} \frac{3r_{\text{KK}}^6}{5r^6 - 2r_{\text{KK}}^6} H_E(r) G_E(x) \\
h_{r\mu} &= \frac{90r^7 r_{\text{KK}}^6}{M_E^2 L^2 (5r^6 - 2r_{\text{KK}}^6)^2} H_E(r) \partial_\mu G_E(x), \tag{4.29}
\end{aligned}$$

where $H_E(r) \equiv S_4(r)$ and $x \equiv x^\mu$, denoting four-dimensional flat space-time. The normalisation constant is obtained from inserting these fluctuations into the supergravity action, which after integrating over the S^4 -part is given by

$$S = \frac{1}{2\kappa_{11}^2} (L/2)^4 \Omega_4 \int d^7x \sqrt{-\det G} \left(R(G) + \frac{30}{L^2} \right), \tag{4.30}$$

with $\Omega_4 = 8\pi^2/3$.

Inserting the metric fluctuations into this 7-dimensional Einstein-Hilbert action with negative cosmological constant leads to

$$\begin{aligned}
& \int d^7x \sqrt{-\det G} \left(R(G) + \frac{30}{L^2} \right) \Big|_{H_G^2} \\
&= -\mathcal{C}_E \int dx^{11} d^4x d\tau \frac{1}{2} [(\partial_\mu G_E)^2 + M_E^2 G_E^2], \tag{4.31}
\end{aligned}$$

with

$$\mathcal{C}_E = \int_{r_{\text{KK}}}^{\infty} \frac{dr r^3}{L^3} \frac{5}{8} H_E(r)^2. \tag{4.32}$$

For the lowest mode $H_E(r)$ we obtain

$$\mathcal{C}_E = 0.057395 [H_E(r_{\text{KK}})]^2 \frac{r_{\text{KK}}^4}{L^3}, \quad (4.33)$$

which deviates from the result given in Ref. [53] by a factor $\frac{1}{2}$ that is missing in (2.19) of [53]. Canonical normalisation of the scalar field $G(x)$ after integrating over x^4 and x^{11} implies

$$\begin{aligned} [H_E(r_{\text{KK}})]^{-1} &= \frac{1}{\sqrt{2}} 0.0097839 \lambda^{1/2} N_c M_{\text{KK}} \\ &= 0.0069183 \lambda^{1/2} N_c M_{\text{KK}}, \end{aligned} \quad (4.34)$$

which differs from [53] by the explicitly written factor $1/\sqrt{2}$.

Let us now consider the fluctuations corresponding to the tensor multiplet, containing a degenerate scalar and tensor mode, denoted by T_4 in 4.1. The explicit form of the fluctuations for the scalar is given by

$$\begin{aligned} h_{11,11} &= -3 \frac{r^2}{L^2} H_D(r) G_D(x), \\ h_{\mu\nu} &= \frac{r^2}{L^2} H_D(r) \left[\eta_{\mu\nu} - \frac{\partial_\mu \partial_\nu}{\square} \right] G_D(x), \end{aligned} \quad (4.35)$$

with $H_D(r) \equiv T_4(r)$, while the nonvanishing components of the tensor fluctuations may be written as

$$h_{11} = -h_{22} = -\frac{r^2}{L^2} H_T(r) G_T(x), \quad (4.36)$$

with $H_T(r) = H_D(r)$. As both modes obey the same eigenvalue equation, we have $M_D = M_T$.

Applying the normalisation condition in analogy to the previous case leads to

$$\begin{aligned} &\int d^7x \sqrt{-\det G} \left(R(G) + \frac{30}{L^2} \right) \Big|_{H_G^2} \\ &= -\mathcal{C}_{D,T} \int dx^{11} d^4x d\tau \frac{1}{2} [(\partial_\mu G_{D,T})^2 + M_{D,T}^2 G_{D,T}^2], \end{aligned} \quad (4.37)$$

with

$$\mathcal{C}_D = 6 \int_{r_{\text{KK}}}^{\infty} \frac{dr r^3}{L^3} H_D(r)^2 \quad (4.38)$$

and

$$\mathcal{C}_T = \int_{r_{\text{KK}}}^{\infty} \frac{dr r^3}{L^3} H_T(r)^2. \quad (4.39)$$

For the lowest eigenmode $H_T(r)$ we obtain

$$\mathcal{C}_T = 0.22547 [H_T(r_{\text{KK}})]^2 \frac{r_{\text{KK}}^4}{L^3}, \quad (4.40)$$

as well as $\mathcal{C}_D = 6\mathcal{C}_T$. This leads to

$$[H_D(r_{\text{KK}})]^{-1} = 0.033588 \lambda^{1/2} N_c M_{\text{KK}} \quad (4.41)$$

and

$$[H_T(r_{\text{KK}})]^{-1} = 0.013712 \lambda^{1/2} N_c M_{\text{KK}}. \quad (4.42)$$

Next, we consider the pseudoscalar glueball with $H_P(r) \equiv V_4(r)$, corresponding to the masses in the third column of Table 4.1. Apart from a nonvanishing 0τ -component of the metric fluctuation that does not enter any relevant equations, this mode reduces to a fluctuation of the Ramond-Ramond field of type IIA string theory, which we denote by $C = C_\tau d\tau$, and hence write

$$C_\tau = H_P(r) G_P(x). \quad (4.43)$$

It is therefore convenient to work in the ten-dimensional framework in order to obtain the normalisation constant. From the Ramond-Ramond action of Eq. 2.14 we get

$$[H_P(r_{\text{KK}})]^{-1} = 0.002046 \lambda^{3/2} \quad (4.44)$$

for the lightest mode, and

$$[H_P(r_{\text{KK}})]^{-1} = 0.001157 \lambda^{3/2} \quad (4.45)$$

for the first excitation.

Finally, we consider the pseudovector glueball with $H_V(r) \equiv N_4(r)$. We will again adopt a ten-dimensional perspective in which the fluctuations of the glueball are given in terms of components of the Kalb-Ramond field as

$$B_{\mu\nu} = A_{\mu\nu 11} = r^3 N_4(r) \tilde{B}_{\mu\nu}(x), \quad (4.46)$$

and

$$A_{\rho 4r} = 6r^2 N_4(r) \epsilon^{\alpha\beta\gamma\delta} \eta_{\rho\alpha} \frac{\partial_\beta}{\square} \tilde{B}_{\gamma\delta}, \quad (4.47)$$

with $\eta^{\rho\mu} \partial_\rho \tilde{B}_{\mu\nu} = 0$, with the transverse polarisation parametrised as

$$\tilde{B}_{\mu\nu} = \frac{1}{\sqrt{\square}} \eta^{\lambda\rho} \eta^{\kappa\sigma} \epsilon_{\mu\nu\lambda\kappa} \epsilon_\rho \partial_\sigma \tilde{V}^{(\epsilon)}(x), \quad (4.48)$$

ϵ_ρ being a spacelike unit vector. The normalisation is chosen in such a way that the hermitean field $\tilde{V}^{(\epsilon)}(x)$ is canonically normalized, i.e.,

$$\begin{aligned} \mathcal{L}_{\tilde{B}} &= -\frac{1}{4} \eta^{\rho\mu} \eta^{\sigma\nu} \tilde{B}_{\mu\nu} (M^2 - \square) \tilde{B}_{\rho\sigma} + \dots \\ &= \mathcal{L}_{\tilde{V}} = -\frac{1}{2} \tilde{V}^{(\epsilon)} (M^2 - \square) \tilde{V}^{(\epsilon)} + \dots, \end{aligned} \quad (4.49)$$

which implies

$$C_B = R_{11} R_4 L^7 \frac{\pi^4}{3\kappa_{11}^2} \int dr r^3 H_V(r)^2 = 1. \quad (4.50)$$

For the normalisation constant of the lightest mode this leads to

$$[H_V(r_{\text{KK}})]^{-1} = 0.009838 L^3 \lambda^{1/2} N_c M_{\text{KK}}. \quad (4.51)$$

4.4 ◆ DUAL OPERATORS

Before comparing the spectrum with results from the lattice, let us write down the operators on the field theory side to which the scalar glueballs are dual. We will do this explicitly for the dilatonic glueball, and follow the approach presented in [54]. Consider the DBI-action for a stack of N_c D4-branes,

$$S_{\text{DBI,D4}} = -T_4 \int d^5x e^{-\Phi} \text{Tr} \sqrt{g_{MN} + 2\pi\alpha' F_{MN}}, \quad (4.52)$$

and insert the dimensional reduction of the dilatonic mode (4.35) according to (2.8) in the presence of nonvanishing F_{MN} . Expanding to linear order in the dilatonic fluctuation leads to

$$S_{\text{DBI,D4}} \propto \int d^4x G_D(x) \mathcal{O}^D, \quad (4.53)$$

with

$$\mathcal{O}^D = +\frac{3}{8} F_{\mu\nu} F^{\mu\nu} - \frac{1}{2} T_{00}^{\text{YM}} + F_{\tau\mu} F_{\tau}^{\mu} - \frac{1}{2} F_{\tau 0}^2 + \dots, \quad (4.54)$$

where the energy-momentum tensor of Yang-Mills theory is given by

$$T_{\text{YM}}^{\mu\nu} = F^{\mu\rho} F^{\nu}_{\rho} - \frac{1}{4} \eta^{\mu\nu} F_{\rho\sigma} F^{\rho\sigma}. \quad (4.55)$$

Repeating the calculation for the exotic mode of (4.29) leads to

$$\mathcal{O}^E = -\frac{5}{8} F_{\mu\nu} F^{\mu\nu} - \frac{1}{2} T_{00}^{\text{YM}} + F_{\tau\mu} F_{\tau}^{\mu} - \frac{1}{2} F_{\tau 0}^2 + \dots \quad (4.56)$$

Dots denote couplings to adjoint scalars due to the presence of the circle. Discarding components corresponding to this compactified dimension, it is noteworthy that there is a nonvanishing coupling to the 00-component of the nonabelian energy-momentum tensor, T_{00}^{YM} . Furthermore, we see that the standard operator $F_{\mu\nu} F^{\mu\nu}$ commonly associated with the dilaton in Yang-Mills theory is only obtained from the difference $\mathcal{O}^D - \mathcal{O}^E$, which unfortunately does not correspond to a distinct linearised gravity solution. A fluctuation

of the string theory dilaton Φ alone would also produce the required term, but once again this does not correspond to the solution of any mode equation.

4.5 ◆ COMPARISON WITH LATTICE RESULTS

Let us conclude this section by stating that the spectrum of glueballs as described above seems to match quite well the results from lattice simulations, after adjusting the mass scale such that the values for the tensor glueballs matched exactly [51]. We show this in Fig. 4.2, plots are taken from [5] and [51]. In both cases we have a low-lying scalar glueball, followed by a scalar, a tensor, and a pseudoscalar in relative proximity to each other. However, there are qualitative differences: the two lowest scalar glueballs in the holographic result do not arise from the same wave equation, as they correspond to the dilatonic and the exotic mode. It is not clear how this would translate into the lattice approach. Furthermore, in the holographic case, the second-lightest scalar and the lightest tensor are exactly degenerate. This is not the case on the lattice side. Finally, we see that in the lattice plot there are states not present in the supergravity result. This concerns both states with other quantum numbers, as well as states with spin larger than 2. The latter can be explained by the fact that the holographic result is obtained in classical gravity which by definition is limited to spins less or equal to 2. One would have to take into account string modes to obtain higher spin states.

Unfortunately, we will see in the next chapter that this picture of reasonable agreement is shattered once flavour degrees of freedom are introduced, and the mass scale is fixed by experimental data.

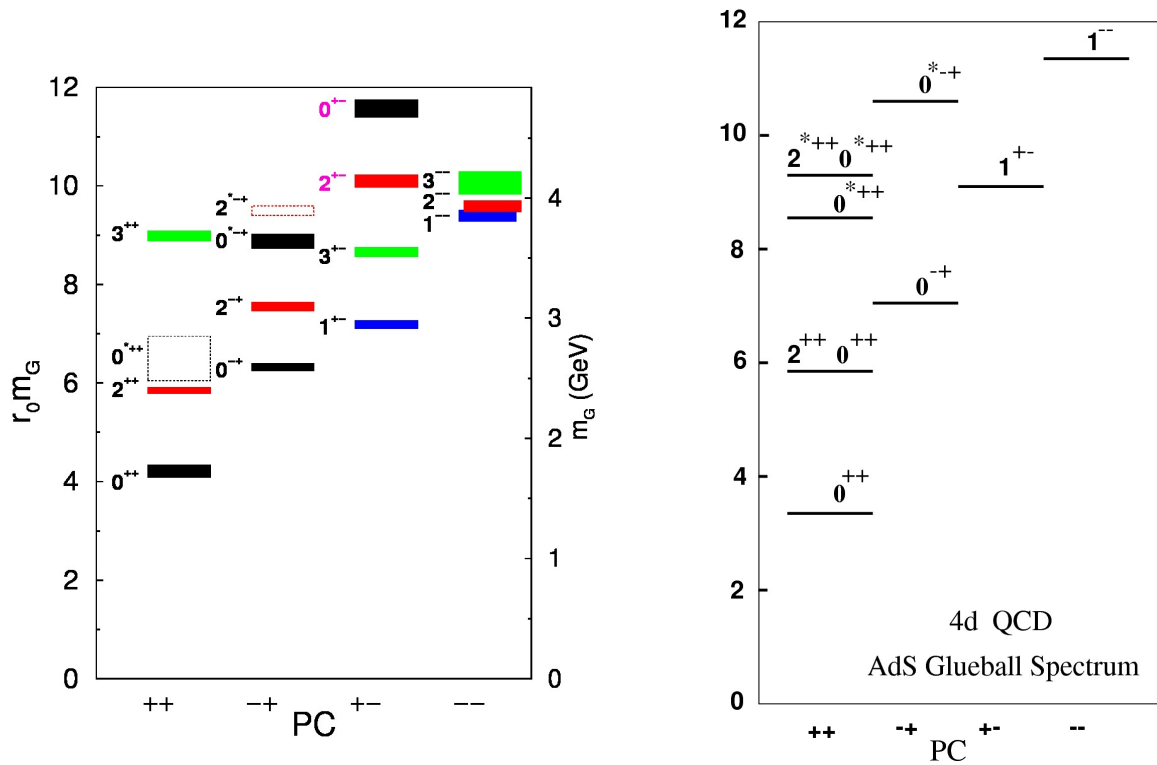


Figure 4.2: Comparison of the spectrum of glueballs on the lattice and from the supergravity calculation as presented by Brower, Mathur, and Tan [51]. The mass scale in the latter is chosen such that the mass of the tensor glueball matches the lattice result.

5 THE SAKAI-SUGIMOTO MODEL

“Don’t be too proud of this technological terror you’ve constructed.”

Dar t h Vader

5.1 INTRODUCING FLAVOUR BRANES

Experimental evidence supports the notion that we do not live in a world of glue, but that we rather must include degrees of freedom known as quarks, if we want to obtain a coherent description of a host of phenomena [6]. This also holds true in the holographic picture: we have to go beyond Witten’s model that has been described in the previous section, and modify it in such a way that it corresponds to description dual to a theory of quarks and gluons.

A successful approach to this problem is due to Sakai and Sugimoto [30], who have supplemented the stack of N_c D4-branes corresponding to Witten’s model by a stack of N_f D8- and anti-D8-branes embedded in a particular way within the cigar-shaped geometry, N_f being the number of quark flavours. As shown in Fig. 5.1, D8 and anti-D8-branes merge at the tip of the cigar for antipodal embedding (i.e., when the stacks of branes are placed at an angle of π away from each other on the circle at infinity). The flavour branes are taken to be in the probe-limit $N_f \ll N_c$, avoiding backreactions on the background geometry. Strings with one endpoint each on a D4-brane and a D8-brane correspond to quarks, and those with one on a D4-brane and one on a anti-D8-brane to anti-quarks. As a consequence, pairs of stacks then may lead to the formation of mesons, bound states of quarks and anti-quarks.

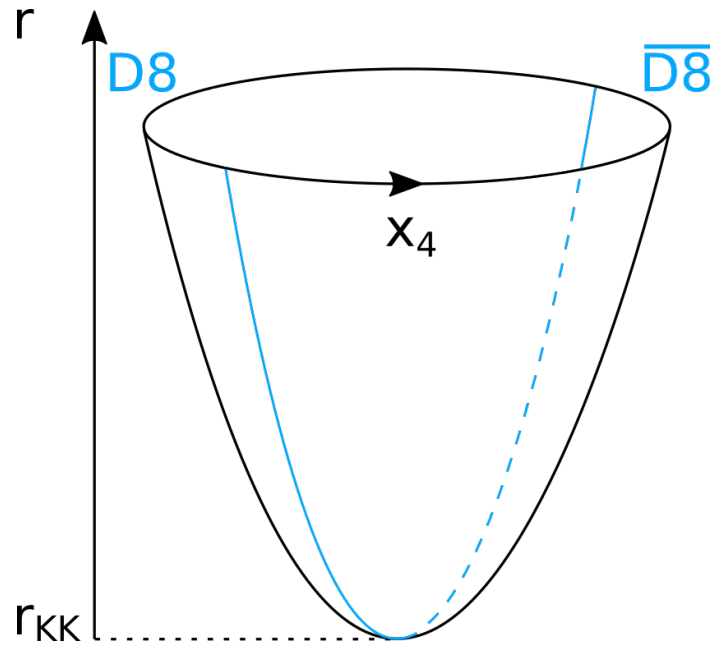


Figure 5.1: Visual representation of D8- and anti-D8-branes, represented by blue lines, embedded into the (x_4, r) subspace of the geometry described by the line element in Eq. (4.1).

The field theory dual to this construction indeed describes the dynamics of mesons. In particular it correctly reproduces the phenomenon of chiral symmetry breaking as known from low-energy QCD. A stack of N_f D8-branes corresponds to a $U(N_f)$ gauge symmetry, translating into a global symmetry of the boundary field theory. A pair of D8- and anti-D8-stacks correspondingly generates a $U(N_f) \times U(N_f)$ symmetry that is broken down to a single copy of $U(N_f)$. This happens because the D8-branes merge with their counterparts at the tip of the cigar. Thus, holography presents us with an interesting geometric interpretation of chiral symmetry breaking, valid at least for this particular model. As we will discuss in the the next section, the degrees of freedom on the D-branes indeed contain the correct number of corresponding Nambu-Goldstone bosons, massless pseudoscalar mesons.

Remarkably, this interpretation of chiral symmetry originating from from an underlying gauge symmetry is in line with what is known as *hidden local symmetry* [56, 57]. Vector mesons are interpreted as gauge bosons of this local symmetry, which is broken in the effective chiral Lagrangian - the ρ meson for example is massive. A direct consequence is

the universality of ρ meson couplings, in agreement with experimental results.

Beyond this, the Sakai-Sugimoto model may also be used to study baryons, as the effective Lagrangian contains a Skyrme-term whose corresponding soliton, the Skyrmion, may be identified with Witten's baryon vertex in the form of D4-branes wrapped around the S^4 part of the geometry. One may also introduce finite baryon density and study how it affects the properties of the model. The complete phase diagram of the theory can then be explored by turning on temperature, and at a certain value a deconfinement phase transition takes place. However, the current work will not focus on these aspects.

5.2 ◆ MESONS AND INTERACTIONS

Mesons and their interactions are described by the world volume theory on the D8- (and anti-D8) branes. For the purpose of writing down the explicit action we make use of the radial coordinates $U \in (U_{\text{KK}}, \infty)$ and $Z \in (0, \infty)$ with $U = r^2/(2L)$ and

$$K(Z) \equiv 1 + Z^2 = \frac{r^6}{r_{\text{KK}}^6} = \frac{U^3}{U_{\text{KK}}^3}, \quad (5.1)$$

where

$$U_{\text{KK}} = \frac{2}{9} g_{YM}^2 N_c M_{\text{KK}} l_s^2. \quad (5.2)$$

In terms of this language, the line element of the geometry of D8-branes at antipodal embedding as represented in Fig. 5.1 is given by

$$ds^2 = \left(\frac{U}{R_{\text{D4}}} \right)^{3/2} \eta_{\mu\nu} dx^\mu dx^\nu + \left(\frac{R_{\text{D4}}}{U} \right)^{3/2} \left[\frac{dU^2}{f(U)} + U^2 d\Omega_4^2 \right], \quad (5.3)$$

with

$$f(U) = 1 - \frac{U_{\text{KK}}^3}{U^3} \quad (5.4)$$

and

$$R_{\text{D4}} = \frac{1}{2} \frac{g_{YM}^2 N_c l_s^2}{M_{\text{KK}}}. \quad (5.5)$$

Furthermore, the dilaton field is given by

$$e^\phi = g_s \left(\frac{U}{R_{D4}} \right)^{3/4}. \quad (5.6)$$

The dynamics of pseudoscalar and vector mesons may be studied by expanding the world volume action of the D8-brane, i.e. by assuming the modes to be given by small fluctuations around the background. Let us begin by considering the DBI action at quadratic order. Extending the range of the coordinate Z to $(-\infty, \infty)$ to account for both D8- and anti-D8-branes we find

$$S_{D8}^{(F^2)} = -\kappa \text{Tr} \int d^4x \int_{-\infty}^{\infty} dZ \left[\frac{1}{2} K^{-1/3} \eta^{\mu\rho} \eta^{\nu\sigma} F_{\mu\nu} F_{\rho\sigma} + K M_{\text{KK}}^2 \eta^{\mu\nu} F_{\mu Z} F_{\nu Z} \right], \quad (5.7)$$

with $K \equiv K(Z)$ and

$$\kappa = (2\pi\alpha')^2 T_{D8} g_s^{-1} \Omega_4 \frac{1}{3} R_{D4}^{9/2} U_{\text{KK}}^{1/2} = \frac{\lambda N_c}{216\pi^3}, \quad (5.8)$$

where $T_{D8} = (2\pi)^{-8} l_s^{-9}$.

It can be shown that kinetic terms for pseudoscalar mesons and a tower of vector mesons arise from this action, as well as mass terms for the latter. This may be seen from the factorised ansatz

$$A_Z = U_{\text{KK}} \phi_0(Z) \pi(x^\nu) \quad (5.9)$$

and

$$A_\mu = \sum_n \psi_n(Z) v_\mu^{(n)}(x^\nu), \quad (5.10)$$

with $\pi(x^\nu) = \pi^a(x^\nu) T^a$ and $v_\mu^{(n)}(x^\nu) = v_\mu^{(n)a}(x^\nu) T^a$, where n denotes the n -th mode of the tower. Generators of the flavour symmetry are chosen to obey the normalisation condition $\text{Tr} T^a T^b = \delta^{ab}$.

Kinetic terms arise under the condition that the functions $\psi_n(Z)$ obey an eigenvalue problem in the form of the second order differential equation

$$-K^{1/3}\partial_Z(K\partial_Z\psi_n) = \lambda_n\psi_n, \quad (5.11)$$

with the boundary conditions $\psi_n(\pm\infty) = 0$ and either $\psi_n|_{Z=0} = 0$ or $\partial_Z\psi_n|_{Z=0} = 0$. The choice between the latter two conditions corresponds to choosing between vector and axial-vector mesons. The eigenvalue is related to the mass m_n of a given meson by $\lambda_n = (m_n/M_{\text{KK}})^2$. The lightest vector meson with $n = 1$ and $\lambda_1 \approx 0.669$ may be identified with the ρ meson, such that $\rho_\mu \equiv v_\mu^{(1)}$, and the lightest axial-vector mode with $\lambda_2 \approx 1.569$ with the $a_1(1260)$ meson. Model predictions for dimensionless ratios of masses of distinct mesons can then be compared with experiment, to good agreement. The square root of the ratio of eigenvalues, $\sqrt{\lambda_2/\lambda_1} \approx 1.53$, is very close to the experimental value for the ratio of masses, $m_{a_1}/m_\rho \approx 1.59$. The second lightest vector-meson may be identified with the excited ρ meson $\rho(1450)$, for which we get $\sqrt{\lambda_3/\lambda_1} \approx 2.07$, also close to the experimental value of $m_{\rho^*}/m_\rho \approx 1.86$. Recent lattice simulations at large N_c extrapolated to zero quark mass [58] put some perspective on this success, as the ratios are computed to be $m_{a_1}/m_\rho \approx 1.86$ and $m_{\rho^*}/m_\rho \approx 2.40$, for which the comparison turns out slightly worse.

Given this remarkable agreement it is not far fetched to go beyond comparing ratios and use the meson spectrum to fit the mass scale of the Witten-Sakai-Sugimoto model. Using the experimental value of the lightest ρ meson leads to a scale of $M_{\text{KK}} \approx 949$ MeV. As we will see later, this fit leads to a series of further quantitative results that are in reasonable agreement with experiment. It also has important consequences for the spectrum of glueballs that later will be discussed in some detail.

Including the pion, the action of the ρ meson arising at quadratic level from Eq. (5.8) turns out to be

$$S = -\text{Tr} \int d^4x \left[\frac{1}{2}(\partial_\mu\pi)^2 + \frac{1}{4}F_{\mu\nu}^2 + m_\rho^2\rho_\mu^2 \right], \quad (5.12)$$

where indices are contracted with the Minkowski metric and $F_{\mu\nu} \equiv \partial_\mu\rho_\nu - \partial_\nu\rho_\mu$, given that the conditions

$$2\kappa \int_{-\infty}^{\infty} dZ K^{-1/3} (\psi_1)^2 = 1 \quad (5.13)$$

and

$$2\kappa (U_{\text{KK}} M_{\text{KK}})^2 \int_{-\infty}^{\infty} dZ K (\phi_0)^2 = 1 \quad (5.14)$$

are obeyed. This leads to a normalisation of ψ_1 with

$$\psi_1(Z=0) \approx 1/\sqrt{5.606\kappa}, \quad (5.15)$$

and to

$$\phi_0 = \frac{1}{U_{\text{KK}} M_{\text{KK}} \sqrt{2\pi\kappa}} \frac{1}{K}. \quad (5.16)$$

An immediate conclusion to draw from Eq. (5.12) is that pions in the construction of Sakai and Sugimoto are massless. As a consequence, all results calculated in this model are to be understood in this chiral limit, and should be treated with some skepticism. Nevertheless, they can be a useful guide in making qualitative and semi-quantitative statements about the interactions of mesons. In later sections we will discuss how to go beyond this limit by modifying the model and see how this affects its predictions.

The pionic part of the DBI action may be recast in another familiar form, namely in that of the so-called chiral Lagrangian. One obtains

$$S_{\text{chiral}} = \frac{f_\pi^2}{4} \int d^4x \text{Tr} (U^{-1} \partial_\mu U)^2, \quad (5.17)$$

with

$$U = \text{P exp} \left[i \int_{-\infty}^{\infty} dZ A_Z \right] \quad (5.18)$$

and

$$f_\pi^2 = \frac{1}{54\pi^4} \lambda N_c M_{\text{KK}}^2. \quad (5.19)$$

The above relation between the pion decay constant f_π and the 't Hooft coupling λ implies a natural way of fixing the latter by fitting the former to its experimental value of $f_\pi = 92.7$ MeV. With $N_c = 3$ and $M_{\text{KK}} \approx 949$, this leads to $\lambda \approx 16.63$.

At this point it is useful to discuss an alternative way of fixing λ . The confining background of D4-branes allows for the definition of a string tension corresponding to Wilson loops connecting heavy quarks at the boundary with large separation along one of the spatial directions, say, in the coordinate x_1 . These loops are represented by fundamental strings minimising their energy by extending along the holographic direction. The value of the string tension is given in terms of the metric by

$$\sigma = \frac{1}{2\pi l_s^2} \sqrt{-g_{00}g_{11}}|_{U=U_{\text{KK}}} = \frac{1}{2\pi l_s^2} \left(\frac{U_{\text{KK}}}{R_{\text{D4}}} \right)^{3/2} = \frac{2\lambda}{27\pi} M_{\text{KK}}^2. \quad (5.20)$$

This string tension cannot be measured experimentally, but may be computed on the lattice. More precisely, the ratio of the ρ meson mass and the square root of the string tension is obtained in the large- N_c limit and comes out at $m_\rho/\sqrt{\sigma} = 1.504(50)$ [58], with the central value leading to $\lambda = 12.55$. We will therefore always compute our results for both values of lambda, and quote them in the form

$$\lambda \approx 16.63 \dots 12.55. \quad (5.21)$$

Now that we have fixed the free parameters, let us proceed and study interactions of mesons arising from the effective action of D-branes. This is important, as we may easily compare with well-known experimental data, and see how the model performs.

The presence of a non-vanishing background three-form implies that the Chern-Simons action of Eq. (2.15) leads to a term that is cubic in the fluctuation of the gauge field. As a consequence, there exists an interaction vertex for two pions and one ρ meson in the form of the Lagrangian

$$\mathcal{L}_{\rho\pi\pi} = -g_{\rho\pi\pi} \epsilon_{abc} (\partial_\mu \pi^a) \rho^{b\mu} \pi^c \quad (5.22)$$

with the coupling constant

$$g_{\rho\pi\pi} = \sqrt{2} \int_{-\infty}^{\infty} dZ \frac{1}{\psi K} \pi_1 = \sqrt{2} \times 24.030 \lambda^{-1/2} N_c^{-1/2}. \quad (5.23)$$

The decay rate of a ρ meson into two pions may be evaluated in the rest frame of the original particle, with the polarisation given by $\epsilon^\mu = (0, \mathbf{e})$, and the momenta of the pions by $p^\mu = (|\mathbf{p}|, \mathbf{p})$ and $q^\mu = (|\mathbf{p}|, -\mathbf{p})$. See Appendix A for details on the calculation of amplitudes making use of Feynman rules. The corresponding result is then given by

$$\mathcal{M} = ig_{\rho\pi\pi} \epsilon^\mu (p_\mu - q_\mu) = 2ig_{\rho\pi\pi} e^\mu p_\mu. \quad (5.24)$$

The decay rate is obtained from this amplitude by taking the square of the absolute value and then averaging over all possible angles as

$$\Gamma_\rho/m_\rho = \frac{1}{4\pi} \int d\Omega \frac{|\mathcal{M}|^2}{16\pi m_\rho^2} = \frac{g_{\rho\pi\pi}^2}{48\pi} \approx \frac{7.659}{\lambda N_c} \approx 0.1535 \dots 0.2034, \quad (5.25)$$

where we compute a dimensionless ratio, and insert values of λ as specified in (5.21), as well as $N_c = 3$. From now on, we will almost exclusively quote results in this form. This numerical result is remarkable, as the experimental value is given by $\Gamma_\rho/m_\rho = 0.191(1)$. Finite quark masses decrease the model prediction by roughly 20%, leading to a slightly worse, but still reasonable result, considering all approximations and deviations from real-world QCD.

The decay of the ω meson into $\pi^0 \pi^+ \pi^-$ was discussed first in [59]. The vertex, which arises from the Chern-Simons action, is proportional λ^{-4} , and the result for $\lambda = 16.63$ is given by $\Gamma = 2.58$ MeV, which is rather far away from the the experimental result of approximately 7.6 MeV. However, using our range of parameter values we obtain $\Gamma \approx 2.58 \dots 7.96$ MeV, for which the experimental data is in good agreement with the model.

These results are encouraging, as we find reasonably good agreement with experimental data for the decay channels of vector and axial-vector mesons. Although it is certainly no guarantee for success, this puts the idea of obtaining a rough estimate of the decay channels for glueballs using the Witten-Sakai-Sugimoto model on a more solid footing.

5.3 ◆ THE MASS OF η_0

The dynamics of pseudoscalar mesons are dominated by chiral symmetry and its breaking. A particularly important role is played by the axial anomaly of the symmetry $U(1)_A$, which is also part of the full chiral symmetry group. It has been shown to be an explanation for the mass of the η' meson that is significantly greater than that of the other pseudoscalar mesons - a fact that cannot be explained by finite quark masses alone. The mass of the η' is related to that of the η_0 meson, which arises before diagonalising the Lagrangian. It is this degree of freedom that actually obtains what is called anomalous mass through the Witten-Veneziano mechanism [60, 61].

Any credible holographic model of low energy QCD should in one way or another reproduce this effect. However, on the level of the DBI and Chern-Simons actions we have considered so far to study the interactions of mesons, there is no trace of it, and all pseudoscalars are massless. Introducing finite quark mass as shown later will also not give rise to this effect. The holographic analogue of the Witten-Veneziano mechanism therefore has to come from somewhere else, and indeed it does.

As laid out in [30], it follows from anomaly cancellation conditions studied in [62] that a mass term for the η_0 meson is hidden in the Ramond-Ramond action of Eq. (2.14). A nonvanishing theta-parameter, which is intimately related to the η_0 meson, arises in the Sakai-Sugimoto model as a nonzero flux of the Ramond-Ramond field strength through a surface Σ parametrised by (U, τ) ¹. It is computed as

$$\theta = \int_{\Sigma} F_2 = \int_{S^1} C_1, \quad (5.26)$$

where $F_2 = dC_1$, S^1 being the circle parametrised by τ at $U \rightarrow \infty$. However, the Ramond-Ramond field strength is not invariant under the $U(1)_A$ part of the gauge symmetry of the world volume theory on the flavour branes. Gauge invariance demands that F_2 is shifted to

¹See [63, 64, 65] for recent developments on the study of theta dependence in the Witten-Sakai-Sugimoto model.

$$\tilde{F}_2 = F_2 + i\text{Tr}(A) \wedge \delta(y)dy, \quad (5.27)$$

from which we obtain

$$\int_{\Sigma} \tilde{F}_2 = \theta + \frac{\sqrt{2N_f}}{f_{\pi}} \eta_0, \quad (5.28)$$

as the radial integral over the trace of the gauge field selects the η_0 part of the pseudoscalar multiplet. It can be shown that the explicit form of \tilde{F}_2 solving the equations of motion is given by

$$\tilde{F}_2 = \frac{4}{3^5 \pi} \lambda^3 M_{\text{KK}}^4 l_s^6 \frac{1}{U^4} \left[\theta + \frac{\sqrt{2N_f}}{f_{\pi}} \eta_0 \right] dU \wedge d\tau. \quad (5.29)$$

Inserting this into the ten-dimensional Ramond-Ramond action, integrating down to four dimensions, and considering the term quadratic in η_0 , we obtain a mass term for η_0 , with the square of the mass given by, in terms of the model parameters,

$$m_0^2 = \frac{N_f}{27\pi^2 N_c} \lambda^2 M_{\text{KK}}^2. \quad (5.30)$$

After inserting numerical values we obtain $m_0 = 967 \dots 730$ MeV, which covers the value of the physical η' meson obtained from diagonalising the Lagrangian, as will be discussed in the next section.

5.4 ◆ INTRODUCING FINITE QUARK MASS

Apart from the mass term for the η_0 that arises from the $U(1)_A$ anomaly, pseudoscalar mesons in the Sakai-Sugimoto model are massless. However, this scenario, corresponding to the chiral limit of zero quark mass, is not in accordance with experimental data. This will inevitably lead to shortcomings in the predictivity of the model with regards to glueball decay, as finite mass may alter results through kinematic effects, as well as by possibly introducing additional couplings of glueballs to the mass terms. It is therefore desirable to study ways of going beyond the chiral limit in the holographic setting.

Let us review first what one should expect to obtain. In addition to the Witten-Veneziano mass term, the mass terms in the effective Lagrangian for the pseudoscalar mesons associated with explicitly broken chiral symmetry for $N_f = 3$ is given by

$$\mathcal{L}_m = -\frac{1}{2}m_\pi^2\pi_0^2 - m_\pi^2\pi_+\pi_- - m_K^2(K_0\bar{K}_0 + K_+K_-) - \frac{1}{2}m_1^2\eta_0^2 - \frac{1}{2}m_8^2\eta_8^2 - \frac{2\sqrt{2}}{3}(m_K^2 - m_\pi^2)\eta_0\eta_8, \quad (5.31)$$

where we have assumed the absence of electromagnetic effects. The mass parameters m_1 and m_8 in this expression are given in terms of the other masses by

$$m_1^2 = \frac{2}{3}m_K^2 + \frac{1}{3}m_\pi^2 \quad (5.32)$$

and

$$m_8^2 = \frac{4}{3}m_K^2 - \frac{1}{3}m_\pi^2. \quad (5.33)$$

The last term in Eq. (5.31) indicates mixing between η_0 and η_8 , and may be removed by introducing new degrees of freedom such that the Lagrangian becomes diagonal. These correspond to the physical states η and η' , and are related to η_0 and η_8 by

$$\eta = \eta_8 \cos \theta_P - \eta_0 \sin \theta_P \quad (5.34)$$

and

$$\eta' = \eta_8 \sin \theta_P + \eta_0 \cos \theta_P, \quad (5.35)$$

where θ_P is known as the pseudoscalar mixing angle. It is expressed in terms of the mass parameters as

$$\theta_P = \frac{1}{2} \arctan \frac{2\sqrt{2}}{1 - \frac{3}{2}m_0^2/(m_K^2 - m_\pi^2)}. \quad (5.36)$$

Finally, the squares of the masses of the physical states are given by

$$m_{\eta,\eta'}^2 = \frac{1}{2}m_0^2 + m_K^2 \mp \sqrt{\frac{m_0^4}{4} - \frac{1}{3}m_0^2(m_K^2 - m_\pi^2) + (m_K^2 - m_\pi^2)^2}. \quad (5.37)$$

It is apparent from the structure of this equation that the η' meson receives much of its mass from the Witten-Veneziano mechanism, as is reflected in experimental data: with a mass of almost 1 GeV, it is considerably heavier than the other pseudoscalar mesons.

Since mesons may be thought of as bound states of quarks, it is not far-fetched to ask whether there exists a relationship between the masses of pseudoscalar mesons and those of quarks, and indeed it does. It is known as the Gell-Mann-Oakes-Renner (GMOR) relation [66] and determines the pion mass in terms of the masses of up- and down-quark, and for $m_u = m_d = m_q$ is roughly given by

$$m_\pi^2 = \frac{2m_q \langle \bar{q}q \rangle}{f_\pi^2} + \mathcal{O}(m_q^2), \quad (5.38)$$

where $\langle \bar{q}q \rangle$ is the quark condensate.

There have been several attempts at understanding this formula from a holographic point of view in the context of the Sakai-Sugimoto model. In [67] it was proposed that finite quark mass arises from a mechanism analogous to a tachyonic mode of a string stretched between two infinitely extended stacks of D8-branes. However, as the correct action implementing this stringy effect within the supergravity approximation of the Sakai-Sugimoto model is not known, it is hard to obtain concrete results. A different approach based on world sheet instantons arising from strings stretched between the D4 – D8 – $\overline{D8}$ -branes of the Sakai-Sugimoto model and regularized by another stack of either D4- or D6-branes was presented in [68]. In this setup it is easier to perform concrete calculations, and indeed the GMOR relation was reproduced successfully. In [69] it was suggested that the two approaches were actually two different points of view of one and the same mechanism. Let us also note that an alternative view has been put forward in [70], namely that finite quark mass arises from non-antipodal embedding of the flavour branes. However, to the knowledge of the author, it is still controversial whether this claim is valid or not.

Let us continue by briefly reviewing the results of [68]. The construction can be thought of as analogous to a holographic realisation of technicolour: another gauge-sector of N'_c D4-branes (which we call D4'-branes) separated from the original stack of D4-branes is introduced, and strings stretching from the D8- $\overline{D8}$ -branes to the D4'-branes correspond to techni-quarks. An important difference to the original Sakai-Sugimoto-model is that

pairs of flavour branes now join at the location of the D4'-branes, as well as at that of the original D4-branes. Spontaneous symmetry breaking now induces massless goldstone modes which have to be decoupled by imposing $N'_c \rightarrow \infty$ and by placing the D4'-branes at the far UV with respect to the D4-branes. Explicit chiral symmetry breaking is induced in the QCD sector through massive gauge bosons arising from open strings between D4- and D4'-branes. More precisely, this configuration of D-branes permits the existence of world sheet instantons bounded by a closed loop that stretches along the D8-, $\overline{D8}$, and D4'-branes.

In the strongly interacting picture, i.e. in weakly coupled gravity, this world sheet translates into an area bounded by a closed loop along the D8- $\overline{D8}$ branes, as the D4' branes are not present as dynamical objects, and are only responsible for the background geometry.

Quark mass arises as follows: open strings stretching from D8- and $\overline{D8}$ -branes to D4-branes correspond to the massless quarks q_L and q_R , while open strings stretching from D8- and $\overline{D8}$ -branes to D4'-branes correspond to the massless quarks q'_L and q'_R . String interactions mediated by massive gauge and scalar bosons² induce a four-point vertex of the form $\bar{q}_L q_R \bar{q}'_L q'_R$, and mass terms therefore arise if one pair of quarks forms a condensate. The quark mass of the "QCD-quarks" is therefore proportional to the condensate of the "technicolour-quarks", i.e. $m_q \propto \langle \bar{q}'_L q'_R \rangle$. In terms of string world sheet instantons, this mass term arises from an instanton action of the form

$$S \propto \int d^4x \text{Tr} \bar{q}_L q_R e^{-S_{\text{NG}}} + \text{h.c.}, \quad (5.39)$$

where S_{NG} is the classical Nambu-Goto action, the trace being taken over the flavour indices of the quarks.

In the case where the QCD-sector is in the weakly coupled regime while the technicolour-sector is strongly coupled, one may evaluate the the Nambu-Goto action explicitly, treating the QCD-branes in the probe approximation, with the result [68]:

²The scalar corresponds to the "tachyonic" mode discussed in [67].

$$S_{\text{NG}} = \frac{U_0 - U'_{\text{KK}}}{2\alpha' M_{\text{KK}}}, \quad (5.40)$$

where U_0 is the position of the D4-branes and U'_{KK} is the Kaluza-Klein radius of the D4'-branes. In the approximation $U_0 \gg U'_{\text{KK}}$, this implies

$$m_q \propto e^{-\pi M_W / M_{\text{KK}}}, \quad (5.41)$$

with the mass of the massive gauge boson given by $M_W = U_0 / (2\pi\alpha')$. But is the Gell-Mann-Oakes-Renner relation, Eq. (5.38), also realised holographically? The answer is yes, and it arises as follows:

In the low energy limit, as shown in the ordinary Sakai-Sugimoto construction, mesons are realised as excitations of gauge fields on pairs of D8-branes. This remains true in the modified version that includes additional D4'-branes. However, the world sheet instanton may now interact with these gauge fields, inducing an interaction term in the instanton action, which is given by

$$S \propto \frac{1}{g_s} \int d^4x \text{P Tr} e^{-S_{\text{NG}} + i \oint dz A_z} + \text{h.c.}, \quad (5.42)$$

where P indicates path ordering, and the integral over z is taken to be along the boundary of the world sheet instanton. With

$$U = e^{i2\pi(x)/f_\pi} \quad (5.43)$$

and

$$\text{Tr} U = \text{P Tr} e^{i \oint dz A_z}, \quad (5.44)$$

we obtain the mass term of the chiral Lagrangian,

$$S = m_\pi^2 f_\pi^2 \text{Tr}(U + U^\dagger), \quad (5.45)$$

which through

$$m_\pi^2 \propto \frac{1}{g_s} e^{-S_{\text{NG}}} \propto m_q \quad (5.46)$$

is consistent with the GOR-relation.

Unfortunately, the proportionality constants in the previous relations have not been evaluated in [68], as the metric corresponding to a multi-center throat geometry arising from multiple stacks of D4-branes is not known. In order to circumvent this problem, the route of replacing the D4'-branes by a stack of D6-branes was taken, a setup that still generates quark mass through world sheet instantons, but makes the calculation possible. This is because the D6-branes are treated in the probe approximation, and hence do not modify the background geometry. It is also possible to calculate the effect of separating D6-branes from each other, generating flavour-dependent quark mass. The analog of Eq. (5.41) is then given by the mass matrix

$$(m_q)_{ij} = \mathcal{N} N' \frac{2\pi M_{\text{KK}}}{g_Y M^2} \delta_{ij} e^{-\pi M_W^{(i)}/M_{\text{KK}}}, \quad (5.47)$$

where N' is the number of D6-branes, $M_W^{(i)}$ is the mass of W-bosons corresponding to each of the branes, and \mathcal{N} is a dimensionless normalisation constant that is assumed to be of order 1. Finally, the square of the pion mass is given by

$$m_\pi^2 = \frac{4g_Y^2 M_c^{3/2} M_{\text{KK}}^3}{3^{9/2} \pi^3 \mathcal{N} f_\pi^2} m_q. \quad (5.48)$$

It is also important that this mechanism generates an additional mass term for the flavour singlet η_0 , in addition to the Witten-Veneziano mass term discussed in the previous chapter, and in line with the discussion above. diagonalising the flavour octet η_8 together with η_0 leads to the physical mass eigenstates η and η' , in accordance with Eq. (5.37). Choosing $\mathcal{M} = \text{diag}(m, m, m_s)$, $m = (m_u + m_d)/2$, with $m_\pi = 140$ MeV and $m_K = 497$ MeV we obtain

$$m_\eta = 518 \dots 476 \text{ MeV}, \quad (5.49)$$

$$m_{\eta'} = 1077 \dots 894 \text{ MeV}, \quad (5.50)$$

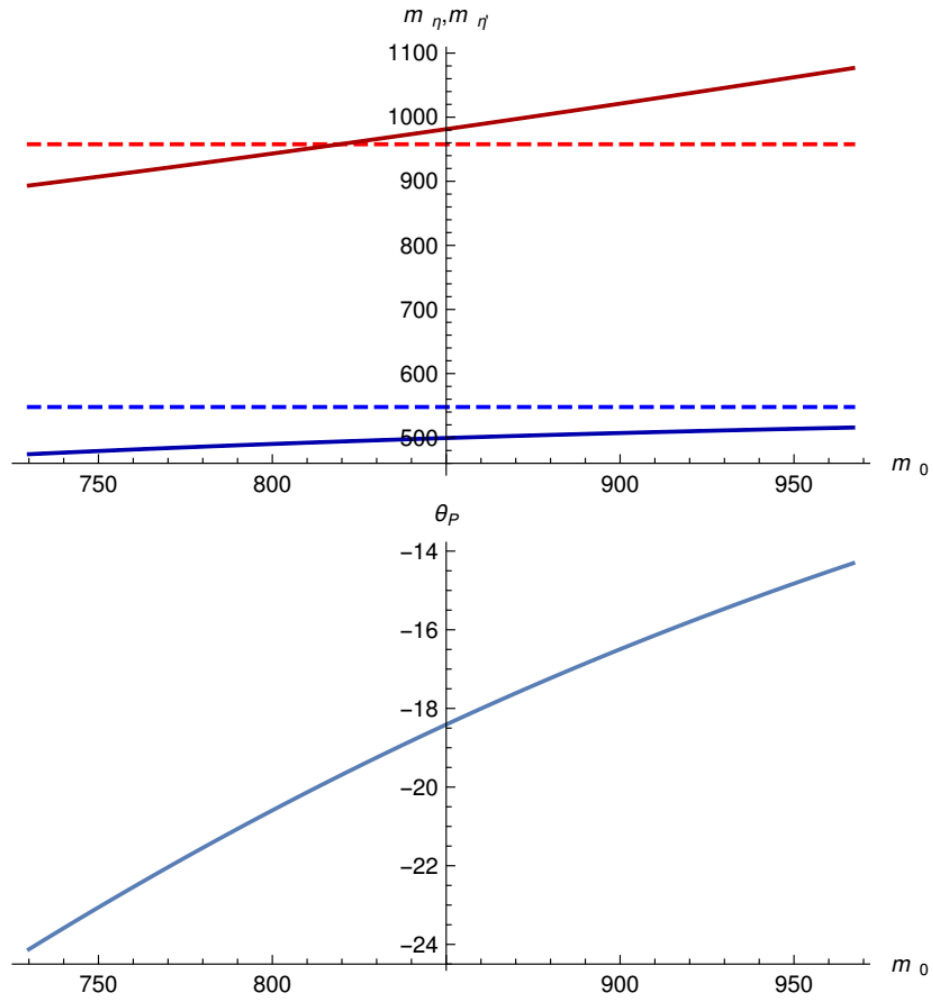


Figure 5.2: The mass of η and η' , as well as the mixing angle θ_P shown as a function of the Witten-Veneziano mass m_0 . Dashed lines correspond to experimental values.

in good agreement with the experimental values $m_\eta \approx 548$ MeV and $m_{\eta'} \approx 958$ MeV, as well as the mixing angle

$$\theta_P = -14.4^\circ \dots -24.2^\circ. \quad (5.51)$$

In [34], the dependence of the above quantities on the Witten-Veneziano mass m_0 (which in turn depends on the 't Hooft coupling $\lambda = 16.63 \dots 12.55$) was plotted, and the resulting graphs are shown in Fig. 5.2. It is noteworthy that the ratio $m_\eta/m_{\eta'}$ never reaches its experimental value of approximately 0.572. The highest possible value is $m_\eta/m_{\eta'} \approx 0.535$, which corresponds to $m_0 \approx 661$ MeV and $\theta_P \approx -28^\circ$, which lies

outside the parameter range we have so far considered. Furthermore, at this point both m_η and $m_{\eta'}$ lie roughly 100 MeV below their physical values.

The values of θ_P are in good agreement with mixing angles cited in the literature. Light meson decays hint towards values around -14° [72, 73], while radiative charmonium decay favours $\theta_P \approx -21^\circ$ [71, 74]. According to [6], the ratio $\Gamma(\eta' \rightarrow 2\gamma)/\Gamma(\eta \rightarrow 2\gamma)$ implies $\theta_P = (-18 \pm 2)^\circ$.

5.5 ◆ THE GLUON CONDENSATE

Having discussed predictions of the Sakai-Sugimoto construction in some detail, it is worth mentioning an additional feature that becomes apparent once we have fixed all model parameters. A nontrivial and highly interesting quantity to study in Yang-Mills theory is the gluon condensate, which is roughly given by the vacuum expectation value of the square of the non-abelian field strength $G_{\mu\nu}^a$, and is defined as

$$C^4 \equiv \left\langle \frac{\alpha_s}{\pi} G_{\mu\nu}^a G^{a\mu\nu} \right\rangle, \quad (5.52)$$

where α_s denotes the coupling constant of the strong interaction.

The gluon condensate was computed for Witten's model in [75] using the technique of holographic renormalisation, and the explicit expression is given by

$$C_{\text{hol}}^4 = \frac{4N_c}{3^7\pi^4} \lambda^2 M_{\text{KK}}^4. \quad (5.53)$$

Inserting the parameters as discussed above (with $N_c = 3$) we obtain

$$C_{\text{hol}}^4 = 0.0126 \dots 0.0072 \text{ GeV}^4, \quad (5.54)$$

as was shown first in [32], where the upper bound is almost identical with the SVZ sum rule result of [76]. Other sum rule calculations lead to smaller and larger results as compared to SVZ [77, 78], while lattice computations lead to significantly larger values. However, the latter are of the same size as ambiguities from the subtraction procedure [79].

5.6 ◆ MASS SCALE AND GLUEBALL SPECTRUM

Finally, we will discuss the impact of fixing the mass scale to $M_{\text{KK}} \approx 949$ MeV by fitting the mass of the ρ meson to its experimental value as described above on the spectrum of glueballs. Let us point out in the beginning that the nice agreement with the lattice result suggested in Fig. 4.2 is ruined, and the story becomes more complicated than initially expected. As shown in Fig. 5.3, the lightest exotic scalar glueball mode is now no longer found at roughly 1.5 GeV, but rather at around 850 MeV, while the lightest degenerate dilatonic scalar and tensor are now found slightly below 1.5 GeV. There are several possible explanations for this mismatch:

1. The lattice results do not capture the whole truth about the spectrum of glueballs. The holographic picture is closer to reality, despite all approximations and deviations from true QCD.
2. The holographic result is not accurate, and the study of glueballs in the Witten-Sakai-Sugimoto model is quantitatively not reliable.
3. Neither is wrong, but a more careful examination of the holographic results is in order.

Explanation 1 seems hard to justify, as lattice results both in the quenched and unquenched approximation, as well as extrapolations to large N_c are very robust, despite suggestions in the literature that a glueball state around or below 1 GeV might exist. We are therefore left to either discard holographic results, or to examine them closer. In light of all the other successes of the Sakai-Sugimoto model in describing features of low energy QCD both qualitatively and quantitatively, we are led to opt for explanation 3, and reexamine the assumptions of the model, and their implications for the spectrum of glueballs.

The lattice results we are comparing the holographic spectrum with are inherently four-dimensional, while the holographic model, possessing an additional compact direction, is five-dimensional. In addition to the presence of Kaluza-Klein scalars, we observe that as

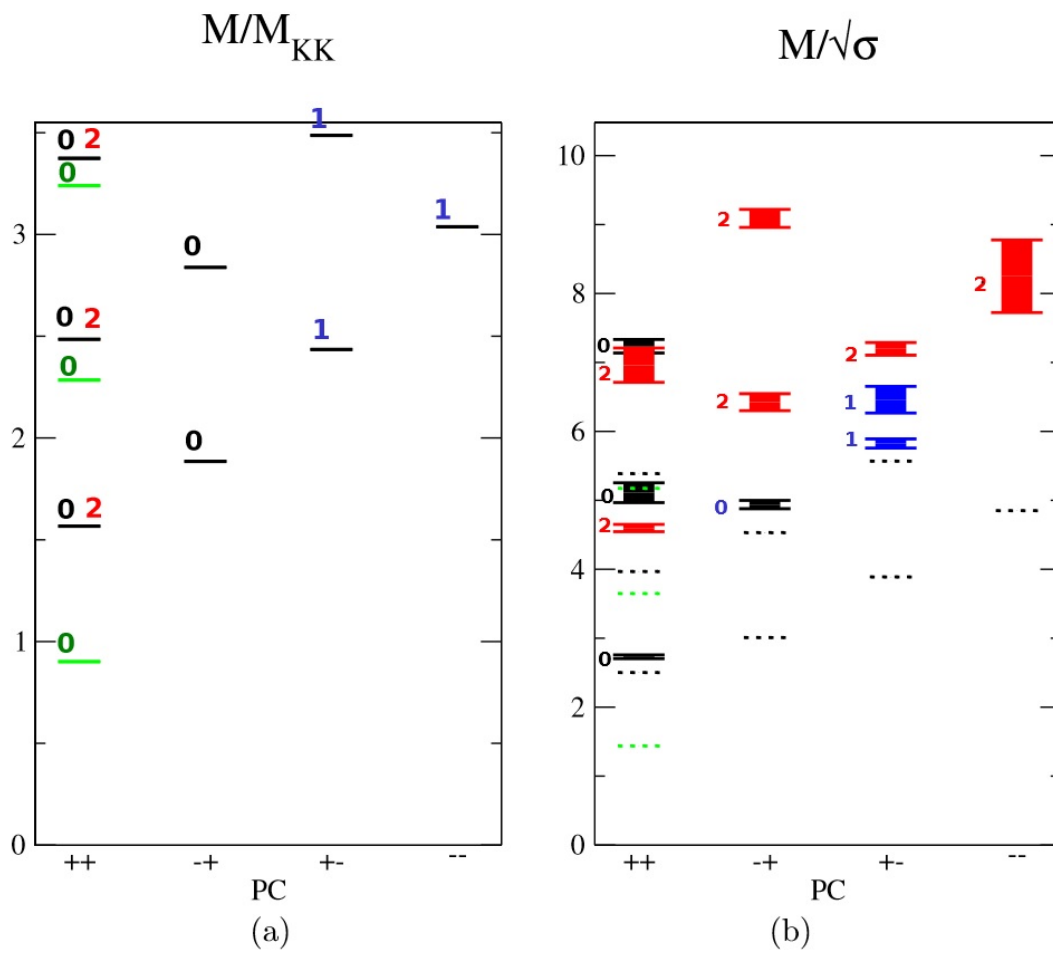


Figure 5.3: The spectrum of glueballs in the Witten-Sakai-Sugimoto model expressed (a) in terms of the Kaluza-Klein mass M_{KK} (b) the square root of the string tension σ for the standard parameters of the model. To the right, we have juxtaposed the large- N_c lattice results of [55].

written down explicitly in Eq. (4.29), the fluctuations corresponding to the lowest lying glueball contain a component along this additional direction. This is why the mode is referred to as exotic, and can be expected to be absent in a four-dimensional version of holographic QCD. The other scalar mode, which is called dilatonic because it mainly affects fluctuations of the dilaton in the ten-dimensional formulation, is not influenced by the fifth direction, and it can be expected to be more or less unchanged in a four-dimensional theory. This is consistent with the fact that it corresponds to the second lightest scalar glueball in the holographic spectrum, whose mass lies relatively close to that of the lightest glueball on the lattice. One possible answer to the above problem therefore seems to be to ignore the exotic mode when comparing with four-dimensional results. However, in the following sections we will nevertheless include this mode and compare its decay patterns to those of experimental glueball candidates and see how it performs in comparison to the dilatonic one. Furthermore, we will extrapolate glueball masses to values of potential glueball candidates in order to get a more realistic picture of the possible decay patterns. This is especially interesting in the case of the tensor glueball, which now comes out much lighter than the lattice suggests.

6 SCALAR GLUEBALL - CHIRAL LIMIT

“One thing’s for sure, we’re all going to be a lot thinner.”

Han Sol o

6.1 GENERALITIES

This section is a description of the results published in the articles [32] and [33], which deal with the decay of scalar glueballs, i.e., those states with $J^{PC} = 0^{++}$. Let us begin with a general conceptual introduction to the idea that is valid for glueballs of other quantum numbers as well.

In the probe approximation of a stack of D-branes in a background sourced by another stack of D-branes, fluctuations of the background spacetime will also affect the geometry of the probe branes. As the world volume of the latter gives rise to a gauge theory, it is plausible that fluctuations of the background may also be absorbed by the probe branes. This can be thought of as a decay process, transforming gravitational excitations into excitations of the gauge fields living on the probe-brane world volume. Translated into the language of the holographic dual, this corresponds to the decay of glueballs into mesons.

The above picture can be made precise by considering the action of the world volume theory of the probe branes in the presence of metric fluctuations induced by the background, as well as excitations of gauge fields. Let us denote this action by $S_{\text{WV}}(\delta A, \delta g)$. Interactions may be quantified by expanding this action in the fluctuations and by ob-

serving whether mixed terms, e.g. $\delta g(\delta A)^2$, are non-vanishing. Interaction vertices are then obtained by inserting explicit factorized forms for the fluctuations and integrating out all extra dimensions. As the resulting expressions are of the form of a conventional field theory Lagrangian, quantities like decay rates and scattering amplitudes may then be derived from them by means of standard quantum field theory methods.

For the computation of the decay rate of a single glueball into several mesons we have to consider terms linear in the metric fluctuation $h_{MN} \equiv \delta g_{MN}$. Wherever the components of the metric tensor enter explicitly, we have to make the replacements

$$g_{MN} \longrightarrow g_{MN} + h_{MN} \quad (6.1)$$

and

$$g^{MN} \longrightarrow g^{MN} - h^{MN}. \quad (6.2)$$

Furthermore, we need an explicit expression for the expression of the square root of the metric determinant for small fluctuations. With $\tilde{g}_{MN} \equiv g_{MN} + h_{MN}$, it can be shown to be given by

$$\sqrt{\tilde{g}} = \sqrt{g} \left[1 + \frac{1}{2} g^{MN} h_{MN} + \frac{1}{8} g^{MN} g^{PQ} h_{MN} h_{PQ} - \frac{1}{4} g^{MN} g^{PQ} h_{MP} h_{QN} + \mathcal{O}(h^3) \right]. \quad (6.3)$$

Terms of higher than linear order will mostly be discarded, even though they may in principle play a role for multi-glueball interactions. In a decay process of a heavy glueball, a lighter glueball may act as an intermediate state which subsequently decays to ordinary mesons. We will comment on this possibility wherever necessary.

The core idea of this thesis is to systematically apply this principle to the probe-branes of the Sakai-Sugimoto model, whose background admits glueball fluctuations, as we have seen earlier. The goal is to obtain a prediction for the decay channels of various glueballs, and to compare them with the data for experimental candidates. In the case of the pseudoscalar glueball, it will also be used to study production channel. The strategy,

which will be shown in more detail in the initial examples, may be split into three distinct subroutines:

1. Derivation of the four-dimensional interaction Lagrangians of glueballs and mesons from the holographic picture by solving mode equations, inserting the resulting fluctuations into the supergravity actions, and integrating out extra dimensions.
2. Computation of amplitudes and subsequently decay rates by using Feynman rules and other traditional quantum field theory techniques.
3. Exploration of the parameter space and comparison with experimental data on glueball candidates, whenever there are any.

In this section we will discuss the decay channels of the scalar glueball, but results for the other glueball states are obtained in a very similar manner, using the same principles. We will first discuss the case of the Sakai-Sugimoto model in its original form, namely in the absence of quark masses, and hence, as dictated by the GOR-relation, in the presence of massless pseudoscalar mesons. One should not expect that this chiral limit leads to accurate predictions for decay rates. This is in part for kinematic reasons, and in part due to possible additional couplings a mass term for pseudoscalars might induce. These aspects are discussed further in Section 6.4. Studying decay channels in the chiral limit nevertheless has the potential lead to a rough understanding of possible glueball decay patterns.

6.2 ◆ DECAY TO TWO PSEUDOSCALARS

We will first consider glueball decay to two pseudoscalar mesons, since the corresponding interaction vertices possess the simplest structure of all possible decay patterns.

As the DBI action is defined within type IIA string theory, but the metric fluctuations are computed in M-Theory, we first have to dimensionally reduce them in order to perform the calculation. Let G_{MN} be the eleven-dimensional, and g_{MN} the ten-dimensional metric. All relevant metric fluctuations, as well as those of the dilaton, reduce as

$$\begin{aligned}
g_{\mu\nu} &= \frac{r^3}{L^3} \left[\left(1 + \frac{L^2}{2r^2} \delta G_{11,11} \right) \eta_{\mu\nu} + \frac{L^2}{r^2} \delta G_{\mu\nu} \right], \\
g_{\tau\tau} &= \frac{r^3 f}{L^3} \left[1 + \frac{L^2}{2r^2} \delta G_{11,11} + \frac{L^2}{r^2 f} \delta G_{\tau\tau} \right], \\
g_{rr} &= \frac{L}{r f} \left[1 + \frac{L^2}{2r^2} \delta G_{11,11} + \frac{r^2 f}{L^2} \delta G_{rr} \right], \\
g_{r\mu} &= \frac{r}{L} \delta G_{r\mu}, \\
g_{\Omega\Omega} &= \frac{rL}{4} \left[1 + \frac{L^2}{2r^2} \delta G_{11,11} \right], \\
\exp [4\Phi/3] &= \frac{r^2}{L^2} \left[1 + \frac{L^2}{r^2} \delta G_{11,11} \right].
\end{aligned} \tag{6.4}$$

Let us begin with the lightest holographic glueball in the form of the exotic polarisation as introduced in Section 4.2. Decay patterns for this mode, which we denote G_E , were first studied in [53]. However, the calculations presented there, as pointed out in [32], contained several errors, which were subsequently corrected in the latter reference. One of them is that the authors of [53] did not include fluctuations in the $g_{\Omega\Omega}$ -component of the metric, contrary to the formula above this paragraph.

Two-body decays are obtained by considering the expansion of the DBI action, Eq. (2.18) to quadratic order in the gauge field. Keeping only terms of the form

$$G \operatorname{Tr}(\pi\pi), \tag{6.5}$$

we end up with all possible interaction vertices that couple a glueball to two pseudoscalar mesons. Interactions of this form are represented by the Feynman diagram of Fig. 6.1. The corresponding Lagrangian is given by

$$\mathcal{L}^{G_E \rightarrow \pi\pi} = -\frac{1}{2} \operatorname{Tr} \left[c_1 \partial_\mu \pi \partial_\nu \pi \frac{\partial^\mu \partial^\nu}{M_E^2} G_E + \check{c}_1 \partial_\mu \pi \partial^\mu \pi G_E \right], \tag{6.6}$$

where the coupling constants are computed as

$$c_1 = \int dZ \frac{\bar{H}_E(Z)}{\pi K(Z)} = \sqrt{2} \times 44.304 \lambda^{-1/2} N_c^{-1} M_{\text{KK}}^{-1} \tag{6.7}$$

and

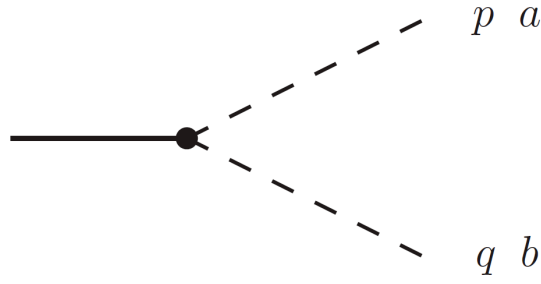


Figure 6.1: Feynman diagram representing the decay of a scalar glueball (thick line) into two pseudoscalars (dashed lines). The labels indicate momenta (p and q) and isospin indices (a and b) of the decay products.

$$\check{c}_1 = \int dZ \frac{H_E(Z)}{4\pi K(Z)} = \sqrt{2} \times 11.590 \lambda^{-1/2} N_c^{-1} M_{\text{KK}}^{-1}, \quad (6.8)$$

where $Z \in (-\infty, \infty)$ and

$$\overline{H}_E(Z) \equiv \left[\frac{1}{4} + \frac{3}{5K(Z) - 2} \right] H_E(Z). \quad (6.9)$$

We will also perform the calculation for the excited mode G_E^* , for which the coupling constants are given by

$$c_1^* = \int dZ \frac{\overline{H}_E^*(Z)}{\pi K(Z)} = \sqrt{2} \times 24.641 \lambda^{-1/2} N_c^{-1} M_{\text{KK}}^{-1} \quad (6.10)$$

and

$$\check{c}_1^* = \int dZ \frac{H_E^*(Z)}{4\pi K(Z)} = \sqrt{2} \times 4.5843 \lambda^{-1/2} N_c^{-1} M_{\text{KK}}^{-1}, \quad (6.11)$$

where \overline{H}_E^* is defined in analogy to the ground state.

The same computation for the dilatonic mode, denoted by G_D , leads to

$$\mathcal{L}^{G_D \rightarrow \pi\pi} = \frac{1}{2} d_1 \text{Tr} \partial_\mu \pi \partial_\nu \pi \left[\eta^{\mu\nu} - \frac{\partial^\mu \partial^\nu}{M_D^2} \right] G_D, \quad (6.12)$$

with the coupling constant

$$d_1 = \int dZ \frac{H_D(Z)}{\pi K(Z)} = 17.226 \lambda^{-1/2} N_c^{-1} M_{\text{KK}}^{-1}. \quad (6.13)$$

For the excited mode, we obtain

$$d_1^* = \int dZ \frac{H_D^*(Z)}{\pi K(Z)} = 11.906 \lambda^{-1/2} N_c^{-1} M_{\text{KK}}^{-1}. \quad (6.14)$$

In order to compute decay rates from these expressions we have to apply the principles laid out in appendix A, correctly taking into account the kinematics of the processes at hand. The corresponding Feynman diagram is displayed in Fig 6.1. We obtain

$$\Gamma_{G_{E,D} \rightarrow \pi\pi} = 3 \times \frac{1}{2} \times \frac{|\mathbf{p}|}{8\pi M_{E,D}^2} |\mathcal{M}_{E,D}|^2, \quad (6.15)$$

\mathbf{p} being the momentum of one of the pions in the rest frame of the glueball. The symmetric nature of this process leads to $|\mathbf{p}| = M_{E,D}/2$, which is also responsible for the symmetry factor $\frac{1}{2}$, while the factor of 3 arises from a sum over all possible isospins. The amplitudes \mathcal{M}_E and \mathcal{M}_D may be computed using Feynman rules for the respective vertices, with the results

$$|\mathcal{M}_E| = |(c_1 + \check{c}_1)p_0 q_0 - \check{c}_1 \mathbf{p} \cdot \mathbf{q}| = (c_1 + 2\check{c}_1) \frac{M_E^2}{4} \quad (6.16)$$

and

$$|\mathcal{M}_D| = |d_1 \mathbf{p} \cdot \mathbf{q}| = d_1 \frac{M_D^2}{4}. \quad (6.17)$$

The explicit expressions and numerical values for the dimensionless ratio of the decay rate and the glueball mass are then given by

$$\Gamma_{G_E \rightarrow \pi\pi} / M_E = \frac{3(c_1 + 2\check{c}_1)^2 M_E^2}{512\pi} \approx \frac{13.79}{\lambda N_c^2} \approx 0.092 \dots 0.122 \quad (6.18)$$

and

$$\Gamma_{G_D \rightarrow \pi\pi} / M_D = \frac{3d_1^2 M_D^2}{512\pi} \approx \frac{1.359}{\lambda N_c^2} \approx 0.009 \dots 0.012, \quad (6.19)$$

where we have used $N_c = 3$, $\lambda = 16.63 \dots 12.55$, $M_E \approx 855$ MeV, and $M_D \approx 1487$ MeV.

Finally, for the excited glueball states we obtain

$$\Gamma_{G_E^* \rightarrow \pi\pi} / M_{E^*} \approx 0.149 \dots 0.197 \quad (6.20)$$

and

$$\Gamma_{G_D^* \rightarrow \pi\pi} / M_{D^*} \approx 0.011 \dots 0.014, \quad (6.21)$$

where the masses are given by $M_{E^*} \approx 2168 \text{ MeV}$ and $M_{D^*} \approx 2358 \text{ MeV}$.

We observe that the results for even the lightest exotic glueball are about one order of magnitude above those of its dilatonic counterpart, despite being much lighter, which appears to be unnatural in the context of interpreting the dilatonic mode as an excited state of the exotic "ground state". This serves as further evidence that the exotic mode should be discarded, in line with the discussions of Section 5.6.

However, at this point is worth mentioning that a broad glueball with a mass of around 1 GeV has been discussed before in the literature. It arises from spectral sum rules, along with a narrow glueball state predicted to have a mass close the lightest glueball of lattice gauge theory, and plays the role of a pure glue component of the $f_0(500)$ (or σ) meson [17, 80, 81, 82]. Along these lines, a speculative alternative to discarding the exotic glueball could therefore be to view it as a holographic dual to such a pure glue component of the σ meson.

Let us conclude this subsection by comparing the above results to experimental data for the isoscalar mesons $f_0(1500)$ and $f_0(1710)$, which possess masses close to lattice predictions for the lightest glueball, and are frequently considered to have a large glue component. Data for the $f_0(1500)$ is available in [6], and the relevant dimensionless ratio for decay into two pions is given by

$$\Gamma^{(\text{exp.})}(f_0(1500) \rightarrow \pi\pi) / (1505 \text{ MeV}) = 0.025(3). \quad (6.22)$$

The model prediction for the exotic glueball, (6.18), is significantly bigger than this, while that of the dilatonic mode, (6.19), albeit closer, is too small.

For the $f_0(1710)$ isoscalar there exist two distinct results for the measurement of the decay widths, one by the BES collaboration, with

$$\Gamma^{(\text{exp.})}(f_0(1710) \rightarrow \pi\pi) / (1722 \text{ MeV}) = 0.017(4), \quad (6.23)$$

and one by the WA102 collaboration, namely

$$\Gamma^{(\text{exp.})}(f_0(1710) \rightarrow \pi\pi)/(1722\text{MeV}) = 0.009(2). \quad (6.24)$$

The prediction for the exotic glueball is still much larger than this, while that for the dilatonic glueball is in very close agreement. Thus we conclude that when considering two-body decay of scalar glueballs, the Witten-Sakai-Sugimoto model in the chiral limit favours the identification of the $f_0(1710)$ isoscalar as a predominant glueball state.

6.3 ◆ DECAY TO FOUR PSEUDOSCALARS

Like the two-body decay channel discussed in the previous section, interaction vertices for decays into more than two pseudoscalars are similarly obtained by considering the expanded DBI action, Eq. (2.18). There are no final states with three pseudoscalars, and as such the next interesting case to consider is four-body decay. It is described by vertices schematically given by

$$G \text{Tr}(\rho\rho), \quad G \text{Tr}(\pi^4), \quad (6.25)$$

where the latter comes from quartic terms in (2.18)f, and leads to a final state that consists exclusively of π^0 mesons, while all other vertices lead to final states made of π^\pm mesons. Beyond this, the Chern-Simons term induces a vertex of the form

$$G \text{Tr}(\rho[\pi, \pi]). \quad (6.26)$$

Vector mesons in the above vertices are not considered as final states, but as intermediate states which further decay to two pseudoscalars, as discussed in an earlier section. The Feynman diagrams arising from all of the above vertices are summarized in Figs. 6.2 and 6.3.

In principle it is also possible to obtain additional vertices due to glueball-glueball couplings as $G \rightarrow 2G \rightarrow 4\pi^0$ and $G \rightarrow G+2\pi^0 \rightarrow 4\pi^0$. However, these are parametrically suppressed. Furthermore, the world volume action of the D8-branes also permits terms of the form

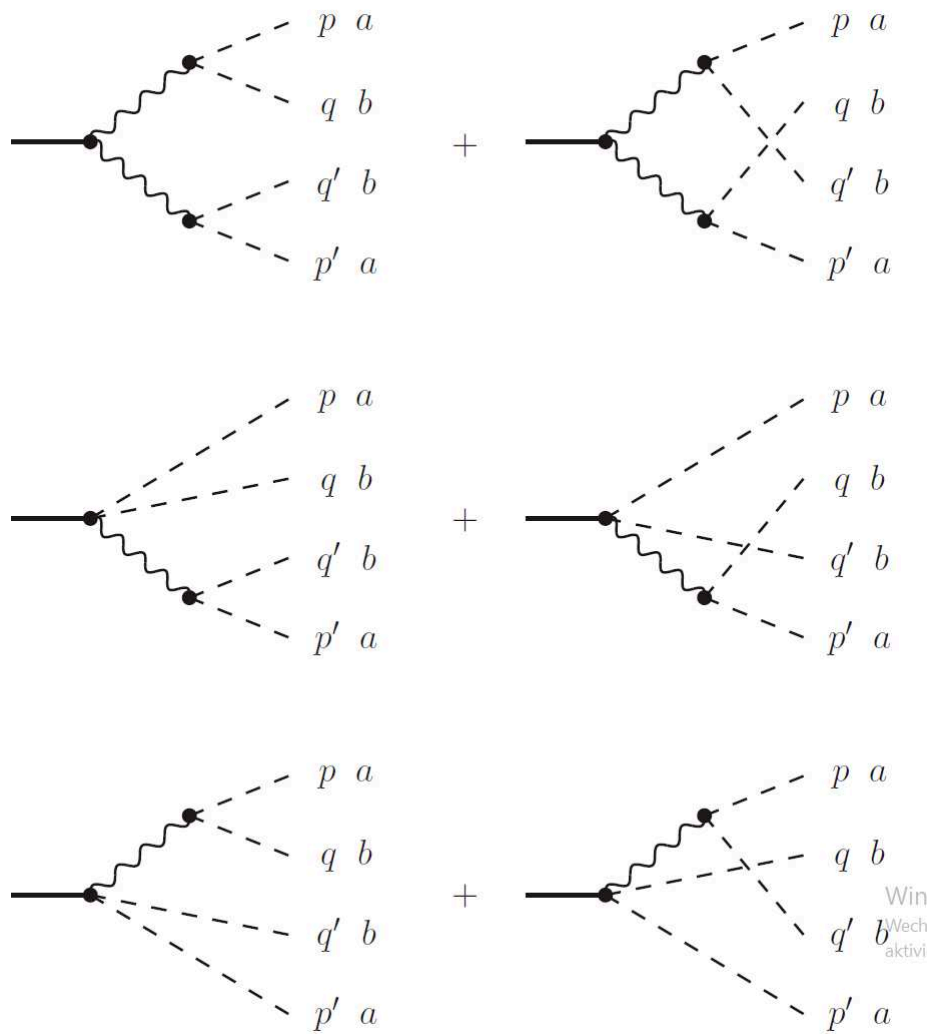


Figure 6.2: Feynman diagrams representing the decay of a scalar glueball (thick line) into four pseudoscalars (dashed lines), partially through intermediate vector mesons (wavy lines). The labels indicate momenta (p , p' , q , and q') and isospin indices (a and b , where $a \neq b$) of the decay products.

$$G \text{Tr}([\pi, \rho]^2), \quad G \text{Tr}(\rho[\rho, \rho]), \quad G \text{Tr}([\rho, \rho]^2), \quad (6.27)$$

which are also suppressed - if at all allowed kinematically, depending on the mass of the glueball under consideration - and will not be considered here.

Let us continue by explicitly showing the corresponding Lagrangian (leaving out the

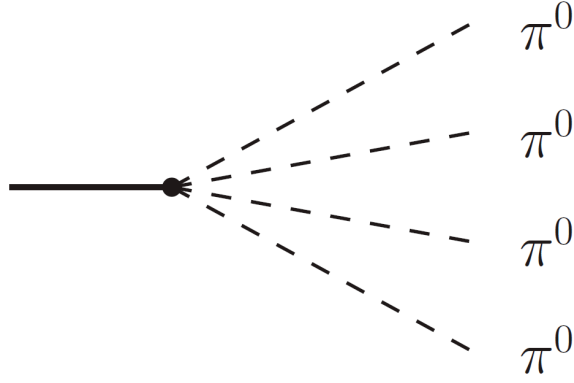


Figure 6.3: Feynman diagram representing the decay of a glueball (thick line) into four π^0 mesons (dashed lines).

$G \rightarrow 4\pi^0$ vertex) for the exotic mode:

$$\begin{aligned}
\mathcal{L}_{G_E} = & -c_2 M_{\text{KK}}^2 \text{Tr} \left[\frac{1}{2} \rho_\mu \rho_\nu \frac{\partial^\mu \partial^\nu}{M_E^2} + \frac{1}{4} (\rho_\mu)^2 \left(1 - \frac{\square}{M_E^2} \right) \right] G_E \\
& - c_3 \text{Tr} \left[\frac{1}{2} \tilde{F}_{\mu\rho} \tilde{F}_\nu^\rho \frac{\partial^\mu \partial^\nu}{M_E^2} - \frac{1}{8} \tilde{F}_{\mu\nu} \tilde{F}^{\mu\nu} \left(1 + \frac{\square}{M_E^2} \right) \right] G_E \\
& - \text{Tr} \left[c_4 \frac{3}{2M_E^2} \rho_\mu \tilde{F}^{\mu\nu} \partial_\nu + \frac{1}{2} \check{c}_2 M_{\text{KK}}^2 \rho_\mu \rho^\mu \right] G_E \\
& - \text{Tr} \left[\frac{1}{4} \check{c}_3 \tilde{F}_{\mu\nu} \tilde{F}^{\mu\nu} + i \check{c}_5 \partial_\mu \pi [\pi, \rho^\mu] \right] G_E \\
& - i c_5 \text{Tr} \left[\partial_\mu \pi [\pi, \rho_\nu] \frac{\partial^\mu \partial^\nu}{M_E^2} + \frac{1}{2} \partial_\mu \pi [\pi, \rho^\mu] \left(1 - \frac{\square}{M_E^2} \right) \right] G_E, \quad (6.28)
\end{aligned}$$

with $\tilde{F}_{\mu\nu} \equiv \partial_\mu \rho_\nu - \partial_\nu \rho_\mu$, where terms proportional to i arise from the Chern-Simons contribution.

The strength of the couplings is again determined by integrals over the holographic coordinate as follows:

$$c_2 = 2\kappa \int dZ K \psi_1^2 \bar{H}_E = \sqrt{2} \times 5.0318 \lambda^{-1/2} N_c^{-1} M_{\text{KK}}^{-1}, \quad (6.29)$$

$$c_3 = 2\kappa \int dZ K^{-1/3} \psi_1^2 \bar{H}_E = \sqrt{2} \times 49.334 \lambda^{-1/2} N_c^{-1} M_{\text{KK}}^{-1}, \quad (6.30)$$

$$c_4 = 2\kappa M_{\text{KK}}^2 \int dZ \frac{20ZK}{(5K-2)^2} \psi_1 \psi_1' H_E = -\sqrt{2} \times 7.4810 \lambda^{-1/2} N_c^{-1} M_{\text{KK}}, \quad (6.31)$$

$$c_5 = \int dZ \frac{\psi_1 \bar{H}_E}{\pi K} = \sqrt{2} \times 1428.1 \lambda^{-1} N_c^{-3/2} M_{\text{KK}}^{-1}, \quad (6.32)$$

$$\check{c}_2 = \frac{1}{2} \kappa \int dZ K \psi_1'^2 H_E = \sqrt{2} \times 2.0970 \lambda^{-1/2} N_c^{-1} M_{\text{KK}}^{-1}, \quad (6.33)$$

$$\check{c}_3 = \frac{1}{2} \kappa \int dZ K^{-1/3} \psi_1^2 H_E = \sqrt{2} \times 12.814 \lambda^{-1/2} N_c^{-1} M_{\text{KK}}^{-1}, \quad (6.34)$$

$$\check{c}_5 = \int dZ \frac{\psi_1 \bar{H}_E}{4\pi K} = \sqrt{2} \times 359.33 \lambda^{-1} N_c^{-3/2} M_{\text{KK}}^{-1}. \quad (6.35)$$

For the dilatonic mode, the analogous expressions are given by

$$\begin{aligned} \mathcal{L}_{G_D} = & \text{Tr} \left[d_2 M_{\text{KK}} \frac{1}{2} \rho_\mu \rho_\nu \left(\eta^{\mu\nu} - \frac{\partial^\mu \partial^\nu}{\square} \right) G_D + d_3 \frac{1}{2} \tilde{F}_{\mu\rho} \tilde{F}_\nu^\rho \left(\eta^{\mu\nu} - \frac{\partial^\mu \partial^\nu}{\square} \right) G_D \right] \\ & + id_5 \text{Tr} \left[\partial_\mu \pi [\pi, \rho_\nu] \left(\eta^{\mu\nu} - \frac{\partial^\mu \partial^\nu}{\square} \right) G_D \right], \end{aligned} \quad (6.36)$$

with

$$d_2 = 2\kappa \int dZ K \psi_1'^2 H_D = 4.3714 \lambda^{-1/2} N_c^{-1} M_{\text{KK}}^{-1}, \quad (6.37)$$

$$d_3 = 2\kappa \int dZ K^{-1/3} \psi_1^2 H_D = 18.873 \lambda^{-1/2} N_c^{-1} M_{\text{KK}}^{-1}, \quad (6.38)$$

and

$$d_5 = \int dZ \frac{\psi_1 H_D}{\pi K} = 512.20 \lambda^{-1} N_c^{-3/2} M_{\text{KK}}^{-1}. \quad (6.39)$$

Furthermore, the vertex corresponding to a direct decay into $4\pi^0$ is given by

$$\mathcal{L}^{G_D \rightarrow 4\pi^0} = 3d_1' [(\partial_\mu \pi^0)^2]^2 G_D - 2d_1' (\partial_\rho \pi^0)^2 (\partial_\mu \pi^0) (\partial_\nu \pi^0) \left(\eta^{\mu\nu} - \frac{\partial^\mu \partial^\nu}{M_D^2} \right) G_D, \quad (6.40)$$

with

$$d'_1 = \frac{3^9 \pi^3}{8 \lambda^3 N_c M_{\text{KK}}^4} \int dZ H_D K^{-8/3} \approx 2.513 \cdot 10^6 \lambda^{-7/2} N_c^{-2} M_{\text{KK}}^{-5}. \quad (6.41)$$

In order to evaluate the decay rates corresponding to the vertices above, we have to compute a many-dimensional phase space integral, which in the case of the decay of a particle of mass M into n massless particles is in general given by

$$\Gamma \propto \frac{1}{2M} \int d\text{LIPS}_4(M) |\mathcal{M}|^2, \quad (6.42)$$

where the square of the absolute value of the amplitude \mathcal{M} is integrated using the *Lorentz Invariant Phase Space* measure, given by

$$d\text{LIPS}_n(M) = (2\pi)^4 \delta^4 \left(M \delta_0^\mu - \sum_{A=1}^n p_A^\mu \right) \prod_{B=1}^n \frac{d^3 p_B}{(2\pi)^3 2p_B^0}. \quad (6.43)$$

Integrals of this type can be evaluated numerically, and we have done so for the computation of glueball four-body decay rates. Fortunately, there exists a closed form of the phase space integral for $\mathcal{M} = 1$, which serves as a useful check of the numerical computation:

$$\int d\text{LIPS}_n(M) = \frac{M^{2n-4}}{2(4\pi)^{2n-3} \Gamma(n) \Gamma(n-1)}, \quad (6.44)$$

where $\Gamma(n)$ is the Gamma function.

In the case of two pairs of identical particles of different isospin indices ($2\pi^a 2\pi^b$ with $a \neq b$), the proportionality factor is $3/4$: a factor of 3 for 3 possible values of the isospin index, and $1/4$ as a symmetry factor to avoid overcounting. For four identical particles ($4\pi^0$), we obtain the factor $1/12$.

In order to finally compute the four-body decay rates of glueballs, it remains to explicitly spell out the amplitude \mathcal{M} for all cases. For $G_D \rightarrow 2\pi^a 2\pi^b$ we obtain

$$\begin{aligned}
i\mathcal{M}_{G_D \rightarrow 2\pi^a 2\pi^b} &= \sqrt{2}g_{\rho\pi\pi}(\Delta_\rho(r) + \Delta_\rho(s))d_5 \mathbf{a} \cdot \mathbf{b} + g_{\rho\pi\pi}^2 \Delta_\rho(r)\Delta_\rho(s)d_2 M_{KK}^2 \mathbf{a} \cdot \mathbf{b} \\
&+ g_{\rho\pi\pi}^2 \Delta_\rho(r)\Delta_\rho(s)d_3 [(a_0 b_0 - \mathbf{a} \cdot \mathbf{b})\mathbf{r} \cdot \mathbf{s} + \mathbf{a} \cdot \mathbf{b}(r_0 s_0 - \mathbf{r} \cdot \mathbf{s})] \\
&- g_{\rho\pi\pi}^2 \Delta_\rho(r)\Delta_\rho(s)d_3 [(a_0 r_0 - \mathbf{a} \cdot \mathbf{r})\mathbf{b} \cdot \mathbf{s} + \mathbf{a} \cdot \mathbf{r}(b_0 s_0 - \mathbf{b} \cdot \mathbf{s})] \\
&+ (q \leftrightarrow q'), \tag{6.45}
\end{aligned}$$

where the momenta p , p' , q , and q' are assigned to individual particles as in Fig. 6.2, and where we define

$$a^\mu \equiv q^\mu - p^\mu, \tag{6.46}$$

$$b^\mu \equiv q'^\mu - p'^\mu, \tag{6.47}$$

$$r^\mu \equiv p'^\mu + q'^\mu, \tag{6.48}$$

and

$$s^\mu \equiv p^\mu + q^\mu, \tag{6.49}$$

with the equality

$$M_D = r^0 + s^0, \tag{6.50}$$

while we take the propagator of intermediate meson states to be given by

$$\Delta_\rho(r) = \frac{1}{r_0^2 - \mathbf{r}^2 - m_\rho^2 + im_\rho \Gamma_\rho}, \tag{6.51}$$

where Γ_ρ is the decay rate of the ρ meson into two pions, and is given through Eq. (5.25).

For the decay $G_D \rightarrow 4\pi^0$ we obtain

$$\begin{aligned}
\mathcal{M}_{G_D \rightarrow 4\pi^0} / (8id_1^2) &= 3[p \cdot qp' \cdot q' + p \cdot p'q \cdot q' + p \cdot q'q \cdot p'] \\
&- p \cdot q\mathbf{p}' \cdot \mathbf{q}' - p' \cdot q'\mathbf{p} \cdot \mathbf{q} - p \cdot p'\mathbf{q} \cdot \mathbf{q}' \\
&- q \cdot q'\mathbf{p} \cdot \mathbf{p}' - p \cdot q'\mathbf{q} \cdot \mathbf{p}' - q \cdot p'\mathbf{p} \cdot \mathbf{q}', \tag{6.52}
\end{aligned}$$

where each of the four four-momenta corresponds to one of the massless pions.

With these expressions we can finally compute the decay rates of the dilatonic glueball into four pions, resulting in

$$\Gamma_{G_D \rightarrow 4\pi} / M_D = 2.4 \times 10^{-3} \dots 3.9 \times 10^{-3}, \quad (6.53)$$

$$\Gamma_{G_D \rightarrow 4\pi^0} / M_D = 4.0 \times 10^{-6} \dots 2.9 \times 10^{-5}. \quad (6.54)$$

We may also perform the analogous computation for an excited dilatonic glueball of $M = 2168 \text{ MeV}$, where the form of the Lagrangian and hence the amplitude remains the same, but the couplings are now determined by

$$d_2^* = -0.9415 \lambda^{-1/2} N_c^{-1} M_{\text{KK}}^{-1}, \quad (6.55)$$

$$d_3^* = 13.680 \lambda^{-1/2} N_c^{-1} M_{\text{KK}}^{-1}, \quad (6.56)$$

and

$$d_5^* = 419.46 \lambda^{-1} N_c^{-3/2} M_{\text{KK}}^{-1}, \quad (6.57)$$

with the result

$$\Gamma_{G_D^* \rightarrow 4\pi} / M_{D^*} = 0.104 \dots 0.142. \quad (6.58)$$

6.4 ◆ DECAY TO TWO VECTOR MESONS

In principle, the vertices above allow for a decay of scalar glueballs to two vector mesons. However, as the ground states of both the dilatonic and the exotic glueballs are too light, pairs of vector mesons only arise as intermediate states in Feynman diagrams. This changes once one considers the first excitations of these modes, with $M_{E^*} = 2168 \text{ MeV}$ and $M_{D^*} = 2358.4 \text{ MeV}$, both being heavier than twice the ρ meson mass. Making use of the vertices for the channel $G^* 2\rho$, we obtain

$$\Gamma_{G_D^* \rightarrow 2\rho} / M_{D^*} \approx \frac{14.330}{\lambda N_c^2} \approx 0.096 \dots 0.127 \quad (6.59)$$

and

$$\Gamma_{G_E^* \rightarrow 2\rho} / M_{E^*} \approx \frac{14.330}{\lambda N_c^2} \approx 0.014 \dots 0.018. \quad (6.60)$$

6.5 ◆ COMPARISON WITH EXPERIMENT

In this section, we compare the results for exotic and dilatonic glueball modes with the experimentally measured decay rates of the glueball candidates $f_0(1500)$ and $f_0(1710)$. More precisely, we compare the dimensionless ratio Γ/M , while extrapolating the glueball mass to the experimental values, which are $M_{f_0(1500)} = 1505 \text{ MeV}$ and $M_{f_0(1710)} = 1722 \text{ MeV}$. Both experimental values and theoretical predictions for $f_0(1500)$ are given in Table 6.1, while those of $f_0(1710)$ are given in Table 6.2. In order to compare with experiment, we have changed the mass of the glueballs from the theoretical prediction to the physical values. This is valid under the assumption that whatever correction to the model changes the mass towards realistic values does not significantly change the interaction terms in the Lagrangians. Given that the predictions for exotic and dilatonic modes differ by orders of magnitude, and that the known decay patterns of $f_0(1500)$ and $f_0(1710)$ are markedly different, we hope that the present results can give at least a rough hint at the correct interpretation of the modes.

Let us begin by noting that the predicted decay rates of scalar glueballs into pseudoscalars, i.e., 2π , 2η , and $2K$, are related by the ratios $3 : 1 : 4$. This is because the model is in the chiral limit, and as a consequence the pseudoscalars are massless. Hence there is neither a contribution from a potential coupling of the glueballs to a mass term, i.e., a term of the form $G\pi^2$, nor a difference in kinematic factors. The ratios arise merely from flavour symmetry, i.e. they account for the multiplicity of particles of the same type. This is a severe shortcoming of the prediction, as the experimental results appear to be strongly influenced by pseudoscalar mass. A remedy is presented in the next chapter, where we include explicit pseudoscalar mass terms.

decay channel	Γ/M (exp.)	Γ/M (exotic)	Γ/M (dilaton)
total	0.072(5)	0.249 ... 0.332	0.027 ... 0.037
$f_0(1500) \rightarrow 4\pi$	0.036(3)	0.003 ... 0.006	0.003 ... 0.005
$f_0(1500) \rightarrow 2\pi$	0.025(2)	0.092 ... 0.122	0.002 ... 0.012
$f_0(1500) \rightarrow 2K$	0.006(1)	0.123 ... 0.163	0.012 ... 0.016
$f_0(1500) \rightarrow 2\eta$	0.004(1)	0.031 ... 0.041	0.003 ... 0.004

Table 6.1: Comparison of the results of the previous section for both exotic and dilaton modes with experimental data for the $f_0(1500)$ isoscalar. The input mass is extrapolated to that of the experimentally measured value of 1505 MeV. Experimental data is taken from [6].

It is clear from the comparison that the exotic glueball is far too broad to be considered a dominant glue component of either the $f_0(1500)$ or the $f_0(1710)$. However, the total decay width of the dilaton glueball is close to that of $f_0(1710)$, and significantly further away from that of $f_0(1500)$. Notably, the prediction for the decay of the $f_0(1500)$ into four pions is roughly one order of magnitude away from the experimental result, where it is the dominant decay channel.

Our results predict a significant decay of $f_0(1710)$ into four pions, when considered to be a predominantly gluonic state, accounting for more than one third of the total decay width. However, the Particle Data Group does not record such a decay channel for the $f_0(1710)$. Considering that there are still large uncertainties with respect to the experimental status of the branching ratios of the mode, our result may be viewed as a prediction that might be checked in future experiments. Beyond this, the holographic approach predicts notable decay into two ω mesons (which in turn decay into pions). The Particle Data Group lists a decay into two ω with the status "seen".

decay channel	Γ/M (exp.)	Γ/M (exotic)	Γ/M (dilaton)
total	0.078(4)	0.252 ... 0.336	0.059 ... 0.076
$f_0(1710) \rightarrow 2K$	0.041(20)/0.047(17)	0.123 ... 0.163	0.012 ... 0.016
$f_0(1710) \rightarrow 2\eta$	0.020(10)/0.022(11)	0.031 ... 0.041	0.003 ... 0.004
$f_0(1710) \rightarrow 2\pi$	0.017(4)/0.009(2)	0.092 ... 0.122	0.009 ... 0.012
$f_0(1710) \rightarrow 4\pi$?	0.006 ... 0.010	0.024 ... 0.030
$f_0(1710) \rightarrow 2\omega \rightarrow 6\pi$	seen	0.00016 ... 0.00021	0.011 ... 0.014

Table 6.2: Comparison of the results of the previous section for both exotic and dilaton modes with experimental data for the $f_0(1710)$ isoscalar. The input mass is extrapolated to that of the experimentally measured value of 1722 MeV. Experimental data is taken from [6], unless when two values are given: in this case values are taken from [83], with experimental input from BES (left, [84]) and WA102 (right, [84]).

7 SCALAR GLUEBALL - MASSIVE QUARKS

"There's always a bigger fish."

Qui-Gon Jinn

7.1 GLUEBALL COUPLING TO THE PSEUDOSCALAR MASS TERM

In Chapter 5 we have shown how quark mass and consequently mass terms for pseudoscalar mesons are incorporated in the Witten-Sakai-Sugimoto model. Unfortunately, a rigorous derivation of the coupling of a scalar glueball to such a mass term is not available. In [33], an educated guess on the form of this coupling was made based on the structure of the mass term induced by the Witten-Veneziano mechanism. We will now revisit this approach.

The proportionality factor in Eq. (5.42) is not known, but it should depend on the holographic coordinate. More generally, as it was phrased in [33], the general form of the mass term, explicitly writing down the tachyonic field $\mathcal{T}(r)$, as well as a factor $h(r)$ accounting for the dependence on the metric field, is proportional to

$$\int d^4x \int_{r_{\text{kk}}}^{\infty} dr h(r) \text{Tr} \left[\mathcal{T}(r) P e^{-i \int dz A_z(x,z)} + \text{h.c.} \right]. \quad (7.1)$$

The right boundary conditions for $\mathcal{T}(r)$ then lead to an expression for the mass matrix, i.e.

$$\mathcal{M} = \text{diag}(m_u, m_d, m_s) \propto \int_{r_{\text{KK}}}^{\infty} dr h(r) \mathcal{T}(r). \quad (7.2)$$

Unfortunately, neither the metric dependence in $h(r)$ nor the tachyon profile $\mathcal{T}(r)$ are known explicitly, so we cannot evaluate the coupling directly. We may, however, consider the coupling of the scalar glueballs (dilaton and exotic) to the Witten-Veneziano mass term. Inserting into the relevant action, we obtain

$$S_{\eta_0 G^2} = -\frac{1}{2} \int d^4x m_0^2 \eta_0^2 (1 - 3d_0 G_D + 5\check{c}_0 G_E), \quad (7.3)$$

with

$$d_0 = 3U_{\text{KK}}^3 \int dU H_D(U) U^{-4} = \frac{17.915}{\lambda^{1/2} N_c M_{\text{KK}}} \quad (7.4)$$

and

$$\check{c}_0 = \frac{3}{4} U_{\text{KK}}^3 \int dU H_E(U) U^{-4} = \frac{15.829}{\lambda^{1/2} N_c M_{\text{KK}}}. \quad (7.5)$$

One possibility would be to assume that there is coupling universality at play, and to take the coupling to the other mass terms to be identical to the above. Another would be to start with the fact that the tachyon field arises from a string stretching between pairs of D8- and anti-D8-branes, and assume that the metric dependence is of the same structure as that in the DBI-action, i.e. $d^9x e^{-\Phi} \sqrt{-g}$. For the dilatonic glueball, this implies a factor of $(1 - 3G_D H_D(r))$, in agreement with Eq. (7.7). For the tachyonic profile, which should be concentrated around the bottom of the cigar geometry, one might try the function that gives rise to the coupling of the glueball to two pseudoscalars, i.e. the metric dependence arising from the term $A_r \partial_\mu^2 A_r$. This would lead to a coupling of the form $\frac{1}{2} m_i^2 P_i^2 3d_1 G_D$, d_1 being the coupling that appears in Eq. (6.12), which differs from d_0 by 4%. It is therefore tempting to assume that the coupling of a scalar glueball to pseudoscalar mass terms is universal, and proceed under the assumption that the coupling is given by

$$\mathcal{L}_{G_D PP}^{(m)} = \frac{1}{2} \sum_i m_i^2 P_i^2 3d_0 G_D. \quad (7.6)$$

This can also be expressed as

$$\mathcal{L}_{G_D PP}^{(m)} = \frac{3}{2} d_0 G_D \mathcal{L}_m, \quad (7.7)$$

where \mathcal{L}_m is given by Eq. (5.31). Consequently, the ratio of decay rate of the dilatonic glueball into two pions and the glueball mass is now given by

$$\Gamma_{G_D \rightarrow \pi\pi} / M_D = \left(1 - 4 \frac{m_\pi^2}{M_D^2}\right)^{1/2} \left(1 + \alpha_D \frac{m_\pi^2}{M_D^2}\right)^2 \frac{3d_1^2 M_D^2}{512\pi}, \quad (7.8)$$

where the first additional factor as compared to Eq. (6.19) is due to kinematics, while the second one arises from the coupling to the mass term. The constant α_D is given by

$$\alpha_D = 4 \left(3 \frac{d_0}{d_1} - 1\right) \approx 8.48. \quad (7.9)$$

The same reasoning applied to the exotic scalar glueball leads to a similar expression:

$$\Gamma_{G_E \rightarrow \pi\pi} / M_E = \left(1 - 4 \frac{m_\pi^2}{M_E^2}\right)^{1/2} \left(1 + \alpha_E \frac{m_\pi^2}{M_E^2}\right)^2 \frac{3(c_1 + 2\check{c}_1)^2 M_E^2}{512\pi}, \quad (7.10)$$

with

$$\alpha_E = 4 \frac{(5\check{c}_0 - \check{c}_1)}{(c_1 + 2\check{c}_1)} \approx 2.630. \quad (7.11)$$

7.2 ◆ RESULTS

The above expressions for decay rates may be evaluated numerically, and generalised to other pseudoscalar mesons. We have only done this for the dilatonic glueball, as the exotic one is not compatible with experimental results, as shown in the previous Chapter. Most importantly, the phenomenon that the decay of the $f_0(1710)$ isoscalar into two kaons is enhanced as compared to that into two pions and two eta mesons is accurately reproduced by our calculation. The holographic prediction for the ratio $\Gamma(\pi\pi)/\Gamma(K\bar{K})$ lies within experimental error bars, while the result for $\Gamma(\eta\eta)/\Gamma(K\bar{K})$ is found within 1.33 standard deviations of the experimental value. In [33] we have called this phenomenon

$f_0(1710)$	exp.	prediction
$\frac{4}{3} \cdot \Gamma(\pi\pi)/\Gamma(K\bar{K})$	$0.55^{+0.15}_{-0.23}$	0.463
$4 \cdot \Gamma(\eta\eta)/\Gamma(K\bar{K})$	1.92 ± 0.60	1.12

Table 7.1: Comparison of the holographic results with experimental data from [6], illustrating the correct reproduction of nonchiral enhancement.

nonchiral enhancement, in contrast to the term *chiral suppression*. This is because in the holographic approach, the massive (nonchiral) case is a modification of the massless (chiral) one, not the other way around. A numerical comparison between our result and experimental data is shown in Table 7.1.

A full comparison of all results, including the chiral case, both for the $f_0(1500)$ and the $f_0(1710)$ isoscalar is shown in Table 7.2. While the agreement is still not good for the $f_0(1500)$ meson (in fact, worse for certain channels), the introduction of quark masses leads to a much better agreement of experimental data for the $f_0(1710)$ meson with the decay patterns of a holographic glueball.

7.3 ◆ CONSTRAINTS ON $\eta\eta'$ DECAY

In the previous two sections, results were obtained under the assumption of universal coupling of a scalar glueball to the pseudoscalar mass term. In [34] this assumption was relaxed and the consequences of a deviation of the coupling due to finite quark mass from that of the coupling to the Witten-Veneziano term were studied. In this section, we describe the results of this investigation.

We assume that any coupling of the dilatonic glueball to a pseudoscalar mass term will be of the form of Eq. (7.7). In order to consider case that the prefactor does not agree with that of the coupling to the Witten-Veneziano mass term, the Equation is changed to

$$\mathcal{L}_{G_D P P}^{(m,x)} = \frac{3}{2} x d_0 G_D \mathcal{L}_m, \quad (7.12)$$

where x is a real parameter of arbitrary value, and $\mathcal{L}_{G_D P P}^{(m,1)} = \mathcal{L}_{G_D P P}^{(m)}$.

With the above Lagrangian, the decay rate into two pions or kaons is now given by

decay	Γ/M (exp.)	(WSS chiral)	(WSS massive)
$f_0(1500)$ (total)	0.072(5)	0.027...0.037	0.057...0.077
$f_0(1500) \rightarrow 4\pi$	0.036(3)	0.003...0.005	0.003...0.005
$f_0(1500) \rightarrow 2\pi$	0.025(2)	0.009...0.012	0.010...0.014
$f_0(1500) \rightarrow 2K$	0.006(1)	0.012...0.016	0.034...0.045
$f_0(1500) \rightarrow 2\eta$	0.004(1)	0.003...0.004	0.010...0.013
$f_0(1710)$ (total)	0.078(4)	0.059...0.076	0.083...0.106
$f_0(1710) \rightarrow 2K$	* $\begin{cases} 0.041(2) \\ 0.047(17) \end{cases}$	0.012...0.016	0.029...0.038
$f_0(1710) \rightarrow 2\eta$	* $\begin{cases} 0.020(10) \\ 0.022(11) \end{cases}$	0.003...0.004	0.009...0.011
$f_0(1710) \rightarrow 2\pi$	* $\begin{cases} 0.017(4) \\ 0.009(2) \end{cases}$	0.009...0.012	0.010...0.013
$f_0(1710) \rightarrow 2\rho, \rho\pi\pi \rightarrow 4\pi$?	0.024...0.030	0.024...0.030
$f_0(1710) \rightarrow 2\omega \rightarrow 6\pi$	seen	0.011...0.014	0.011...0.014

Table 7.2: Comparison of the holographic result with measurement, showing all relevant decay branches both for the $f_0(1500)$ and the $f_0(1710)$ isoscalar meson. Experimental data is taken from [6], unless when two values are given: in this case values are taken from [83], with experimental input from BES (left, [84]) and WA102 (right, [84]).

$$\Gamma(G_D \rightarrow PP) = \frac{n_P d_1^2 M_D^3}{512\pi} \left(1 - 4 \frac{m_P^2}{M_D^2}\right)^{1/2} \left(1 + \alpha_D^{(x)} \frac{m_P^2}{M_D^2}\right)^2 \quad (7.13)$$

with

$$\alpha_D^{(x)} = 4 \left(3 \frac{d_0}{d_1} x - 1\right) \approx 4(3.120x - 1), \quad (7.14)$$

where, $n_P = 3$ for pions, and $n_P = 4$ for kaons. For η mesons, mixing of η and η' implies that $\alpha_D^{(x)}$ has to be replaced by

$$\alpha_{D,\eta}^{(x)} = 4 \left[3 \frac{d_0}{d_1} \left(x + \sin^2 \theta_P \frac{m_0^2}{m_\eta^2} (1-x)\right) - 1\right]. \quad (7.15)$$

In the case of a decay of a glueball into two η' mesons, if permitted kinematically, the expression would be

$$\alpha_{D,\eta'}^{(x)} = 4 \left[3 \frac{d_0}{d_1} \left(x + \cos^2 \theta_P \frac{m_0^2}{m_{\eta'}^2} (1-x)\right) - 1\right]. \quad (7.16)$$

Beyond its influence on the decay rate into two η mesons, $\eta - \eta'$ mixing also leads to a nonvanishing decay of a scalar glueball into an η and an η' meson, for which the Lagrangian is given by

$$\mathcal{L}_{G_D \eta \eta'}^{(m,x)} = -\frac{3}{2}(1-x)d_0 \sin(2\theta_P) m_0^2 G_D \eta \eta'. \quad (7.17)$$

The corresponding decay rate reads

$$\Gamma(G_D \rightarrow \eta \eta') = \frac{|\mathbf{p}|}{8\pi M_D^2} \left(\frac{3}{2}(1-x)d_0 \sin(2\theta_P) m_0^2\right)^2, \quad (7.18)$$

with

$$|\mathbf{p}| = \frac{1}{2M_D} \sqrt{[M_D^2 - (m_\eta + m_{\eta'})^2][M_D^2 - (m_\eta - m_{\eta'})^2]}. \quad (7.19)$$

In Figures 7.1 and 7.2 we compare the results as a function of the parameter x with experimental data, where we have set the glueball mass to that of the $f_0(1500)$ and $f_0(1710)$ isoscalars, respectively. Experimental values are taken from [6], except for the upper bound for the decay into $\eta \eta'$ in Fig. 7.2, which comes from [74]. In the comparison

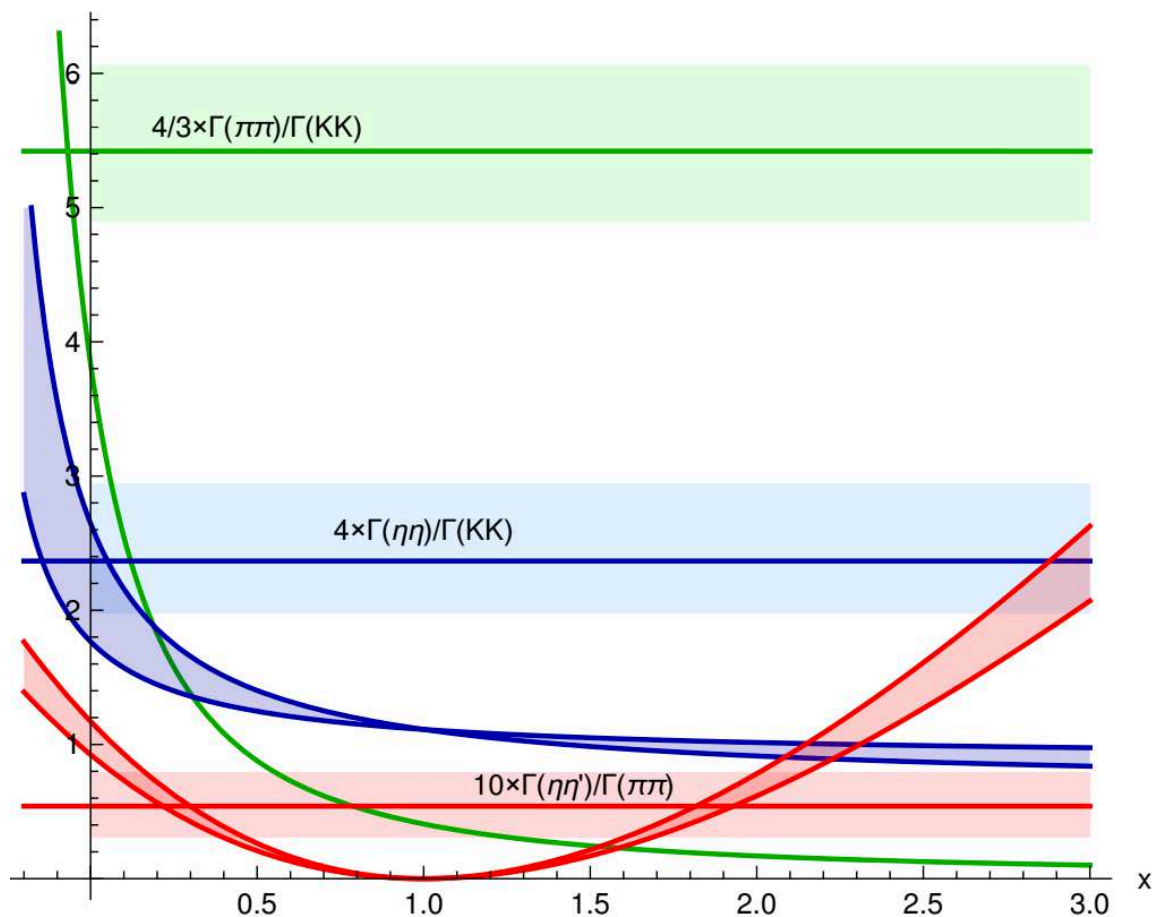


Figure 7.1: Comparison of the model prediction for ratios of glueball decay rates into pseudoscalar mesons as a function of the parameter x to experimental data [6], where horizontal lines indicate the value, and coloured areas the error bars. The mass of the glueball is set to that of the $f_0(1500)$ isoscalar. Ranges for theoretical values follow from the variation of the 't Hooft coupling between 12.55 and 16.63.

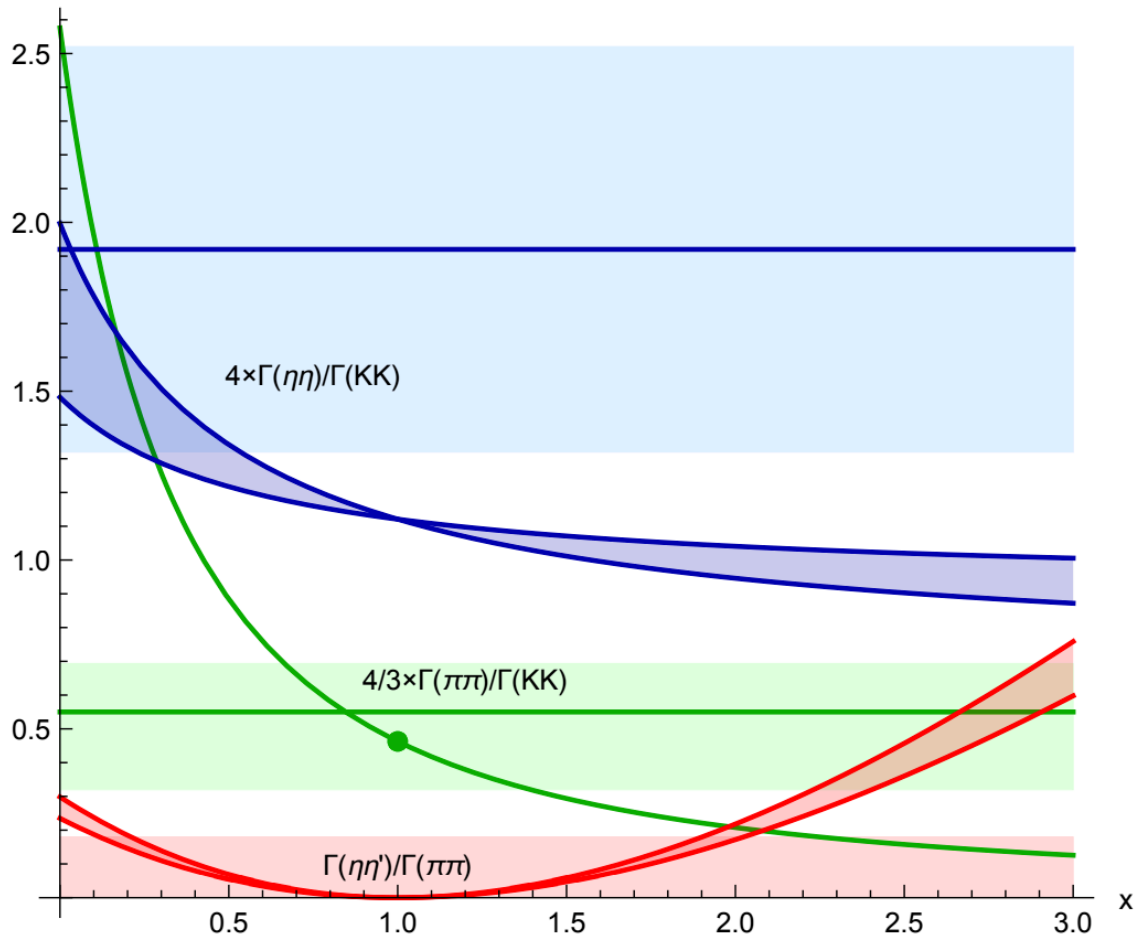


Figure 7.2: Comparison of the model prediction for ratios of glueball decay rates into pseudoscalar mesons as a function of the parameter x to experimental data [6, 74], where horizontal lines indicate the value, and coloured areas the error bars. The mass of the glueball is set to that of the $f_0(1710)$ isoscalar. Ranges for theoretical values follow from the variation of the 't Hooft coupling between 12.55 and 16.63, while green dot denotes the value corresponding to $x = 1$ that was found in [33] and linked to nonchiral enhancement.

with $f_0(1500)$ data, we see that there is agreement only when $x \approx 0$. While this is a possibility, the previous Chapter has shown that $f_0(1500)$ does not come out as good as $f_0(1710)$ due to too low decay rates into two and four pions. For $f_0(1710)$ we see that there is, in accordance with (7.14), an important point at $x \approx 0.32$, where $\alpha_D^{(x)}$ vanishes. For $x > 0.32$ we obtain $\Gamma(G_D \rightarrow \pi\pi) < \Gamma(G_D \rightarrow KK)$, and hence nonchiral enhancement, while for $x < 0$ we obtain the opposite of what is observed in experiment. Interestingly, it is now possible to establish a correlation between nonchiral enhancement and the value of the decay into η and η' . We may deduce a constraint, an upper bound on the possible value of the ratio $\Gamma(G_D \rightarrow \eta\eta')/\Gamma(G_D \rightarrow \pi\pi)$ by requiring the holographic prediction for $4/3 \times \Gamma(G_D \rightarrow \pi\pi)/\Gamma(G_D \rightarrow KK)$ to remain within the experimental error bars. In other words: how large may the ratio $\Gamma(G_D \rightarrow \eta\eta')/\Gamma(G_D \rightarrow \pi\pi)$ be while still having nonchiral enhancement compatible with experiment? The answer is that the upper bound is given by a value of approximately 0.04, less than the experimental bound of 0.18 from [74].

8 TENSOR GLUEBALL

“Sir, it’s very possible this asteroid is not stable.”

C-3PO

8.1 VERTICES

The Lagrangian describing the interactions of a tensor glueball is obtained in complete analogy to the scalar case, i.e., by dimensionally reducing the mode of Eq. (4.36), inserting it into the DBI action, and integrating out all extra dimensions. The resulting expression is given by

$$\mathcal{L}_T = \text{Tr} \left[\frac{1}{2} t_1 \partial_\mu \pi \partial_\nu \pi G_T^{\mu\nu} + \frac{1}{2} t_2 M_{\text{KK}}^2 \rho_\mu \rho_\nu G_T^{\mu\nu} + \frac{1}{2} t_3 \tilde{F}_{\mu\rho} \tilde{F}_\nu^\rho G_T^{\mu\nu} + i t_5 \partial_\mu \pi [\pi, \rho_\nu] G_T^{\mu\nu} \right], \quad (8.1)$$

where the transverse traceless tensor $G_T^{\mu\nu}$ encodes possible polarisations of the glueball, i.e., $G_T^{\mu\nu} = \epsilon^{\mu\nu} G_T$, and the constants t_i are related to those in the dilatonic Lagrangian by $t_i = \sqrt{6} d_i$.

In [32] only the first three terms were considered, as they suffice for a few interesting physical predictions. In the following sections, we will summarise these results.

8.2 DECAY TO TWO PIONS

Making use of the above Lagrangian, we may again compute the decay rate of the glueball into two pions by applying Feynman rules. Since the tensor glueball admits different

polarisations, there are two options: we may average over all possible polarisations, or we may choose a fixed polarisation and integrate over the orientation of the coordinate system. We take the latter route, choosing the polarisation $\epsilon^{11} = -\epsilon^{22} = 1$. In the rest frame of the glueball, the scattering amplitude is then given by

$$|\mathcal{M}_T| = |t_1(p_x^2 - p_y^2)|, \quad (8.2)$$

with

$$p_x = |\mathbf{p}| \cos \phi \sin \theta, \quad (8.3)$$

$$p_y = |\mathbf{p}| \sin \phi \sin \theta, \quad (8.4)$$

and

$$|\mathbf{p}| = M_T/2, \quad (8.5)$$

with

$\phi \in [0, 2\pi)$ and $\theta \in [0, \pi)$. For the dimensional ratio of the decay rate and the mass of the lightest tensor glueball, this implies

$$\Gamma_{T \rightarrow \pi\pi}/M_T = \frac{3}{32\pi M_T^2} \int \frac{d\Omega}{4\pi} |\mathcal{M}_T|^2 = \frac{1}{640\pi} |t_1|^2 M_T^2 = 0.0145 \dots 0.0193, \quad (8.6)$$

while for the first excited tensor mode, we obtain

$$\Gamma_{T^* \rightarrow \pi\pi}/M_{T^*} = \frac{3}{32\pi M_{T^*}^2} \int \frac{d\Omega}{4\pi} |\mathcal{M}_{T^*}|^2 = \frac{1}{640\pi} |t_1^*|^2 M_{T^*}^2 = 0.0175 \dots 0.0233. \quad (8.7)$$

8.3 ◆ DECAY TO TWO VECTOR MESONS

According to the holographic prediction, the mode corresponding to the lightest tensor glueball is too light to decay into two ρ or ω mesons, but the first excited mode with $M_{T^*} = 2358.4$ MeV lies above the relevant mass threshold. The expression for the ratio

of decay rate and glueball mass involves a sum over all possible polarisations of the vector mesons, and is given by

$$\begin{aligned}\Gamma_{T^* \rightarrow 2\rho}/M_{T^*} &= 3 \frac{\sqrt{(M_{T^*}/2)^2 - m_\rho^2}}{16\pi M_{T^*}^2} \int \frac{d\Omega}{4\pi} \sum_{\lambda_1, \lambda_2=1}^3 |\mathcal{M}_{\epsilon_T}(\lambda_1, \lambda_2)|^2 \\ &\approx \frac{21.236}{\lambda N_c^2} \approx 0.142 \dots 0.188,\end{aligned}\quad (8.8)$$

with the explicit expression for the amplitude

$$\begin{aligned}\mathcal{M}_{\epsilon_T}(\lambda_1, \lambda_2) &= \epsilon_\mu(p, \lambda_1) \epsilon_\nu(q, \lambda_2) \left[t_2^* M_{\text{KK}}^2 \epsilon_T^{\mu\nu} \right. \\ &\quad \left. - t_3^* (p_\rho \epsilon_T^{\rho\sigma} q_\sigma \eta^{\mu\nu} + p_\rho q^\rho \epsilon_T^{\mu\nu} - p^\nu \epsilon_T^{\mu\rho} q_\rho - q^\mu \epsilon_T^{\nu\rho} p_\rho) \right],\end{aligned}\quad (8.9)$$

as well as the integral

$$\begin{aligned}\int \frac{d\Omega}{4\pi} \sum_{\lambda_1, \lambda_2=1}^3 |\mathcal{M}_{\epsilon_T}(\lambda_1, \lambda_2)|^2 &= 2(t_2^* M_{\text{KK}}^2/m_\rho^2)^2 \left[\frac{2}{15} (\mathbf{p}^2)^2 + \frac{2}{3} m_\rho^2 \mathbf{p}^2 + m_\rho^4 \right] \\ &\quad + 4t_2^* t_3^* M_{\text{KK}}^2 \left[\frac{4}{3} \mathbf{p}^2 + m_\rho^2 \right] \\ &\quad + 2(t_3^*)^2 \left[\frac{8}{15} (\mathbf{p}^2)^2 + 2m_\rho^2 \mathbf{p}^2 + m_\rho^4 \right],\end{aligned}\quad (8.10)$$

with $p^0 = q^0 = M_{T^*}/2$, $\mathbf{p} = -\mathbf{q}$, and $\mathbf{p}^2 = (M_{T^*}/2)^2 - m_\rho^2$. The factor of 3 in Eq. (8.8) arises from the possible isospin values of the ρ meson. Consequently, the result for the ω meson is 1/3 of the value for the ρ meson, i.e.,

$$\Gamma_{T^* \rightarrow 2\omega}/M_{T^*} \approx \frac{7.079}{\lambda N_c^2} \approx 0.047 \dots 0.063.\quad (8.11)$$

8.4 ◆ RESULTS

As the model value of the mass of the lightest tensor glueball (1487 MeV) is unfortunately far away from both the lattice result (≈ 2.4 GeV) and the mass of possible experimental candidates (around and above 2 GeV), we will extrapolate the glueball mass to different

values, i.e. 2 GeV and 2.4 GeV, in order to obtain a more realistic picture of the possible decay patterns.

The results are summarized in Table 8.1. The extrapolation has a considerable effect on the decay branches, as the mass of the glueball is now large enough to allow for a decay into two ρ , ω , K^* , or ϕ mesons. We have also incorporated masses for pseudoscalars by a phase space factor of the form $(1 - 4m^2/M_T^2)^{5/2}$, which seems sufficient, given that a tensor glueball would not couple linearly to a potential pseudoscalar mass term. We have done the same for the K^* and ϕ mesons, whose masses differ notably from m_ρ , i.e., $m_{K^*} \approx 890$ MeV and $m_\phi \approx 1020$ MeV. In addition, we have adjusted the coupling constant t_2 such that it corresponds to a coupling of the tensor glueball to a mass terms with aforementioned masses.

The consequence of all the above considerations is that the holographic approach predicts a tensor glueball around or above 2 GeV to be a very broad state with a rich variety of decay channels. For 2.4 GeV we obtain a tensor glueball that is much broader than all f_2 mesons listed in [6]. With a mass of 2 GeV, the total decay width ($\Gamma \approx 600 \dots 900$) is not identical to, but at least in the same order of magnitude of that of the $f_2(1950)$ meson with $\Gamma = 472(18)$ MeV, which is considered a potential glueball candidate.

decay channel	M (MeV)	Γ/M
$T \rightarrow 2\pi$	1487	0.013 ... 0.018
$T \rightarrow 2K$	1487	0.004 ... 0.006
$T \rightarrow 2\eta$	1487	0.0005 ... 0.0007
total	1487	$\approx 0.02 \dots 0.03$
$T \rightarrow 2\rho \rightarrow 4\pi$	2000	0.135 ... 0.178
$T \rightarrow 2K^* \rightarrow 2K2\pi$	2000	0.119 ... 0.177
$T \rightarrow 2\omega \rightarrow 6\pi$	2000	0.045 ... 0.059
$T \rightarrow 2\pi$	2000	0.014 ... 0.018
$T \rightarrow 2K$	2000	0.010 ... 0.013
$T \rightarrow 2\eta$	2000	0.0018 ... 0.0024
total	2000	$\approx 0.32 \dots 0.45$
$T \rightarrow 2K^* \rightarrow 2K2\pi$	2400	0.173 ... 0.250
$T \rightarrow 2\rho \rightarrow 4\pi$	2400	0.159 ... 0.211
$T \rightarrow 2\omega \rightarrow 6\pi$	2400	0.053 ... 0.070
$T \rightarrow 2\phi$	2400	0.032 ... 0.051
$T \rightarrow 2\pi$	2400	0.014 ... 0.019
$T \rightarrow 2K$	2400	0.012 ... 0.016
$T \rightarrow 2\eta$	2400	0.0025 ... 0.0034
total	2400	$\approx 0.45 \dots 0.62$

Table 8.1: Decay rates of the tensor glueball for 3 different values of the mass, including the model prediction of 1487 MeV.

9 PSEUDOSCALAR GLUEBALL

"You'll find I'm full of surprises."

Luke Skywalker

9.1 VERTICES

Interaction vertices of a pseudoscalar glueball may be obtained from the fact that both the glueball fluctuations (4.43) and the η_0 field (as shown in Section 5.3) appear in the Ramond-Ramond action (2.14). In [35], the following modification of the two-form field strength (5.29) was considered:

$$\tilde{F}_2 \rightarrow \tilde{F}_2 + dC'_1, \quad (9.1)$$

where the glueball fluctuation is contained in the τ -component of the one-form C'_1 as

$$C'_\tau = H_P(U)G_P(x). \quad (9.2)$$

Instead of r we use the coordinate U because the explicit solution for \tilde{F}_2 is given in terms of the latter in Eq. (5.29).

Writing down the Ramond-Ramond action with the above solution explicitly in terms of components, we obtain

$$S_{\text{RR}} = -\frac{1}{4\pi(2\pi l_s)^6} \int d^{10}x \sqrt{-g} \left[g^{mn} g^{\tau\tau} \partial_m C'_\tau \partial_n C'_\tau + g^{UU} g^{\tau\tau} \frac{c^2}{U^8} \left(\theta + \frac{\sqrt{2N_f}}{f_\pi} \eta_0(x) \right)^2 + 2g^{mU} g^{\tau\tau} \partial_m C'_\tau \frac{c}{U^4} \left(\theta + \frac{\sqrt{2N_f}}{f_\pi} \eta_0(x) \right) \right], \quad (9.3)$$

with

$$c \equiv \frac{4\lambda^3 M_{\text{KK}}^4 l_s^6}{3^5 \pi}. \quad (9.4)$$

Note that there are no direct couplings of the pseudoscalar glueball to pseudoscalar mesons other than those contained in the η_0 field, i.e., η and η' . However, the presence of metric components in Eq. (9.3) allows for a coupling through intermediate glueballs. Schematically, the resulting Lagrangian looks like, with $\tilde{G} \equiv G_P(x)$,

$$\mathcal{L}_{\tilde{G}} = -\frac{1}{2} \partial_\mu \tilde{G} \partial^\mu \tilde{G} - \frac{1}{2} m_P^2 \tilde{G} - \frac{1}{2} m_0^2 \eta_0^2 + \mathcal{L}_{\eta_0^2 G} + \mathcal{L}_{\tilde{G} \eta_0 G} + \mathcal{L}_{\tilde{G}^2 G} + \mathcal{O}(G^2), \quad (9.5)$$

where G denotes any scalar or tensor glueball mode. For the lightest pseudoscalar glueball we obtain

$$\mathcal{L}_{\tilde{G} \eta_0 G} = \tilde{d}_0 \tilde{G} \eta_0 G_D + \tilde{c}_0 \tilde{G} \eta G_E + \tilde{c}'_0 \partial_\mu \tilde{G} \eta_0 \partial^\mu G_E + \tilde{c}''_0 \tilde{G} \eta_0 \frac{\square - M_E^2}{M_E^2} G_E, \quad (9.6)$$

$$\mathcal{L}_{\eta_0^2 G} = \frac{1}{2} m_0^2 \eta_0^2 (3d_0 G_D - 5\check{c}_0 G_E) + \frac{1}{2} \bar{c}_0 m_0^2 \eta_0^2 \frac{\square - M_E^2}{M_E^2} G_E, \quad (9.7)$$

and

$$\mathcal{L}_{\tilde{G}^2 G} = \mathcal{L}_{\tilde{G}^2 G_{D,T}} + \mathcal{L}_{\tilde{G}^2 G_E} \quad (9.8)$$

with

$$\mathcal{L}_{\tilde{G}^2 G_{D,T}} = \tilde{d}_1 \left[\frac{1}{2} \partial_\mu \tilde{G} \partial^\mu \tilde{G} - \frac{1}{8} \partial_\mu \tilde{G} \partial_\nu \tilde{G} \frac{\partial^\mu \partial^\nu}{\square} \right] G_D + \frac{1}{2} \tilde{d}_2 m_P^2 \tilde{G}^2 G_D + \frac{\sqrt{6}}{8} \tilde{d}_1 \partial_\mu \tilde{G} \partial_\nu \tilde{G} T^{\mu\nu} \quad (9.9)$$

and

$$\begin{aligned}\mathcal{L}_{\tilde{G}^2 G_E} &= \frac{1}{2} \tilde{c}_1 \partial_\mu \tilde{G} \partial^\mu \tilde{G} G_E + \frac{1}{2} \tilde{c}_2 m_P^2 \tilde{G}^2 G_E + \tilde{c}_3 \partial_\mu \tilde{G} \partial_\nu \tilde{G} \frac{\partial^\mu \partial^\nu}{M_E^2} G_E \\ &+ \tilde{c}_4 \partial_\mu \tilde{G} \partial^\mu \tilde{G} \frac{\square - M_E^2}{M_E^2} G_E + \tilde{c}_5 m_P^2 \tilde{G}^2 \frac{\square - M_E^2}{M_E^2} G_E.\end{aligned}\quad (9.10)$$

The coupling constants are given by

$$\begin{aligned}d_0 &= 3U_{\text{KK}}^3 \int dU H_D(U) U^{-4} \\ &= 17.915 \times \lambda^{-1/2} N_c^{-1} M_{\text{KK}}^{-1},\end{aligned}\quad (9.11)$$

$$\begin{aligned}\tilde{d}_0 &= \tilde{\alpha} \frac{54\sqrt{3} U_{\text{KK}}^3 \pi N_f^{1/2}}{\lambda^{1/2} N_c^{1/2}} \int dU \partial_U H_P(U) H_D(U) dU \\ &= 2.5833 \times \lambda^{1/2} N_f^{1/2} N_c^{-3/2} M_{\text{KK}},\end{aligned}\quad (9.12)$$

$$\begin{aligned}\tilde{d}_1 &= -\frac{8}{\sqrt{6}} \tilde{\alpha} R^3 \int dU U H_P(U)^2 H_T(U) f(U)^{-1} \\ &= 42.484 \times \lambda^{-1/2} N_c^{-1} M_{\text{KK}}^{-1},\end{aligned}\quad (9.13)$$

$$\begin{aligned}\tilde{d}_2 &= -6\tilde{\alpha} \int dU [H_D(U) H_P(U)^2 U f(U)^{-1} R^3 \\ &\quad - M_P^{-2} U^4 H_P(U) \partial_U H_P(U) \partial_U H_D(U)] \\ &= 27.106 \times \lambda^{-1/2} N_c^{-1} M_{\text{KK}}^{-1},\end{aligned}\quad (9.14)$$

$$\begin{aligned}\tilde{c}_0 &= \frac{3}{4} U_{\text{KK}}^3 \int dU H_E(U) U^{-4} \\ &= 15.829 \times \lambda^{-1/2} N_c^{-1} M_{\text{KK}}^{-1},\end{aligned}\quad (9.15)$$

$$\begin{aligned}\bar{c}_0 &= \frac{3}{2} U_{\text{KK}}^3 \int dU H_E(U) U^{-4} \left(\frac{1}{4} + \alpha\right) \\ &= 26.837 \times \lambda^{-1/2} N_c^{-1} M_{\text{KK}}^{-1},\end{aligned}\quad (9.16)$$

$$\begin{aligned}
\tilde{c}_0 &= -\tilde{\alpha} \frac{45\sqrt{3}U_{\text{KK}}^3\pi N_f^{1/2}}{2\lambda^{1/2}N_c^{1/2}} \int dU \partial_U H_P(U) H_E(U) \\
&= -4.8795 \times \lambda^{1/2} N_f^{1/2} N_c^{-3/2} M_{\text{KK}},
\end{aligned} \tag{9.17}$$

$$\begin{aligned}
\tilde{c}'_0 &= \frac{45\sqrt{3}\pi N_f^{1/2}}{U_{\text{KK}}^3 \lambda^{1/2} N_c^{1/2} M_E^2} \int dU U^2 \alpha^2 H_P(U) H_E(U) \\
&= -1.0042 \times \lambda^{1/2} N_f^{1/2} N_c^{-3/2} M_{\text{KK}},
\end{aligned} \tag{9.18}$$

$$\begin{aligned}
\tilde{c}'' &= \tilde{\alpha} \frac{9\sqrt{3}U_{\text{KK}}^3\pi N_f^{1/2}}{\lambda^{1/2}N_c^{1/2}} \int dU \partial_U H_P(U) H_E(U) \left(\frac{1}{4} + \alpha\right) \\
&= 2.0502 \times \lambda^{1/2} N_f^{1/2} N_c^{-3/2} M_{\text{KK}},
\end{aligned} \tag{9.19}$$

$$\begin{aligned}
\tilde{c}_1 &= 2\tilde{\alpha} \int dU U R^3 f(U)^{-1} H_P(U)^2 H_E(U) (1 - \alpha) \\
&= -19.3023 \times \lambda^{-1/2} N_c^{-1} M_{\text{KK}},
\end{aligned} \tag{9.20}$$

$$\begin{aligned}
\tilde{c}_2 &= -\frac{5}{2} \frac{\tilde{\alpha}}{M_P^2} \int dU U^4 (\partial_U H_P(U))^2 H_E(U) \\
&= -40.9678 \times \lambda^{-1/2} N_c^{-1} M_{\text{KK}}^{-1},
\end{aligned} \tag{9.21}$$

$$\begin{aligned}
\tilde{c}_3 &= -\tilde{\alpha} \int dU U R^3 f(U)^{-1} H_P(U)^2 H_E(U) \left(\frac{1}{4} + \alpha\right) \\
&= -8.78243 \times \lambda^{-1/2} N_c^{-1} M_{\text{KK}},
\end{aligned} \tag{9.22}$$

$$\tilde{c}_4 = -\frac{1}{2} \tilde{c}_3, \tag{9.23}$$

$$\begin{aligned}\tilde{c}_5 &= \frac{1}{2} \frac{\tilde{\alpha}}{M_P^2} \int dUU^4 (\partial_U H_P(U))^2 H_E(U) \left(\frac{1}{4} + \alpha_E\right) \\ &= 7.65685 \times \lambda^{-1/2} N_c^{-1} M_{\text{KK}}^{-1},\end{aligned}\tag{9.24}$$

with

$$\tilde{\alpha} = -\frac{1}{4\pi(2\pi l_s)^6} \frac{2\pi}{M_{\text{KK}}} V_4\tag{9.25}$$

and

$$\alpha = \frac{3}{5K - 2}.\tag{9.26}$$

It is noteworthy that for the pseudoscalar glueball with either η or η' , i.e., there is no term proportional containing exclusively the product $\tilde{G}\eta_0$. Furthermore, a mixing term arising from a similar mechanism that generates finite quark mass in the holographic approach is unlikely, as Ramond-Ramond fields do not couple directly to fundamental strings. In [86] an alternative derivation of the Witten-Veneziano mechanism in the Sakai-Sugimoto model that implies kinetic mixing was presented. Mixing with η_0 leads to additional decay channels, and the results in the following sections correspond to an unmixed pseudoscalar. However, relatively recent lattice computations do not show evidence for significant unquenching effects that would be a consequence of strong mixing of a pseudoscalar glueball with radially excited η/η' mesons [87, 88, 89].

9.2 ◆ RESULTS - DECAY RATES

Decay rates may be obtained from the above Lagrangians in analogy to the previous sections, making use of Feynman rules. As stated in the previous section, decay into final states consisting only of pseudoscalar mesons may happen only through the presence of an intermediate glueball. Since it has proven to be the better choice for a mode describing a scalar glueball comparable to experiment, we will restrict ourselves to vertices including the dilatonic glueball, and not consider the exotic one.

An important observation about possible decay patterns follows directly from Eq. (9.6) without the need for a calculation: any potential final state will always contain at least one η or η' meson. This differs from results obtained in the extended linear sigma model [90], as well as with large- N_c chiral Lagrangians [91], where the dominant decay mode of a pseudoscalar glueball is $K\bar{K}\pi$.

For the purpose of obtaining a broader picture than that conveyed by just considering the model result for the mass of the pseudoscalar glueball, $M_P \approx 1789$ MeV, we have treated M_P as a free parameter and studies how decay rates behave as a function of it. This is important because finite decay involving an on-shell scalar glueball is only possible above a threshold, i.e., when $M_P > M_G + M_\eta$ for decays involving $G\eta$, and $M_P > M_G + M_{\eta'}$ for decays involving $G\eta'$, where $G \equiv G_D$. The decay widths corresponding to these two channels, for values of λ varied between 12.55 and 16.63, are shown in Fig. 9.1 both for $M_G = 1.5$ GeV and $M_G = 1.723$ GeV. Decay rates for the channel $G\eta'$ grow significantly faster as a function of M_P than their $G\eta$ counterparts.

Pseudoscalar glueball decay with final states involving only pseudoscalar mesons is also possible, even below the aforementioned threshold. This is because as shown in Chapters 6 and 7, a scalar glueball decays into pairs of pseudoscalar mesons, and may appear as an intermediate (off-shell) state in a decay channel of the form $\tilde{G} \rightarrow G\eta^{(\prime)} \rightarrow PP\eta^{(\prime)}$, where $P = K, \pi, \eta, \eta'$. The results can be seen in Fig. 9.2. We have used $x = 1$ for the coupling of the scalar glueball to the pseudoscalar mass terms (see Chapter 7). We see that for a glueball mass of 2.6 GeV, as predicted by lattice QCD, and below, the pseudoscalar glueball is a narrow state, given that there are no decay channels that lie beyond the reach of the Witten-Sakai-Sugimoto model.

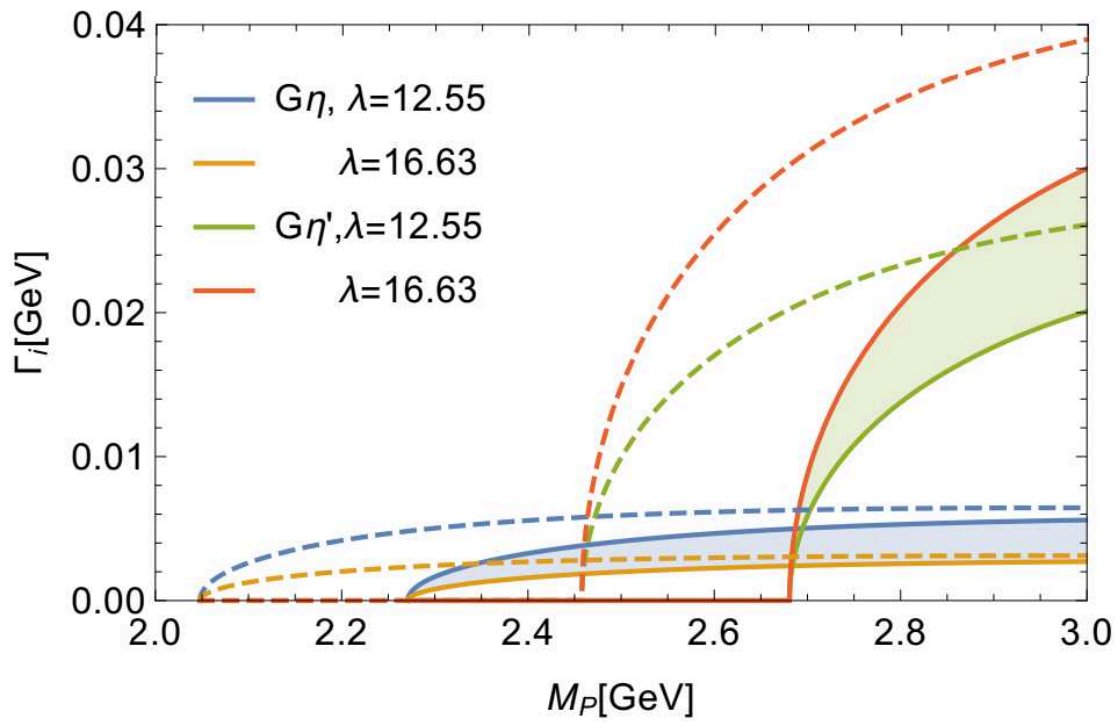


Figure 9.1: Pseudoscalar glueball decay rate into a scalar glueball and an η/η' meson plotted as a function of its mass. The scalar glueball is taken to be the dilatonic mode with mass adjusted to either approximately that of $f_0(1500)$ (dashed lines) or $f_0(1710)$ (solid lines).

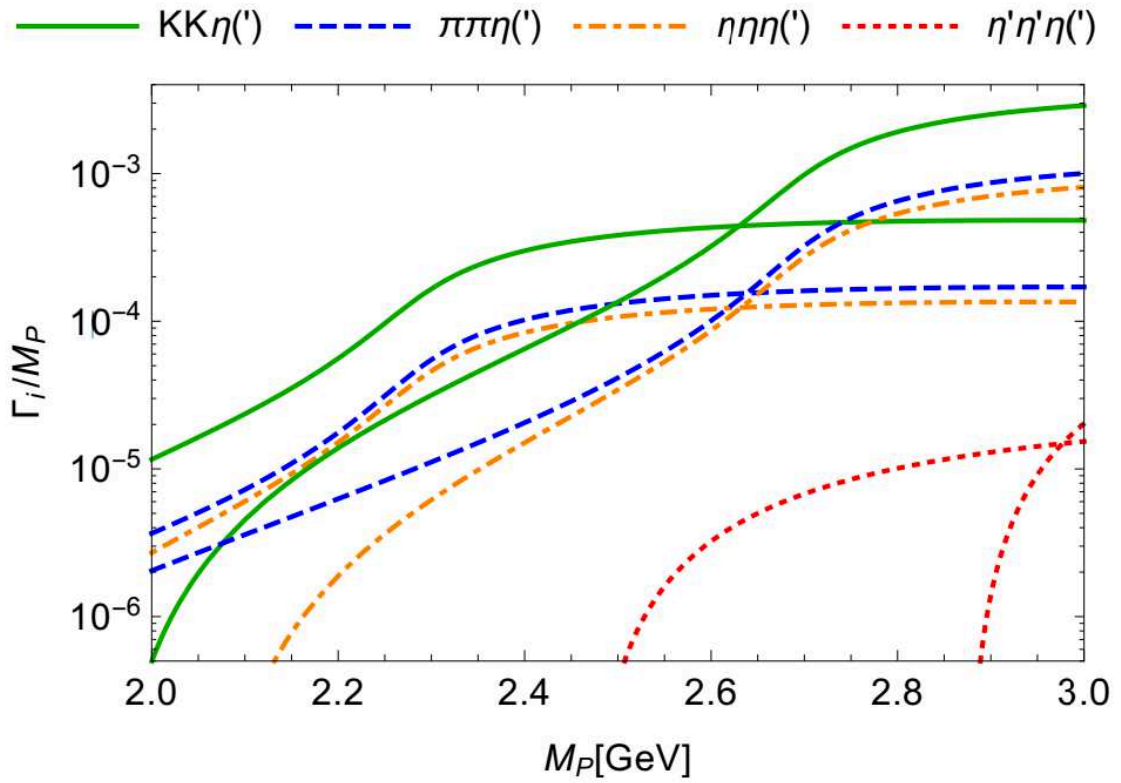


Figure 9.2: Partial decay widths of the form $\tilde{G} \rightarrow G\eta' \rightarrow PP\eta'$ for $P = K, \pi, \eta, \eta'$. Lines of identical colour correspond to the choices of scalar glueball mass (equal to approximately that of $f_0(1500)$ or $f_0(1710)$), where the heavier choice corresponds to a line starting further to the right.

9.3 ◆ RESULTS - PRODUCTION RATES

As we have seen, the pseudoscalar glueball does not, unlike its scalar and tensor counterparts, couple directly to $q\bar{q}$ mesons that are not involved in the Witten-Veneziano mechanism. This serves as an indication that it is not as easily produced in radiative J/ψ decays as the other glueballs, and severely limits its possible production channels: within the approximation considered so far, it may only arise through decay channels of the form $G_{D,T}^* \rightarrow \eta^{(\prime)}\tilde{G}$ and $G_{D,T}^* \rightarrow \tilde{G}\tilde{G}$ meson with $G_{D,T}^*$ denoting excited scalar or tensor glueballs. Since the required energies for these processes are above the mass of J/ψ , excited ψ mesons or the Υ meson might be necessary for these channels. Another possibility for the production of pseudoscalar glueballs would be processes described by off-shell scalar and tensor glueballs that could be found in the future PANDA experiment at FAIR. Beyond these options, a potential production mechanism for pseudoscalar glueballs might be central exclusive production in high-energy hadron collision involving double Pomeron or Reggeon exchange, corresponding to tensor glueball, ρ and ω meson trajectories. In Fig. 9.3 we see the Feynman diagrams associated with these processes, as well as the parametric dependence of the amplitudes. Note that $\tilde{G}\eta_0$ is only possible through processes involving scalar glueballs, while $\tilde{G}\tilde{G}$ can involve tensor glueballs, in accordance with Eqs. (9.6) and (9.9). The natural-parity violating coupling of two tensor glueballs (Pomerons) to η_0 required for the existence of the bottom diagram in Fig.9.3 is possible due to the Chern-Simons part of the D8-brane action.

Production rates corresponding to the aforementioned processes are calculated the same way as decay rates. Assuming that all possible channels are known in which the particle of interest, in our case the pseudoscalar glueball, appears as a final state, the production rate is simply the sum of all individual decay rates for these channels. In the following, we will consider this separately for processes with either $\tilde{G}\eta'$ or $\tilde{G}\tilde{G}$ as final states, and present the results as ratios over the production rate of $\eta'\eta'$. This is because the production rates of $\tilde{G}\tilde{G}$ and $\eta'\eta'$ are of the same order in λ and N_c , making the ratio well determined for fixed meson mass. In particular, we obtain for the amplitudes of the decay of an excited scalar glueball:

$$\mathcal{M}(G^* \rightarrow \tilde{G}\eta') \propto \lambda^{1/2} N_f^{1/2} N_c^{-3/2}, \quad (9.27)$$

$$\mathcal{M}(G^* \rightarrow \tilde{G}\tilde{G}) \propto \lambda^{-1/2} N_c^{-1}, \quad (9.28)$$

and

$$\mathcal{M}(G^* \rightarrow \eta'\eta') \propto \lambda^{-1/2} N_c^{-1} .nk \quad (9.29)$$

The corresponding production rates, which we denote by the letter N , are then proportional to the square of the absolute value of the above amplitudes:

$$N(\tilde{G}\eta') \propto |\mathcal{M}(G^* \rightarrow \tilde{G}\eta')|^2 \propto \lambda N_f N_c^{-3}, \quad (9.30)$$

$$N(\tilde{G}\tilde{G}) = |\mathcal{M}(G^* \rightarrow \tilde{G}\tilde{G})|^2 \propto \lambda^{-1} N_c^{-2}, \quad (9.31)$$

and

$$N(\eta'\eta') = |\mathcal{M}(G^* \rightarrow \eta'\eta')|^2 \propto \lambda^{-1} N_c^{-2}. \quad (9.32)$$

The numerical results for $N(\tilde{G}\eta')/N(\eta'\eta')$ and $N(\tilde{G}\tilde{G})/N(\eta'\eta')$ are shown in Fig. 9.4 as a function of the energy of the excited scalar glueball for a pseudoscalar glueball mass of 2.6 GeV. We vary the 't Hooft coupling within the usual range between $\lambda = 12.55$ and $\lambda = 16.63$. We see that even though the threshold for the process is higher, the production rate of two pseudoscalar glueballs is much larger than that of the pseudoscalar glueball and η' pair. In order to further illustrate this, we directly compare $N(\tilde{G}\tilde{G})$ and $N(\tilde{G}\eta')$ in Fig. 9.5 by plotting their ratio for two different values of the pseudoscalar glueball mass, i.e., 2.37 GeV and 2.6 GeV.

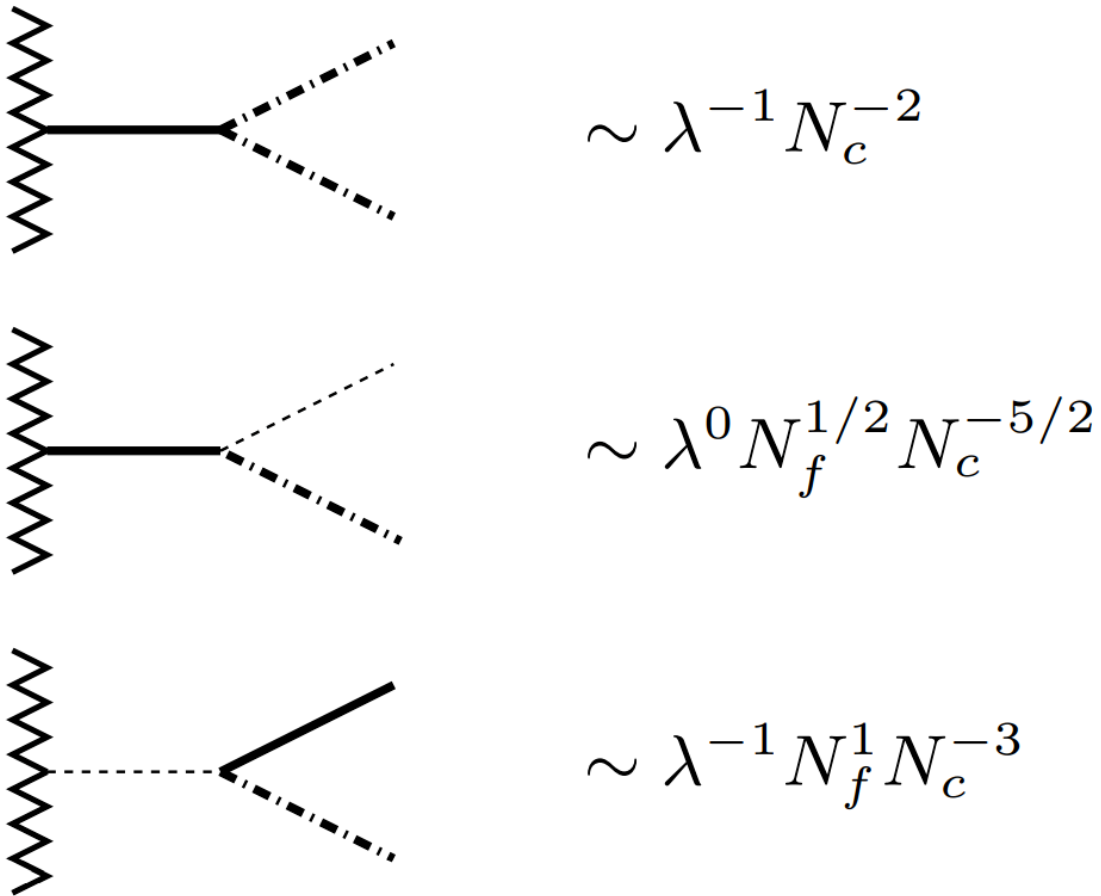


Figure 9.3: Feynman diagrams contributing to pseudoscalar glueball production, as well as the parametric dependence of the corresponding amplitudes. Dotted lines correspond to η/η' mesons, dash-dotted lines to pseudoscalar glueballs, and full lines to scalar, and in the uppermost diagram also to tensor glueballs. Zigzag lines represent double Pomerons, for the first two lines also Reggeons.

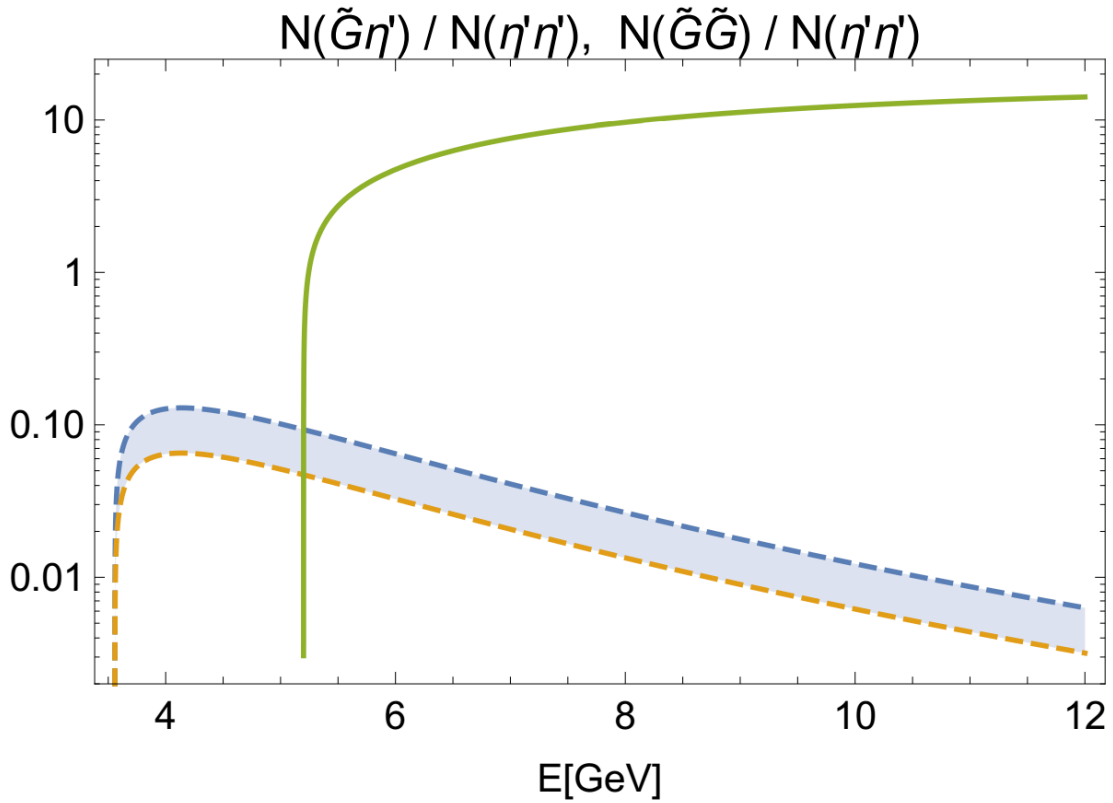


Figure 9.4: Ratios of production rates of either $\tilde{G}\tilde{G}$ (green line) or $\tilde{G}\eta'$ (dashed lines) and $\eta'\eta'$ pairs, corresponding to the first two diagrams in the previous figure. The pseudoscalar glueball is taken to have a mass of 2.6 GeV, and graphs are plotted as a function of the center of mass energy of the produced pair. The ratio $N(\tilde{G}\tilde{G})/N(\eta'\eta')$ is independent of the 't Hooft coupling, whereas the upper dashed line corresponds to $\lambda = 12.55$ and the lower to $\lambda = 16.63$.

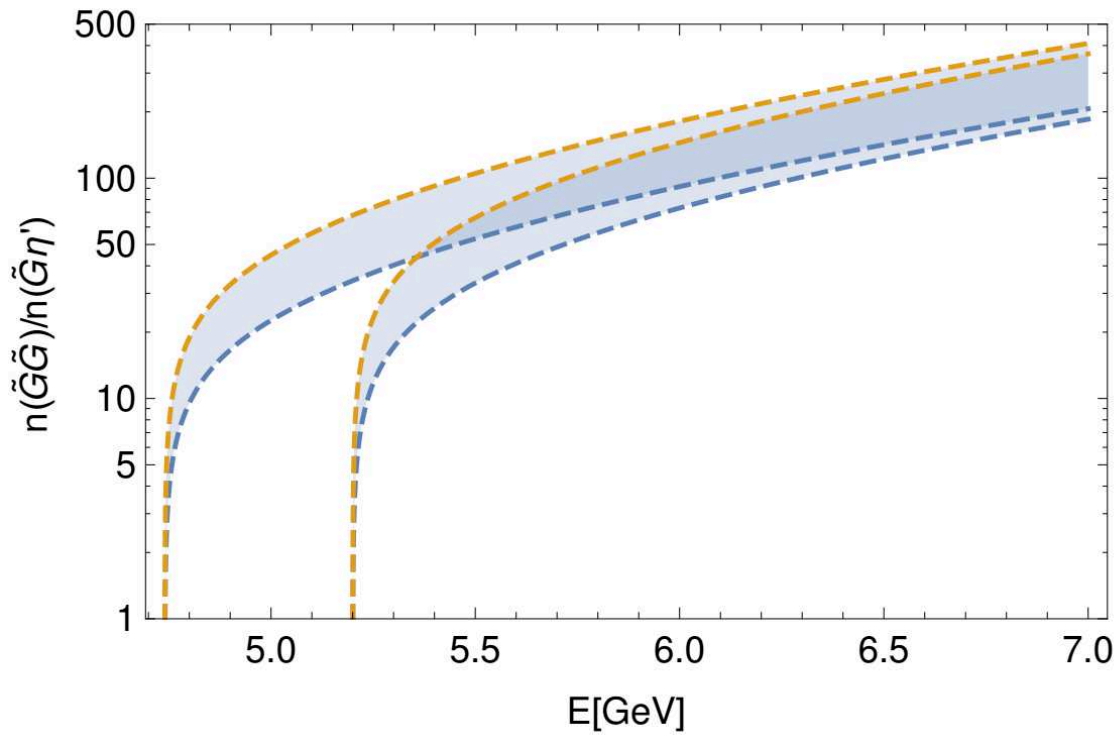


Figure 9.5: The ratio of production rates of the pairs $\tilde{G}\tilde{G}$ and $\tilde{G}\eta'$ as a function of the center of mass energy of the produced pair for a pseudoscalar glueball mass of either 2.37 GeV (graphs with lower production threshold) and 2.6 GeV. Upper and lower lines correspond to $\lambda = 12.55$ and $\lambda = 16.63$, respectively.

10 PSEUDOVECTOR GLUEBALL

“Judge me by my size, do you?”

Yoda

10.1 VERTICES

Interaction vertices for the pseudovector glueball may in principle arise from inserting the corresponding fluctuations of the Kalb-Ramond field (4.46) into both the DBI-action (2.16) and the Chern-Simons action (2.19) of the flavour branes. We will begin with the latter, and then show that vertices that come from the former are parametrically suppressed.

The Chern-Simons action contains a term linear in the Kalb-Ramond field, which is obtained from partial integration, and is given by

$$S_{\text{CS}}^{(B_2)} = \frac{1}{2} (2\pi l_s^2)^2 T_8 L^3 \pi^2 g_s^{-1} \text{Tr} \int A_1 \wedge F_2 \wedge B_2. \quad (10.1)$$

In analogy to the earlier chapters, inserting both glueball and meson fluctuations, and integrating over all extra dimensions leads to a four-dimensional effective Lagrangian for glueball-meson interactions:

$$\begin{aligned} \mathcal{L}_{\tilde{B}\text{IV}}^{\text{CS}} = & b_1 (\Pi^a \partial_\mu V_\nu^a + V_\mu^a \partial_\nu \Pi^a) \star \tilde{B}^{\mu\nu} \\ & - i b_2 \text{Tr} (T^a [T^b, T^c]) \Pi^a V_\mu^b V_\nu^c \star \tilde{B}^{\mu\nu}, \end{aligned} \quad (10.2)$$

with $\star \tilde{B}^{\mu\nu} = \frac{1}{2} \epsilon^{\mu\nu\rho\sigma} \tilde{B}_{\rho\sigma}$, as well as the coupling constants

$$\begin{aligned}
b_1 &= \frac{1}{4} T_8 (2\pi^2 l_s^2 r_{\text{KK}} L)^2 g_s^{-1} \int r^3 \phi_0 \psi_1 H_V(Z) dZ \\
&= 56.027 \times \lambda^{-1/2} N_c^{-1},
\end{aligned} \tag{10.3}$$

and

$$\begin{aligned}
b_2 &= \frac{3}{8} T_8 (2\pi^2 l_s^2 r_{\text{KK}} L)^2 g_s^{-1} \int r^3 \phi_0 \psi_1^2 H_V(Z) dZ \\
&= 2571.72 \times \lambda^{-1} N_c^{-3/2}.
\end{aligned} \tag{10.4}$$

Next, we turn to the DBI action. We will consider the expansion of the DBI action to quartic order, Eq. (2.18), as it turns out that potential lower order interaction terms vanish. Consequently, there is also no mixing of the pseudovector glueball and any of the vector mesons. In order to obtain an estimate of the magnitude of the nonzero terms, we set $N_f = 1$ and obtain

$$\begin{aligned}
\mathcal{L}_{\tilde{B}\Pi V}^{\text{DBI}} &= \bar{b}_1 F^{\nu\rho} F_{\rho\sigma} F^{\sigma\mu} \tilde{B}_{\mu\nu} + \bar{b}_2 F^{\rho\sigma} F_{\rho\sigma} F^{\mu\nu} \tilde{B}_{\mu\nu} + \bar{b}_3 \partial^\rho \Pi \partial_\rho \Pi F^{\mu\nu} \tilde{B}_{\mu\nu} \\
&\quad + \bar{b}_4 V^\rho \partial_\rho \Pi F^{\mu\nu} \tilde{B}_{\mu\nu} + \bar{b}_5 V^\rho V_\rho F^{\mu\nu} \tilde{B}_{\mu\nu},
\end{aligned} \tag{10.5}$$

with $F^{\mu\nu} \equiv \partial^\mu V^\nu - \partial^\nu V^\mu$ and the coupling constants

$$\begin{aligned}
\bar{b}_1 &= \frac{1}{16} \frac{L^3 N_c}{M_{\text{KK}}^2 \pi^2} \int dZ K^{-5/6} \psi_1^3 H_V(Z) \\
&= 0.0000375351 \times \lambda^{-2} N_c^{-3/2},
\end{aligned} \tag{10.6}$$

$$\bar{b}_2 = -\bar{b}_1/4, \tag{10.7}$$

$$\begin{aligned}
\bar{b}_3 &= -\frac{1}{10368} \frac{M_{\text{KK}}^4 L^9 N_c}{\pi^2} \int dZ K^{1/2} \phi_0^2 \psi_1 H_V(Z) \\
&= -0.0000168453 \times \lambda^{-2} N_c^{-3/2},
\end{aligned} \tag{10.8}$$

$$\begin{aligned}\bar{b}_4 &= \frac{1}{288} \frac{M_{\text{KK}}^2 L^6 N_c}{\pi^2} \int dZ K^{1/2} \phi_0 H_V(Z) \partial_Z \psi_1 \\ &= -0.00875721 \times \lambda^{-2} N_c^{-3/2},\end{aligned}\tag{10.9}$$

$$\begin{aligned}\bar{b}_5 &= -\frac{1}{32} \frac{L^3 N_c}{\pi^2} \int dZ K^{1/2} \psi_1 (\partial_Z \psi_1)^2 H_V(Z) \\ &= -1.78464 \times \lambda^{-2} N_c^{-3/2}.\end{aligned}\tag{10.10}$$

These vertices are consistently suppressed by a factor of λ^{-1} with respect to their counterparts from the Chern-Simons action, and their numerical values are much smaller. We therefore conclude that their contributions are negligible.

Beyond the interaction terms discussed above, the DBI action leads to a correction to the mass of the pseudovector glueball, arising from a nonvanishing term proportional to $B_{\mu\nu} B^{\mu\nu}$. It is given by

$$\delta\mathcal{L} = -\frac{1}{4} \delta M^2 \eta^{\rho\mu} \eta^{\sigma\nu} \tilde{B}_{\mu\nu} \tilde{B}_{\rho\sigma},\tag{10.11}$$

with

$$\delta M^2 = 0.0035066 \times \frac{N_f}{N_c} \lambda^2 M_{\text{KK}}^2,\tag{10.12}$$

implying an increase of the glueball mass by roughly 8%, from 2311 MeV to 2416...2493 MeV. However, there is a caveat to this: the term is only present on the world volume of the flavour branes, and is therefore not consistent with the solution of the linearised equations presented in Section 4.2, which arises on the higher-dimensional background. A consistent computation of the actual mass correction would require the incorporation of backreactions of the flavour branes on the background, and a subsequent solution of the mode equation on this modified geometry.

decay channel	Γ/M
$\pi\rho$	0.3624 ... 0.4803
KK^*	0.1945 ... 0.2578
$\eta\omega$	0.0530 ... 0.0941
$\eta\phi$	0.0086 ... 0.0076
$\eta'\omega$	0.0168 ... 0.0203
$\eta'\phi$	0.0020 ... 0.0079
$\pi\rho\rho$	0.2595 ... 0.4556
$\pi K^* K^*$	0.0213 ... 0.0375
$KK^*\rho$	0.0032 ... 0.0056
$KK^*\rho$	0.0011 ... 0.0019
total	0.9225 ... 1.3685

Table 10.1: Decay rates of the pseudovector glueball based on the interaction vertices in Eq. (10.2).

10.2 ◆ RESULTS

In Table 10.1 we show the results for Γ/M for all decay channels arising from Eq. (10.2). The sum of all channels is of order 1, making the pseudoscalar glueball a broad resonance even before extrapolating the mass to higher values than predicted by the model. Doing the latter would lead to even larger decay rates. At present, to the knowledge of the author there are no experimental results supporting or contradicting this prediction, and furthermore there are no other theoretical studies of pseudoscalar glueball decay, which makes the work presented in this Chapter unique.

11 CONCLUSION

“Now, witness the power of this fully operational battle station.”

Empir or Pal pat ine

The Witten-Sakai-Sugimoto model, an instance of gauge/gravity duality, is a versatile tool for studying properties of hadrons, bound states of quarks and gluons. Within this framework, it is possible to determine not only the mass spectrum, but also full four-dimensional effective Lagrangians describing the interactions of these states. Consequently one may calculate decay and production rates, as well as scattering cross sections, even though the latter were not treated in this work. The model is based on a solution to the low energy limit of string theory, and therefore only contains a small number of parameters that have to be fixed by experimental input. We have used this approach to study interactions of glueballs and quark-antiquark mesons, and compared our predictions with experimental data of various glueball candidates. A number of nontrivial results concerning the identification of the lightest scalar, but also about pseudoscalar, pseudovector, and tensor glueballs were produced. It remains to be seen whether future experiments aimed at identifying glueballs will confirm our predictions.

Let us conclude this summary with words of caution. Despite all the interesting results that are in good agreement with experimental data, the holographic approach laid out in this work relies on several approximations that introduce some uncertainty to our results. One reason is that the gauge theory considered is not precisely QCD, but a five-dimensional theory that only looks like four-dimensional QCD below a certain compactification scale. Fitting the mass scale so that the lightest vector meson is matched with the ρ meson, we obtain a compactification scale of around 1 GeV. Beyond this scale, Kaluza-Klein

states in principle have to be included. However, we have not considered them, as we were only interested in states with a counterpart in QCD. Furthermore, the supergravity approximation is strictly only valid for large N_c , whereas for the purpose of comparing with QCD we have inserted $N_c = 3$ into all formulae. The precise magnitude of correction terms is not known. The same is true for large but fixed 't Hooft coupling λ , which is also necessary for the supergravity limit to hold. Because of this, it should be viewed as an uncontrolled approximation to large- N_c QCD.

An important step towards a more precise holographic description of QCD phenomena would be to compute these correction terms under the assumption that gauge/gravity duality is valid beyond the supergravity limit. Furthermore, let us note that since the construction of Sakai and Sugimoto relies on the probe approximation of the flavour branes, i.e., $N_f \ll N_c$, it would be of great interest to study how the incorporation of backreactions, which were considered in [92], would change our results.

Finally, we want to mention that in the Witten-Sakai-Sugimoto model degrees of freedom compatible with scalar quark-antiquark mesons in QCD are absent. These degrees of freedom should arise as string modes, which are not present since we are working in the supergravity approximation. This implies that there is no possibility of studying mixing effects for the scalar glueball, which are considered in some phenomenological models. It would be an interesting to see a solution to this problem that would allow for a top-down holographic prediction of mixing matrices. In the meantime, we have to assume that our results are only valid under the assumption that the glueball candidates we compare them with have a large glue component.

A COMPUTING AMPLITUDES

In this appendix we summarise formulas that are used silently in the calculation of decay rates in the main body of this work. All of these are standard and can be found in text books on quantum field theory or relevant review articles.

We exclusively consider the decay of a particle of mass M in its rest frame, the frame in which the particle's four-momentum is given by $p^\mu = (M, 0, 0, 0)^T$. The infinitesimal decay rate to N particles is given by

$$d\Gamma = \frac{(2\pi)^4}{2M} |\mathcal{M}|^2 d\Phi_N(p^\mu, p_1^\mu, \dots, p_N^\mu) \quad (\text{A.1})$$

where \mathcal{M} is the Lorentz invariant amplitude of the process and $d\Phi_N$ is an infinitesimal part of the phase space of the final states:

$$d\Phi_N(p^\mu, p_1^\mu, \dots, p_N^\mu) = \delta^4(P^\mu - \sum_{i=1}^N p_i^\mu) \prod_{i=1}^N \frac{d^3 p_i}{(2\pi)^3 2E_i}, \quad (\text{A.2})$$

where p_i^μ is the four-momentum and E_i the energy of a given decay product. The amplitude \mathcal{M} may in general be complex and is completely determined by the Lagrangian of the underlying theory. While it can be derived rigorously for each process, it is easier to construct it according to the Feynman rules, a simple set of rules that allows for writing down the amplitude by examining the structure of Feynman diagrams. In our case, we have used the following:

- Vertices are given by i times the momentum space representation of the corresponding interaction term in the Lagrangian.
- Internal lines amount to propagators of the form $-i/(k^2 - m^2 + im\Gamma)$, where

$k^2 \equiv \vec{k} \cdot \vec{k}$, \vec{k} being the spatial momentum of the internal particle, m its mass, and Γ its decay width.

An important modification appears when at least one of the particles involved in the process is polarised, which happens when the involved particles are described by either vectors or tensors. In this case the standard strategy to obtain a sensible result is to average over polarisations of the initial state, and to sum over polarisations of the decay products. This is because in an ordinary collider experiment, information about the polarisation of the initial state is not available, so one averages under the assumption that statistically all polarisations occur equally often.

Assume that we are looking at a process in which one of the decay products is a vector particle. Then the decay amplitude can be written as

$$\mathcal{M} \equiv \mathcal{M}^\mu \epsilon_\mu^\lambda, \quad (\text{A.3})$$

where ϵ_μ^λ is one of two polarisation vectors in the massless, and one of three in the massive case. Then the square of the amplitude, including the sum over polarisations, is given by

$$|\mathcal{M}|^2 = \sum_\lambda \mathcal{M}^\mu \overline{\mathcal{M}^\nu} \epsilon_\mu^\lambda \bar{\epsilon}_\nu^\lambda. \quad (\text{A.4})$$

Then one may take advantage of the useful relation (in mostly + signature)

$$\sum_\lambda \epsilon_\mu^\lambda \bar{\epsilon}_\nu^\lambda = \eta_{\mu\nu} + \frac{p_\mu p_\nu}{m^2}, \quad (\text{A.5})$$

where p_μ is the four-momentum of the polarised particle, and m is its mass. Note that the last term would be absent for a massless particle.

BIBLIOGRAPHY

- [1] J. M. Maldacena, *The Large N limit of superconformal field theories and supergravity*, Int. J. Theor. Phys. **38** (1999) 1113 [Adv. Theor. Math. Phys. **2** (1998) 231].
- [2] H. Fritzsche and M. Gell-Mann, *Current algebra: Quarks and what else?*, eConf C **720906V2** (1972) 135].
- [3] H. Fritzsche and P. Minkowski, *Ψ Resonances, Gluons and the Zweig Rule*, Nuovo Cim. A **30** (1975) 393.
- [4] A. M. Jaffe and E. Witten, *Quantum Yang-Mills theory*, <https://www.claymath.org/sites/default/files/yangmills.pdf>.
- [5] C. J. Morningstar and M. J. Peardon, *The Glueball spectrum from an anisotropic lattice study*, Phys. Rev. D **60** (1999) 034509.
- [6] P. A. Zyla *et al.* [Particle Data Group], *Review of Particle Physics*, PTEP **2020** (2020) 083C01.
- [7] C. Amsler and F. E. Close, *Is $f_0(1500)$ a scalar glueball?*, Phys. Rev. D **53** (1996) 295.
- [8] W. J. Lee and D. Weingarten, *Scalar quarkonium masses and mixing with the lightest scalar glueball*, Phys. Rev. D **61** (2000) 014015.
- [9] F. E. Close and A. Kirk, *Scalar glueball $q\bar{q}$ mixing above 1 GeV and implications for lattice QCD*, Eur. Phys. J. C **21** (2001) 531.
- [10] C. Amsler and N. A. Tornqvist, *Mesons beyond the naive quark model*, Phys. Rept. **389** (2004) 61.

- [11] F. E. Close and Q. Zhao, *Production of $f_0(1710)$, $f_0(1500)$, and $f_0(1370)$ in J/ψ hadronic decays*, Phys. Rev. D **71** (2005) 094022.
- [12] F. Giacosa, T. Gutsche, V. E. Lyubovitskij and A. Faessler, *Scalar nonet quarkonia and the scalar glueball: Mixing and decays in an effective chiral approach*, Phys. Rev. D **72** (2005) 094006.
- [13] M. Albaladejo and J. A. Oller, *Identification of a Scalar Glueball*, Phys. Rev. Lett. **101** (2008) 252002.
- [14] V. Mathieu, N. Kochelev and V. Vento, *The Physics of Glueballs*, Int. J. Mod. Phys. E **18** (2009) 1.
- [15] S. Janowski, D. Parganlija, F. Giacosa and D. H. Rischke, *The Glueball in a Chiral Linear Sigma Model with Vector Mesons*, Phys. Rev. D **84** (2011) 054007.
- [16] S. Janowski, F. Giacosa and D. H. Rischke, *Is $f_0(1710)$ a glueball?*, Phys. Rev. D **90** (2014) no.11, 114005.
- [17] S. Narison, *Masses, decays and mixings of gluonia in QCD*, Nucl. Phys. B **509** (1998) 312.
- [18] P. Minkowski and W. Ochs, *Identification of the glueballs and the scalar meson nonet of lowest mass*, Eur. Phys. J. C **9** (1999) 283.
- [19] P. Minkowski and W. Ochs, *The Glueball among the light scalar mesons*, Nucl. Phys. Proc. Suppl. **121** (2003) 123.
- [20] W. Ochs, *Scalar mesons: In search of the lightest glueball*, Nucl. Phys. Proc. Suppl. **174** (2007) 146.
- [21] L. Burakovsky and P. R. Page, *Tensor glueball meson mixing phenomenology*, Eur. Phys. J. C **12** (2000) 489.
- [22] S. R. Cotanch and R. A. Williams, *Tensor glueball photoproduction and decay*, Phys. Lett. B **621** (2005) 269.

- [23] V. V. Anisovich, *Systematization of tensor mesons and the determination of the 2^{++} glueball*, JETP Lett. **80** (2004) 715 [Pisma Zh. Eksp. Teor. Fiz. **80** (2004) 845].
- [24] V. V. Anisovich, M. A. Matveev, J. Nyiri and A. V. Sarantsev, *Sector of the 2^{++} mesons: Observation of the tensor glueball*, Int. J. Mod. Phys. A **20** (2005) 6327 [Int. J. Mod. Phys. A **20** (2005) 0502842].
- [25] F. Giacosa, T. Gutsche, V. E. Lyubovitskij and A. Faessler, *Decays of tensor mesons and the tensor glueball in an effective field approach*, Phys. Rev. D **72** (2005) 114021.
- [26] A. Masoni, C. Cicalo and G. L. Usai, *The case of the pseudoscalar glueball*, J. Phys. G **32** (2006) R293.
- [27] C. M. Richards *et al.* [UKQCD Collaboration], *Glueball mass measurements from improved staggered fermion simulations*, Phys. Rev. D **82** (2010) 034501.
- [28] E. Gregory, A. Irving, B. Lucini, C. McNeile, A. Rago, C. Richards and E. Rinaldi, *Towards the glueball spectrum from unquenched lattice QCD*, JHEP **1210** (2012) 170.
- [29] W. Sun *et al.*, *Glueball spectrum from $N_f = 2$ lattice QCD study on anisotropic lattices*, arXiv:1702.08174 [hep-lat].
- [30] T. Sakai and S. Sugimoto, *Low energy hadron physics in holographic QCD*, Prog. Theor. Phys. **113** (2005) 843.
- [31] E. Witten, *Anti-de Sitter space, thermal phase transition, and confinement in gauge theories*, Adv. Theor. Math. Phys. **2** (1998) 505.
- [32] F. Brünner, D. Parganlija and A. Rebhan, *Glueball Decay Rates in the Witten-Sakai-Sugimoto Model*, Phys. Rev. D **91** (2015) no.10, 106002 Erratum: [Phys. Rev. D **93** (2016) no.10, 109903].
- [33] F. Brünner and A. Rebhan, *Nonchiral enhancement of scalar glueball decay in the Witten-Sakai-Sugimoto model*, Phys. Rev. Lett. **115** (2015) no.13, 131601.

- [34] F. Brünner and A. Rebhan, *Constraints on the $\eta\eta'$ decay rate of a scalar glueball from gauge/gravity duality*, Phys. Rev. D **92** (2015) no.12, 121902.
- [35] F. Brünner and A. Rebhan, *Holographic QCD predictions for production and decay of pseudoscalar glueballs*, Phys. Lett. B **770** (2017) 124.
- [36] F. Brünner, J. Leutgeb and A. Rebhan, *A broad pseudovector glueball from holographic QCD*, Phys. Lett. B **788** (2019), 431-435.
- [37] G. 't Hooft, *Dimensional reduction in quantum gravity*, arXiv:gr-qc/9310026.
- [38] L. Susskind, *The World As A Hologram*, J. Math. Phys. **36**, 6377 (1995).
- [39] G. 't Hooft, *A Planar Diagram Theory for Strong Interactions*, Nucl. Phys. B **72** (1974), 461.
- [40] H. Nastase, *Introduction to AdS-CFT*, [arXiv:0712.0689 [hep-th]].
- [41] S. Gubser, I. R. Klebanov and A. M. Polyakov, *Gauge theory correlators from non-critical string theory*, Phys. Lett. B **428** (1998), 105-114.
- [42] E. Witten, *Anti-de Sitter space and holography*, Adv. Theor. Math. Phys. **2** (1998), 253-291.
- [43] O. Aharony, S. S. Gubser, J. M. Maldacena, H. Ooguri and Y. Oz, *Large N field theories, string theory and gravity*, Phys. Rept. **323** (2000), 183-386.
- [44] M. Ammon and J. Erdmenger, "Gauge/gravity duality,."
- [45] G. Veneziano, *Construction of a crossing - symmetric, Regge behaved amplitude for linearly rising trajectories*, Nuovo Cim. A **57** (1968) 190.
- [46] J. Dai, R. G. Leigh and J. Polchinski, *New Connections Between String Theories*, Mod. Phys. Lett. A **4** (1989) 2073.
- [47] J. Polchinski, *String theory. Vol. 2: Superstring theory and beyond*.

- [48] K. Becker, M. Becker and J. H. Schwarz, *String theory and M-theory: A modern introduction*.
- [49] E. Cremmer, B. Julia and J. Scherk, *Supergravity Theory in 11 Dimensions*, Phys. Lett. **76B** (1978) 409.
- [50] A. A. Tseytlin, *On nonAbelian generalization of Born-Infeld action in string theory*, Nucl. Phys. B **501** (1997) 41.
- [51] R. C. Brower, S. D. Mathur and C. I. Tan, *Glueball spectrum for QCD from AdS supergravity duality*, Nucl. Phys. B **587** (2000) 249.
- [52] N. R. Constable and R. C. Myers, *Spin two glueballs, positive energy theorems and the AdS / CFT correspondence*, JHEP **9910** (1999) 037.
- [53] K. Hashimoto, C. I. Tan and S. Terashima, *Glueball decay in holographic QCD*, Phys. Rev. D **77** (2008) 086001.
- [54] A. Hashimoto and Y. Oz, *Aspects of QCD dynamics from string theory*, Nucl. Phys. B **548** (1999), 167-179.
- [55] B. Lucini, A. Rago and E. Rinaldi, *Glueball masses in the large N limit*, JHEP **1008** (2010) 119.
- [56] M. Bando, T. Kugo, S. Uehara, K. Yamawaki and T. Yanagida, *Is rho Meson a Dynamical Gauge Boson of Hidden Local Symmetry?*, Phys. Rev. Lett. **54** (1985) 1215.
- [57] M. Bando, T. Kugo and K. Yamawaki, *Nonlinear Realization and Hidden Local Symmetries*, Phys. Rept. **164** (1988) 217.
- [58] G. S. Bali, F. Bursa, L. Castagnini, S. Collins, L. Del Debbio, B. Lucini and M. Panero, *Mesons in large-N QCD*, JHEP **1306** (2013) 071.
- [59] T. Sakai and S. Sugimoto, *More on a holographic dual of QCD*, Prog. Theor. Phys. **114** (2005) 1083.

- [60] E. Witten, *Current Algebra Theorems for the $U(1)$ Goldstone Boson*, Nucl. Phys. B **156** (1979) 269.
- [61] G. Veneziano, *$U(1)$ Without Instantons*, Nucl. Phys. B **159** (1979) 213.
- [62] M. B. Green, J. A. Harvey and G. W. Moore, *I-brane inflow and anomalous couplings on d-branes*, Class. Quant. Grav. **14** (1997) 47.
- [63] F. Bigazzi, A. L. Cotrone and R. Sissa, *Notes on Theta Dependence in Holographic Yang-Mills*, JHEP **08** (2015), 090.
- [64] L. Bartolini, F. Bigazzi, S. Bolognesi, A. L. Cotrone and A. Manenti, *Neutron electric dipole moment from gauge/string duality*, Phys. Rev. Lett. **118** (2017), 091601.
- [65] L. Bartolini, F. Bigazzi, S. Bolognesi, A. L. Cotrone and A. Manenti, *Theta dependence in Holographic QCD*, JHEP **02** (2017), 029.
- [66] M. Gell-Mann, R. J. Oakes and B. Renner, *Behavior of current divergences under $SU(3) \times SU(3)$* , Phys. Rev. **175** (1968) 2195.
- [67] O. Bergman, S. Seki and J. Sonnenschein, *Quark mass and condensate in HQCD*, JHEP **0712** (2007) 037.
- [68] K. Hashimoto, T. Hirayama, F. L. Lin and H. U. Yee, *Quark Mass Deformation of Holographic Massless QCD*, JHEP **0807** (2008) 089.
- [69] R. McNees, R. C. Myers and A. Sinha, *On quark masses in holographic QCD*, JHEP **0811** (2008) 056.
- [70] N. Evans and E. Threlfall, *Quark Mass in the Sakai-Sugimoto Model of Chiral Symmetry Breaking*, arXiv:0706.3285 [hep-th].
- [71] J. M. Gerard and E. Kou, *η - η' masses and mixing: A Large $N(c)$ reappraisal*, Phys. Lett. B **616** (2005), 85-92.
- [72] **KLOE** Collaboration, F. Ambrosino et al., *A Global fit to determine the pseudoscalar mixing angle and the gluonium content of the η' meson*, JHEP **07** (2009), 105.

- [73] J. M. Gerard and A. Martini, *Ultimate survival in anomalous $\psi(2S)$ decays*, Phys. Lett. B **730** (2014), 264-266.
- [74] **WA102** Collaboration, D. Barberis et al., *A Study of the $\eta\eta$ channel produced in central $p p$ interactions at 450-GeV/c*, Phys. Lett. B **479** (2000), 59-66.
- [75] I. Kanitscheider, K. Skenderis and M. Taylor, *Precision holography for non-conformal branes*, JHEP **0809** (2008) 094.
- [76] M. A. Shifman, A. I. Vainshtein and V. I. Zakharov, *QCD and Resonance Physics. Theoretical Foundations*, Nucl. Phys. B **147** (1979) 385.
- [77] B. L. Ioffe, *QCD at low energies*, Prog. Part. Nucl. Phys. **56** (2006) 232.
- [78] S. Narison, *Gluon Condensates and precise $\overline{m}_{c,b}$ from QCD-Moments and their ratios to Order α_s^3 and $\langle G^4 \rangle$* , Phys. Lett. B **706** (2012) 412.
- [79] G. S. Bali, C. Bauer and A. Pineda, *Model-independent determination of the gluon condensate in four-dimensional $SU(3)$ gauge theory*, Phys. Rev. Lett. **113** (2014) 092001.
- [80] S. Narison, *QCD tests of the puzzling scalar mesons*, Phys. Rev. D **73** (2006) 114024.
- [81] G. Mennessier, S. Narison and W. Ochs, *Glueball nature of the $\sigma/f_0(600)$ from $\pi\pi$ and $\gamma\gamma$ scatterings*, Phys. Lett. B **665** (2008) 205.
- [82] R. Kaminski, G. Mennessier and S. Narison, *Glueonium nature of the $\sigma/f_0(600)$ from its coupling to $K\bar{K}$* , Phys. Lett. B **680** (2009) 148.
- [83] D. Parganlija, *Quarkonium Phenomenology in Vacuum*, [arXiv:1208.0204 [hep-ph]].
- [84] M. Ablikim, J. Bai, Y. Ban, J. Bian, X. Cai, et al., *Partial wave analyses of $J/\psi \rightarrow \gamma\pi^+\pi^-$ and $\gamma\pi^0\pi^0$* , Phys. Lett. B **642** (2006), 441-448.
- [85] D. Barberis et al. [WA102], *A Coupled channel analysis of the centrally produced K^+K^- and $\pi^+\pi^-$ final states in pp interactions at 450 GeV/c*, Phys. Lett. B **462** (1999), 462-470.

- [86] J. Leutgeb and A. Rebhan, *Witten-Veneziano mechanism and pseudoscalar glueball-meson mixing in holographic QCD*, Phys. Rev. D **101** (2020), 014006.
- [87] C. M. Richards *et al.* [UKQCD], *Glueball mass measurements from improved staggered fermion simulations*, Phys. Rev. D **82** (2010), 034501.
- [88] E. Gregory, A. Irving, B. Lucini, C. McNeile, A. Rago, C. Richards and E. Rinaldi, *Towards the glueball spectrum from unquenched lattice QCD*, JHEP **10** (2012), 170.
- [89] W. Sun, L. C. Gui, Y. Chen, M. Gong, C. Liu, Y. B. Liu, Z. Liu, J. P. Ma and J. B. Zhang, *Glueball spectrum from $N_f = 2$ lattice QCD study on anisotropic lattices*, Chin. Phys. C **42** (2018), 093103.
- [90] W. I. Eshraim, S. Janowski, F. Giacosa and D. H. Rischke, *Decay of the pseudoscalar glueball into scalar and pseudoscalar mesons*, Phys. Rev. D **87** (2013), 054036.
- [91] G. J. Gounaris and H. Neufeld, *Why $\iota(1460)$ decays mainly into $K\bar{K}\pi$?*, Phys. Lett. B **213** (1988), 541. [Erratum: Phys. Lett. B **218** (1988), 508.]
- [92] B. A. Burrington, V. S. Kaplunovsky and J. Sonnenschein, *Localized Backreacted Flavor Branes in Holographic QCD*, JHEP **02** (2008), 001.